Using satellite tagging and molecular techniques to improve the ecologically sustainable fisheries management of shortfin makos (*Isurus oxyrinchus*) in the Australasian region

Tactical Research Fund

Rogers, P.J[a]., Corrigan[b], S. and Lowther[c]. A.

July 2015

FRDC Project No. 2011/077

[a]SARDI Aquatic Sciences, West Beach, South Australia.
[b]Hollings Marine Laboratory, 331 Fort Johnson, Charleston, USA.
[c]Norwegian Polar Institute, Hjalmar Johansensgata, Tromsø 9296, Norway

ISBN: 978-1-921563-81-2

Using satellite tagging and molecular techniques to improve the ecologically sustainable fisheries management of shortfin makos (*Isurus oxyrinchus*) in the Australasian region. Tactical Research Fund.

2011/077

2015

Ownership of Intellectual property rights

This publication (and any information sourced from it) should be attributed to Rogers, P. J., Corrigan, S., and Lowther, A. South Australian Research and Development Institute (Aquatic Sciences) 2015, *Using satellite tagging and molecular techniques to improve the ecologically sustainable fisheries management of shortfin makos (Isurus oxyrinchus) in the Australasian region. Tactical Research Fund.* Adelaide, July.

Creative Commons licence

Disclaimer

Researcher Contact Details

Name:	SARDI Aquatic Sciences
Address:	2 Hamra Avenue
	West Beach
Fax:	08 8207 5481
Phone:	0882075344
Email:	paul.rogers@sa.gov.au

FRDC Contact Details

Address:	25 Geils Court
	Deakin ACT 2600
Phone:	02 6285 0400
Fax:	02 6285 0499
Email:	frdc@frdc.com.au
Web:	www.frdc.com.au

In submitting this report, the researcher has agreed to FRDC publishing this material in its edited form.

Contents

Tables

Figures

Acknowledgments

This study was supported by funding provided by the Fisheries Research and Development Corporation Tactical Research Fund (Shark Futures). Additional support was provided by Nature Foundation SA Inc., Department for Environment and Natural Resources (DEWNR), Australian Geographic Society, Victorian DEPI Recreational Fishing Trust, SARDI Aquatic Sciences, and Flinders University. Procedures were undertaken under SARDI/PIRSA Ministerial exemptions (Section 115; 9902094, and S59; 9902064), DEWNR Permit U25570, Environment Australia, EPBC Act 1999 Permit E20120068 and Flinders University's Animal Welfare Committee approval (Project 309). Drs Simon Goldsworthy and Bradley Page assisted with funding support for the tag deployments in 2008/09 and the ARGOS satellite network coverage. Conventional game fish tagging data used in this report were provided by the NSW DPI Game Fish Tagging Program funded by the NSW recreational Fishing Saltwater Trust as per the terms of the data licence agreement between SARDI and NSW DPI (22 January 2014). We thank Phil Bolton and Adam Welfare from NSW DPI for their assistance with our queries regarding the conventional tagging data. Flinders University provided use of laboratory facilities to analyse tissue samples during a related preliminary project funded by Seaworld. We thank the International participants and Barry Bruce, the primary investigator of the FRDC funded workshop, *Shark futures - a synthesis of available data on mako and porbeagle sharks in Australasian waters: Current status and future directions* for constructive input and support of this project. Drs Andrew Oxley, Nicole Patten and an FRDC assigned reviewer provided valuable comments and suggestions to assist the improvement of the final version of this report. We also thank the following people for their invaluable assistance during satellite tag deployments: John Collinson, Anton Blass, Callan Henley, Shane Gill (*FV* Rahi Aroha), Dennis and Kerry Heineke, Adam Todd (*FV* Shaka-Zura), Paul Irvine, Steve Toranto, Phil Stroker, Clinton Adlington (*FV* Home Strait), Shane Sanders and Brodie Carter (*FV* Baitwaster), Charlie Huveneers, Matt Heard, Mick Drew, Crystal Beckmann (SARDI), Slavko Kolega, Chris Meletti (Sekol, *MV* Lucky-S), Mark Lewis and Bruce Barker (CSIRO). Four sharks were tagged with support from an aligned project funded by the Victorian Department of Primary Industries Recreational Fishing Licence Trust Account Large Grants Program. Tissue samples for genetic analyses were provided by: Malcolm Francis, Clinton Duffy, Nuno Queiroz, Gonzalo Mucientes, Geremy Cliff, William White, Charlie Huveneers, Lindsay Marshall, Matias Braccini, Rory McAuley, Julian Peperrell, Rima Jabado, Alan Foulis, Gavin Naylor, John Collinson, Paul Irvine, Steve Toranto, Shane Sanders, Brodie Carter, Adam Todd, Dennis and Kerry Heineke, Ashley and Neville Dance, and Greg Barea. Luciano Beheregaray and Gavin Naylor provided funding and infrastructure support for the genetic analyses. Dovi Kacev and John Hyde (NOAA/NMFS) developed the microsatellite markers and we thank them for sharing primer sequences.

Abbreviations

Australian Fisheries Management Authority (AFMA)

Commission for the Conservation of Southern Bluefin Tuna (CCSBT)

Commonwealth Scientific and Industrial Research Organisation (CSIRO)

Convention on International Trade in Endangered Species of Wild Flora and Fauna (CITES)

Convention on Migratory Species (CMS)

Department for Environment and Natural Resources (DEWNR)

Exclusive Economic Zone (EEZ)

Ecologically Related Species Working Group (ERSWG)

Environmental Protection Biodiversity and Conservation Act 1999 (EPBC Act 1999)

Game Fishing Association of Australia (GFAA)

Great Australian Bight (GAB)

Fisheries Research and Development Corporation (FRDC)

Highly Migratory Species (HMS)

International Game Fishing Association (IGFA)

International Union of Conservation of Nature (IUCN)

Indian Ocean Tuna Commission (IOTC)

International Commission for the Conservation of Atlantic Tunas (ICCAT)

National Oceanic and Atmospheric Administration (NOAA)

Regional Fisheries Management Organisation (RFMO)

South Australian Research and Development Institute (SARDI)

Secretariat of Pacific Community (SPC)

Species Survival Commission (SSC)

Sub-Tropical Front (STF)

Threatened Endangered and Protected Species (TEPS)

Western Central Pacific Fisheries Commission (WCPFC)

Executive Summary

This study used a multi-disciplinary approach to investigate the patterns of population structure, spatial connectivity, and contemporary effective population size of the shortfin mako (*Isurus oxyrinchus*). It represents the first comprehensive study of the connectivity of this Highly Migratory Species (HMS) species in the Southern Hemisphere.

Listing of the shortfin mako under the *Environmental Protection Biodiversity and Conservation Act* (EPBC Act, 1999) in 2010 was debated by recreational/game fishers. This was followed by an amendment to allow that sector to continue to target shortfin makos. Points of contention included a perception that there was: 1) limited information available to assess links between shortfin mako populations in Australian waters and those in the Northern Hemisphere, and 2) limited information on the movement and mixing of shortfin makos that support Australian fisheries.

The Fisheries Research and Development Corporation funded an Australasian Mako Shark Workshop in 2012. Information on the population structure of the shortfin mako was identified as a research gap and this provided part of the impetus for this project.

The shortfin mako represents a significant recreational and game fish target and bycatch species of pelagic fisheries that target tuna and billfish.

Methodologies used included spatial analyses of long-term satellite telemetry and conventional tagging data from southern and eastern Australia, and analyses of DNA data from the mitochondrial (DNA sequence) and nuclear (microsatellite) genomes from samples collected between New Zealand, Australasia and Indo-Pacific, western Indian Ocean and North Atlantic Ocean.

We used ARGOS tracking data and a (C)orrelated (RA)ndom (W)alk (L)ibrary (CRAWL) model and state-space framework to establish spatial parameters, including mean rate of movement per day (ROM), minimum cumulative distance travelled, and distal displacement distances for each tagged individual.

A total of 7,328 shortfin makos were conventionally tagged and released in Australian waters by recreational and game fishing anglers (NSW DPI Game Fish Tagging Program) between 1973 and 2014. Of these, 158 (2.2% of 7,328) were recaptured between 1977 and 2013. Displacement distances from the tagging sites ranged between 0 and 5,940 km (mean = 532 ± 62.04 km).

The maximal extents of migrations by satellite tagged shortfin makos were north to -12.13°S, south to -46.00°S, east to 174.69°E and west to 49° E. The spatial scales of movements over periods up to 1.8 years ranged between 8,776–24,213 linear km in the Great Australian Bight, Indian Ocean and Coral Sea, and up to 10,838 km in a ~1 year period between the eastern Bass Strait, New Zealand, and New Caledonia regions.

Analyses of mitochondrial DNA suggested there was limited population structure within Australian management jurisdictions, although southern Australia and New Zealand may be connected via patterns of step-wise mitochondrial gene flow.

Cross-equatorial mitochondrial gene flow was limited. Both Northern Hemisphere sampling sites showed significant differentiation from those in the Southern Hemisphere. There was some evidence of reduced mitochondrial gene flow across the Indian Ocean between Australasia and South Africa, however this requires further investigation.

In contrast to the results based on mitochondrial DNA, microsatellite data indicated high connectivity between all sampling locations within Australian management jurisdictions, and with neighbouring sampling sites in South Africa and the Northern Hemisphere. However, given the results from the mitochondrial DNA, we caution against interpreting this to mean that shortfin mako be managed as a single panmictic stock since the migration rate necessary to eradicate a signal of stock structure is less than would be required to replenish overharvested populations by migration.

Contrasting levels of mitochondrial and microsatellite structure at the ocean basin level may indicate that sex-biased dispersal is occurring at this geographic scale. There was a trend toward male-biased dispersal evident in analyses based on smaller spatial scales, however this was not statistically supported. Several caveats to the statistical power of this analysis are discussed. It was recommended that sex-biased dispersal is reassessed based on a larger sample size of both tracking and genetic data derived from mature individuals of known sex.

Estimates of contemporary effective population size mostly ranged between the orders of 100s to 1,000s. Estimated effective population size for the Australasian region (Indo-Pacific, eastern, southern, Western Australia and New Zealand) was 2,550.6 (95% CI = 831 – ∞). Difficulties associated with estimating effective population size in large populations, including some unavoidable violations of

analysis assumptions, are discussed.

In summary, based on the 36 year conventional tagging data-set, a 7-year satellite tracking dataset, and microsatellite and mitochondrial DNA analyses from 365 samples collected in six key regions, the most appropriate ecological scale at which to manage the population fished in Australian State and Commonwealth waters are the boundaries of the Australian and Central Indo Pacific Region (New Zealand – south west Pacific – Australasian/Indo Pacific Region). This will need to be refined as further satellite tracking data are collected and as we collect genetic data from the north and south east Pacific Ocean, and southern Indian Ocean.

Future research should seek to improve satellite tracking and genetic datasets for adult shortfin makos, identify regions in the Australasian and Central Indo-Pacific Region used for nursery, pupping and parturition, and to improve information on the size of breeding populations.

Keywords: Shortfin mako, *Isurus oxyrinchus*, stock structure, connectivity, movement, migration.

Introduction

Background

There is a growing awareness of the important functional roles of top predators, including pelagic sharks (Dulvy et al. 2008; Ferretti et al. 2010), in maintaining marine ecosystem health. Consequently, there is an increasing expectation that fisheries impacts be managed appropriately. Highly migratory species (HMS) of pelagic sharks represent an ecologically, commercially and socially important, but challenging group to manage due to their cryptic nature, ongoing uncertainties regarding their distributions and abundance, and high mobility with a propensity to move across multi-jurisdictional management boundaries (Heithaus et al. 2008; Baum and Worm 2009). Incorporating information regarding the distributions, movement patterns, genetic structure and sizes of pelagic shark populations is therefore crucial to the development of effective management strategies.

Australia is a major fishing nation in the Southern Hemisphere, contributing substantially to pelagic shark target catch and bycatch in this region. Australia is a signatory to multiple international treaties and assessment entities. These include the Convention on Migratory Species (CMS), the Convention on International Trade in Endangered Species of Wild Flora and Fauna (CITES) and the International Union of the Conservation of Nature (IUCN) Species Survival Commission (SSC); all of which call for the integration of modern investigations into the ecological and demographic attributes of HMS, to guide conservation and management options. Nevertheless these areas represent existing knowledge gaps for the majority of pelagic shark species with ranges that extend into this region.

The shortfin mako (Family: Lamnidae, *Isurus oxyrinchus*) is a globally iconic, oceanic pelagic shark species with an extensive temperate and tropical distribution (Compagno et al. 2005), ranging across multiple international and high seas management jurisdictions. It is thus an excellent example of a species that presents substantial challenges in terms of sustainable fisheries and bycatch management in high seas of Australasia and the Indo-Pacific. Bycatch in commercial pelagic long-line fisheries targeting tunas, broadbill swordfish and billfish represent a key source of mortality of shortfin makos in Australian Commonwealth and neighbouring jurisdictions (Stevens 1992; Bruce 2014). Between 1998 and 2011, there were ~852 t (trunk wt) of shortfin makos recorded in Australian Commonwealth managed fisheries, with the majority (757 and ~17.7 t) taken in the Eastern and Western Tuna and Billfish Fisheries (ETBF and WTBF; Bruce 2014). In the early 2000s the Australian Fisheries

Management Authority (AFMA) banned at-sea finning of sharks, which has had important implications for the sustainable management of Australasian stocks. Landing and retaining of live shortfin makos is currently not permitted in State and Commonwealth fisheries, however dead individuals can still be retained under trip limits of 20 shark for all species combined. These sharks can be finned legally once they have been landed on shore.

Previous genetic studies of the shortfin mako showed significant mitochondrial structuring between the Pacific and Atlantic Ocean basins, as well as cross-equatorial sub structure within ocean basins, and between the southeast and southwest Pacific Ocean (Heist et al. 1996; Schrey and Heist 2003). However, the null hypothesis of a single globally panmictic genetic stock could not be rejected based on data from nuclear microsatellite markers (Schrey and Heist 2003). Together these patterns indicate that gene flow at a global scale is male mediated in shortfin mako, while females exhibit greater philopatry to ocean basins (Schrey and Heist 2003). Philopatry in coastal and offshore oceanic areas has also been suggested to occur in white sharks (*Carcharodon carcharias*) that migrate between these areas in the Pacific Ocean (Jorgensen et al. 2010). Tagging data for shortfin makos also indicate differentiation between Northern and Southern Hemisphere populations. Following more than 21,000 standard and satellite tag deployments globally, only one individual has been reported to cross the equator (Holts 1988; Holts and Bedford 1993; Francis et al. 2001; Klimley et al. 2002; Kohler et al. 2002; Sepulveda et al. 2004; Loefer et al. 2005; Holdsworth and Saul 2010; Stevens et al. 2010; Wraith and Kohin 2010; Abascal et al. 2011; Block et al. 2011). Additionally, satellite tracking studies have shown that while shortfin makos exhibit both broad-scale movements and periods of fidelity in the Southern and Indian Oceans (Rogers et al. 2015), they also exhibit similar patterns in the northwest Atlantic Ocean, the southeast, central and northeast Pacific Ocean (Vetter et al. 2008; Abascal et al. 2011; Block et al. 2011; Loefer et al. 2005; Musyl et al. 2011), and the southwest Pacific Ocean off eastern Australia (Stevens et al. 2010).

High mobility does not imply high gene flow (Palumbi 2003). Animals may move for reasons that are unrelated to reproductive activity [for example, in response to prey distribution or habitat preferences], which doesn't translate into genetic connectivity between regions. Other factors, such as sex-biased dispersal, geographical and ecological barriers to movement, recent evolutionary history or an historical demographic event may also promote genetic structure in HMS (Avise 2004). Although studies to date have provided critical insights into the movement ecology of shortfin mako, more information is needed to determine the appropriate spatial scale at which to manage this species in Australasian waters. Specifically, the extent of connectivity between locations within the Southern Hemisphere is

poorly understood, as this region has previously received only low geographic sampling coverage. Tagged animals have mostly been tracked in the Northern Hemisphere while DNA sampling has been conducted only at the ocean basin level. Developing sound management strategies for shortfin makos in Australasian waters requires determining whether any unrecognised local substructure exists throughout the region and between neighbouring jurisdictions.

An understanding of movement ecology for management purposes therefore requires that movement be directly quantified in order to identify critical habitats, but also that the genetic consequences of movement are understood (i.e. gene flow), as these are intimately related to population persistence (Nams 2006; Dingle and Drake 2007). Tracking methods are useful for obtaining direct estimates of dispersal and fine-scale movement of individuals. Molecular methods allow assessments of genetic connectivity over broader spatial scales. We therefore employed the multi-disciplinary approach of combining satellite tracking, conventional tagging, and DNA datasets to investigate the spatial scales of movements and population structure of shortfin makos sampled around Australia and those in neighbouring regions (e.g. Indian Ocean and New Zealand waters).

Genetic data may be used to estimate the contemporary effective population size (CN_e). For fisheries management purposes, CN_e can be thought to approximate the recent average number of breeding individuals that have contributed to the observed genetic diversity within a population (Luikart et al. 2010; Hare et al. 2011). Reductions in population size can be associated with loss of genetic diversity and adaptive variation, increased inbreeding and the accumulation of deleterious alleles, all of which have negative consequences for long term population survival and evolutionary potential (Frankham et al. 2010). Estimating CN_e therefore, indicates not only the breeding population size, but can also provide a measure of population genetic health. Genetic monitoring and CN_e estimation has featured heavily in conservation plans for terrestrial organisms but has only been a focus in marine conservation planning in recent years. To date, CN_e has been estimated for few elasmobranch species (Ahonen et al. 2009; Portnoy et al. 2009; Chapman et al. 2011; Nance et al. 2011; Blower et al. 2012). There is scope for more widespread estimation of CN_e as an evaluation tool for marine populations, complementing existing stock assessment methods (Luikart 1998; Hare et al. 2011).

Need

Concern for shortfin mako populations in the Northern Hemisphere led to the listing of this species as ‘Critically Endangered’ in the Mediterranean and ‘Vulnerable’ in other regions,

including the North Atlantic by the International Union for Conservation of Nature Species Survival Commission on 22 February 2007. Shortfin mako was subsequently CMS listed (Appendix II: Migratory) which led to nomination under the Australian Commonwealth *Environment Protection Biodiversity and Conservation Act* (EPBC Act, 1999). In November 2009, the Australian Commonwealth Government Department of the Environment released information online stating that from 29 January 2010, shortfin mako, longfin mako (*I. paucus*), and porbeagle (*Lamna nasus*) were to be listed under the EPBC Act, making it an offence to kill, injure, take, trade, keep or move shortfin mako in Commonwealth waters. EPBC Act provisions also afforded protection measures for each species in State (out to 3 nm), and Commonwealth waters.

The EBPC listing was debated and petitioned against by recreational, game and charter fishers. Most of the conjecture was raised in Victoria, Tasmania and New South Wales, where recreational fishers target shortfin makos. This led to an amendment to the EPBC Act that allowed recreational fishers to continue to target shortfin makos. Points of contention included that there was: 1) limited information available to assess connectivity between Australian shortfin mako populations and those in the Northern Hemisphere, and 2) limited information regarding the movements of the shortfin makos that support the Victorian recreational fishery, and their connectivity with populations in other regions of Australia. In early February 2012, the Australasian Mako Shark Workshop, which was run by CSIRO in Hobart and funded by the Fisheries Research and Development Corporation (FRDC), aimed to identify key research priorities for shortfin makos. Participants included scientists from the CSIRO, Fisheries Departments of Tasmania, Victoria, New South Wales, Queensland, South Australia and Western Australia, and overseas experts from New Zealand, USA, and Secretariat of Pacific Community (SPC). Government officials from AFMA and the Department of Environment also attended, as did representatives from the World Wide Fund for Nature, Humane Society International and the game fishing sector (GFAA). AFMA representatives indicated that information on the abundance of shortfin makos was a key priority for management of tuna and billfish fisheries. This process highlighted that in Australian jurisdictions, commercial fisheries catches of shortfin makos have predominantly occurred in eastern Australian waters, with 1,257–3,288 (mean = 2,009) individual sharks being landed per year, with 87% retained and 13% discarded (Bruce 2014). Collecting further information about the genetic population structure of shortfin makos in the region was also identified as a key research priority.

Objectives

This study aimed to assess population connectivity of shortfin makos within Australasian and neighbouring waters by combining empirical satellite-tracking and conventional tagging data with DNA data from mitochondrial and nuclear genomes. The resultant information will be used to inform management strategies for shortfin makos in Australian and neighbouring high seas jurisdictions, where this species ranges across multiple State, Commonwealth and international boundaries. A multi-disciplinary approach to assessing connectivity in this pelagic shark species is considered more powerful for detecting and defining management boundaries when compared to single-discipline approaches because it allows consideration of movements that may not be related to reproductive activity, but may reveal critical habitat, while also indicating the extent of genetic connectivity between locations.

The specific aims of this study were:

1. To use new genetic data to assess the patterns of population genetic structure of shortfin makos in the Australasian and neighbouring regions;
2. To compare the geographic scale of genetic connectivity with movement patterns determined from conventional and satellite tagging;
3. To use the data to determine the contemporary effective population size of identified spatially discrete stocks;
4. To integrate the genetic and movement data with that generated during a larger global population structure study with special reference to elucidating the degree of cross-equatorial dispersal.

Methodology

Conventional tag-recapture

Conventional tag-recapture data were collected for 158 shortfin makos (*Isurus oxyrinchus*) by recreational, game and commercial fishers in State and Commonwealth managed waters of South Australia, Victoria, New South Wales, Queensland, and Western Australia during the New South Wales Department of Primary Industries (DPI) Game Fish Tagging Program. This tagging program began in 1973 and provides recreational and game fishers with independently numbered stainless steel head plastic identification tags and tag cards to record capture and release information, including the method of capture, condition on release, species identification, date and location of capture (lat-long), and an estimate of size and weight. Conventional tagging data were returned by anglers and fishing clubs and stored in the NSW DPI Game Fish Tagging Program database. Figure 1 shows tagging locations for recaptured shortfin makos between 1973 and 2014. Appendix 1 provides summary details of all tag-recapture events.

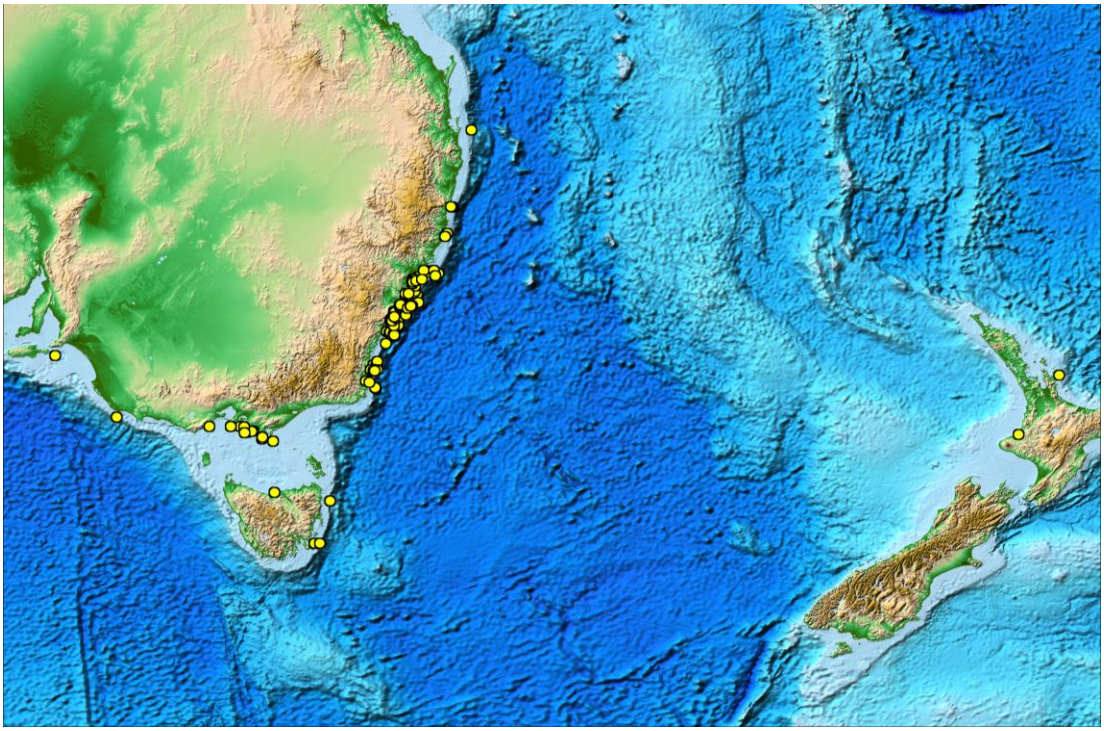

Figure 1. Tagging locations of recaptured shortfin makos in Australia and New Zealand between 1973 and 2014 (indicated by yellow symbols) (Bathymetry source: NOAA ETOPO1 Global relief bathymetry layer (Amante and Eakins 2009).

Capture and tagging techniques

Conventional tagging of sharks occurs via the following steps: a shark is hooked on game fishing equipment and brought along-side the vessel by an angler; the leader is held while a designated tagger uses a tag pole with a stainless steel applicator needle to apply the tag into the musculature near the first dorsal fin; the shark is released by removing the hook(s) using a purpose built de-hooking device, or the leader is cut as close to the shark's mouth/hook(s) as possible. Following a recapture, the fishers record the tag ID number, species, date, location (lat-long), estimated or actual size (if landed and retained), and physical condition upon release (if applicable).

Data analyses

The spatial scale of movement of each tagged shark was estimated by plotting the tag-recapture locations over the NOAA ETOPO1 Global relief bathymetry layer (Amante and Eakins 2009) using MapInfo Ver. 11.5 (Mapinfo Corporation, New York) geographical information systems (GIS) software, removing erroneous locations (i.e. locations on land). Minimum displacement distances (mean, standard error and 5–95th percentiles) travelled between the tagging and recapture locations were measured along with the number of days at liberty. We calculated the individual bearings (direction) between the tagging and recapture locations. Percentage frequencies based on bearing estimates (40° bins) were examined using wind-rose plots in OriginPro 9.1 software (OriginLab, Northampton, USA).

Satellite tagging

A total of 13 satellite tags were deployed in the Great Australian Bight (GAB), southeastern South Australia, western and eastern Victoria between 2008 and 2013 (Fig. 2). Satellite tags were deployed at locations in continental shelf and shelf slope waters of the GAB and the south-east coast of South Australia in 2008 and 2009, and in shelf waters of southwestern Victoria and Bass Strait in 2012 and 2013. Tag deployment sites, locations and bathymetric and oceanographic features mentioned in this report are shown in Figure 2. In Bass Strait, two tags were deployed at a single location. Deployment summary details, including shark size, sex and tagging locations are provided in Table 1. Tags deployed included five different dorsal fin mounted configurations, including Sirtrack™ KiwiSat 202, Sirtrack K2F161A, Wildlife Computers™ (WC) Smart Position or Temperature (SPOT), and data collecting

Argos tags (SPLASH) and Mk10A. Sirtrack 202 tags and SPOTs were programmed to transmit daily, whereas the SPLASH and Sirtrack K2F161A tags were duty-cycled to transmit at a 2-day frequency to maximise battery life.

Capture and satellite tagging techniques

Satellite tag deployments were from a demersal automatic long-line vessel, and a CSIRO chartered tuna fishery vessel in the central and eastern GAB. Game fishing vessels were used in the Bonney Upwelling Region of the southeastern GAB and eastern Bass Strait (Fig. 1, Table 1). Sharks were captured using either a 12 mm diameter rope and 70 mm diameter rubber buoy, attached to ~1 m of stainless steel cable leader (2 mm diameter) and several types of circle hooks (12/0–14/0), or by game fishers using standard game fishing tackle. Depending on the weather/vessel, some small-medium sharks were lifted from the water using either a solid aluminium or collapsible rubber sling. Once on-board, sharks were supported and restrained using a wet, high-density foam mattress, they were aerated using a reinforced deck-hose and their eyes covered. Larger sharks were handled, maintained and supported in the water in an aluminium cradle (Fig. 3). Sharks were sexed and total length (TL) measured or estimated against sling markings of known-length increments.

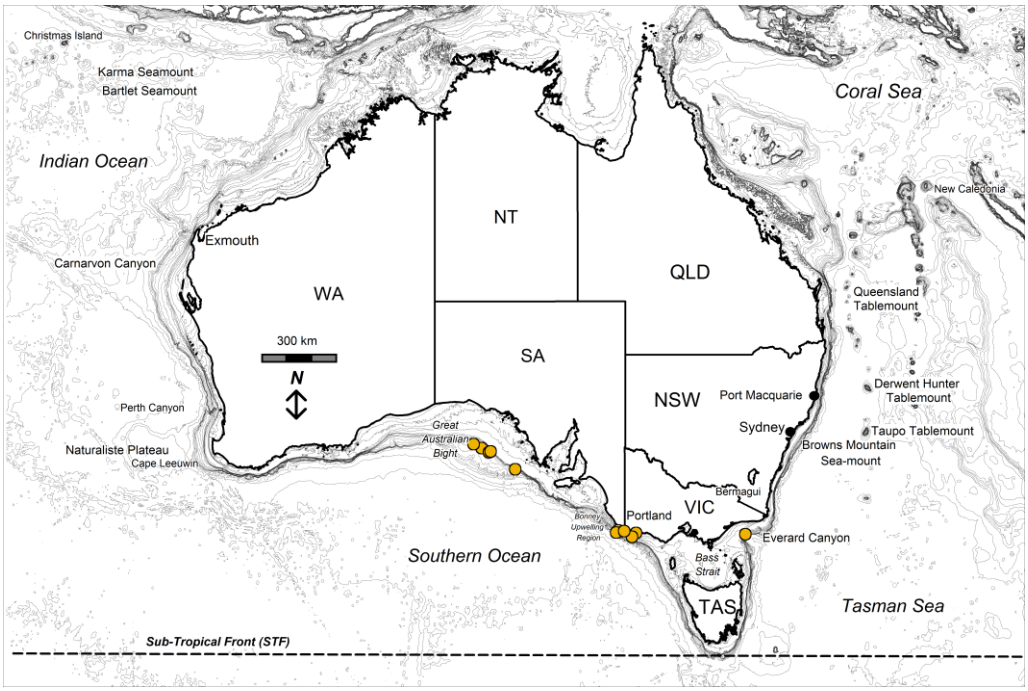

Figure 2. Locations, bathymetric and oceanographic features mentioned in the text of the report. Dashed line approximates the latitude of the Subtropical Front. Orange symbols show locations where satellite tags were deployed on shortfin makos (Bathymetry source: GeoScience Australia, 2009).

Figure 3. Cradle used to handle shortfin makos during deployment of satellite tags.

Table 1. Tag deployment statistics for satellite tracked shortfin makos between 2008 and 2013. **denotes tag still reporting at the time of report preparation.

Shark # ARGOS ID	Tag type and manufacturer	Location	Deployment date	Sex	TL (cm)	Time at liberty (days)	ARGOS position estimates cls 3–B
M1 55947	Sirtrack 202	-34.15, 132.42	11-03-08	M	170	672	1589
M2 55951	WC SPLASH	-33.96, 131.95	01-06-08	F	180	496	702
M3 52465	WC SPOT	-33.75, 131.45	30-03-09	F	180	458	1255
M4 52471	WC SPOT	-38.17, 140.55	09-05-09	M	215	262	803
M5 115559	WC Mk10A	-38.50, 141.68	17-12-12	F	260	320	1671
M6 115562	WC Mk10A	-38.49, 141.43	28-6-12	F	270	249	1372
M7 52466	WC SPLASH	-34.18, 132.41	04-06-08	F	200	469	594
M8 52478	WC SPOT	-35.07, 134.07	22-11-09	M	170	324	1279
M9 115561	WC Mk10A	-38.28, 140.43	05-05-12	M	220	320	1522
M10 55952	WC SPLASH	-34.13, 132.52	31-03-09	F	240	482	528
M11 115162**	Sirtrack 161A	-38.36, 148.57	10-7-13	F	180	311	383
M12 115159**	Sirtrack 161A	-38.36, 148.57	11-7-13	F	190	318	452
M13 52481	WC SPLASH	-38.21, 140.94	07-05-09	M	170	551	1221

Sexual maturity was assessed rapidly based on physical characteristics and size at maturity for each sex following Francis and Duffy (2005). Steps were taken to minimise handling time and mitigate associated stress during the tagging procedure. Specifically, the stainless steel tag bolts were pre-glued into each tag using Araldite™ epoxy; a modified Stanley™ bench-clamp attached to a tag shape template was used to enable holes to be drilled in the dorsal fin that accurately matched the spacing of the tag bolts. Satellite tags were attached to the first dorsal fin of each shark using only two or 3.5 mm diameter stainless steel bolts, nylex lock-nuts and washers. Lock-nuts were fastened using a cordless drill and deep socket and the total length of each animal was estimated (± 10 cm) from increments marked on the cradle. Prior to the release of each shark, bolt cutters were used to remove the hook or cut it in half in a manner that would allow loss of the hook remnant from the jaw.

Data analyses

Satellite tags transmitted signals to the low polar orbiting environmental satellite network receiver stations, which were forwarded to ARGOS centres in France and the USA (ARGOS, 2008). ARGOS position estimates were accessed using Telnet and Tera Term Pro software. Position data were downloaded in seven location classes (cls) ranging from highest to lowest between 3, 2, 1, 0, A, B and Z (no positions) with manufacturer predicted accuracies of 3 = <250 m, 2 = 250–500 m, 1 = 500–1500 m and 0–B = >1500 m, Z = no position (www.argos-system.org). ARGOS position estimation error has also been directly compared to GPS positions and the 68th percentile errors were 3 = 0.49 km, 2 = 1.01 km, 1 = 1.2 km, 0 = 4.18 km, A = 6.19 km, and B = 10.28 km (Costa et al. 2010). Positions of all classes were mapped using circular symbols in the GIS software package, MapInfo Ver. 11.5 (Mapinfo Corporation, New York) on the NOAA ETOPO1 Global relief bathymetry layer (Amante and Eakins 2009) and the Australian bathymetry and topography grid at 250 m resolution (GeoScience Australia 2009). Raw ARGOS data were pre-processed to remove extreme outliers, positions on land and those with unclassified error estimates (cls-Z). Filtering of ARGOS data were undertaken by estimating locations using a Kalman filter under a continuous-time state-space framework using the (C)orrelated (RA)andom (W)alk (L)ibrary 'CRAWL' package in R Ver. 2.15.2 (Johnson et al. 2008; R core team 2013). Locations were interpolated along each filtered track to reduce sampling bias due to irregular transmission of ARGOS location data. We calculated the mean and frequency of individual bearings from the tagging locations to each CRAWL filtered position. To establish a set of spatial scale-based movement parameters, we estimated mean rate of movement per day (ROM), minimum cumulative distance travelled based on the individual CRAWL filtered tracks and

distal displacement distances for each individual (difference between tagging location and most distant location). Statistical results were reported as mean ± standard error with 5th and 95th percentiles, unless otherwise stated.

Population genetics

Sample collection and DNA extraction

Tissue samples were obtained from 389 shortfin makos collected from commercial, recreational and game fisheries. Tissue was preserved in either 95% ethanol or salt-saturated 20% DMSO and moved to a freezer (-20°C) as soon as possible following landing. Some tissue samples were extracted from dried fins from fishery samples collected off eastern Australia. Genomic DNA was extracted using a modified salting out protocol (Sunnucks and Hales 1996). Samples were collected from six regions throughout the Southern Hemisphere (N = 275: Indo-Pacific, eastern Australia, southern Australia, Western Australia, New Zealand and South Africa; Fig. 4). Two regions from the Northern Hemisphere (n samples = 114: Northern Atlantic and Northern Indian) were also sampled to assess connectivity between hemispheres. Locations within the broad regions where samples were collected included, one off Western Australia, three in the GAB and Bonney Upwelling region, seven off eastern Australia, one in the South China Sea, one in Taiwan, one in central Indonesia, 11 off New Zealand, one unspecified location in the North East Atlantic Ocean (off Portugal), nine locations off Oman, and 27 locations off South Africa (Fig. 4). Some samples could not be amplified for both mitochondrial and microsatellite markers, thus final sample sizes for these markers differ. Table 2 shows the number of samples genotyped and included in final analyses per marker type and per region. Although samples were grouped into broad geographic regions, wherever possible there was considerable spatial coverage of sampling within regions to ensure that fine scale geographic structure could be detected if present (Fig. 4).

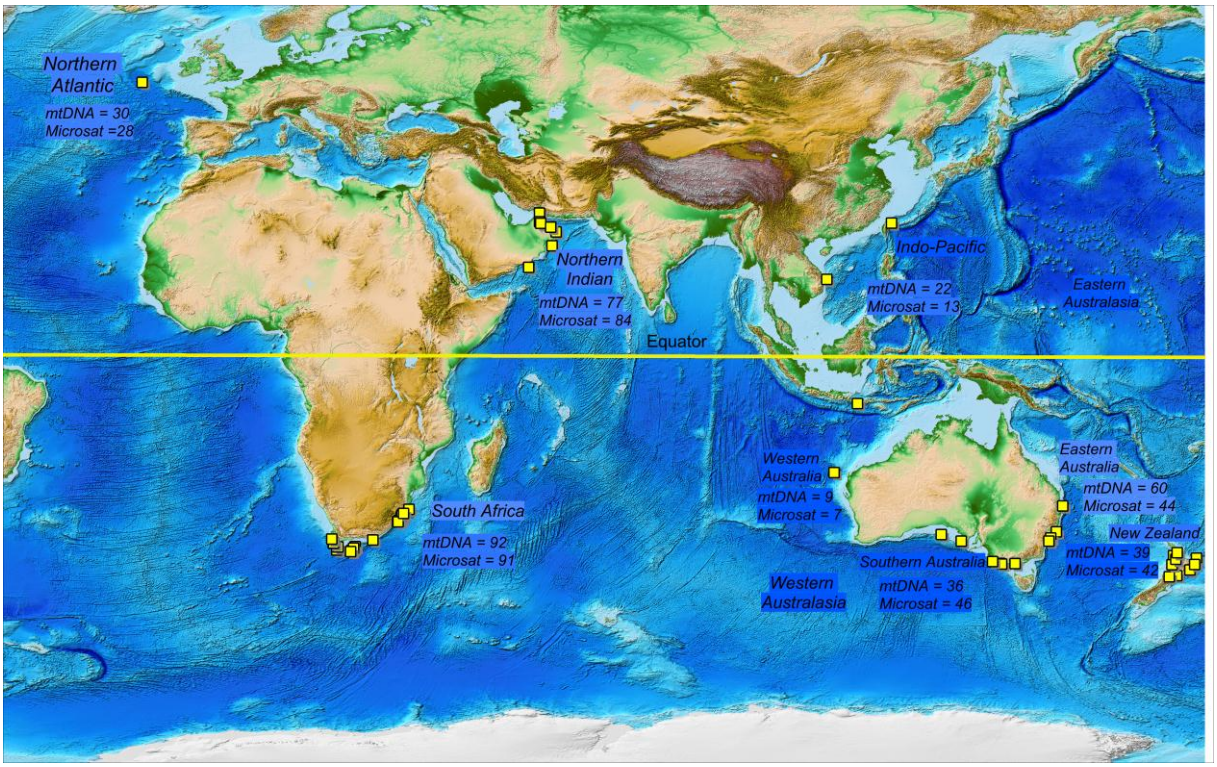

Figure 4. Regions and locations where tissue samples of shortfin makos were collected for genetic analyses in the Southern and Northern Hemispheres. Locations sampled within regions are represented by the yellow square symbols. Regions include the Northern Atlantic, South Africa, Northern Indian, Western Australia, Indo Pacific, southern and eastern Australia and New Zealand. Western and southern Australia were grouped to comprise southwestern Australasia and the Indo-Pacific and eastern Australia were grouped to comprise eastern Australia for some analyses.

Genotyping

A total of 791 base pairs of the mitochondrial DNA control region was amplified by Polymerase Chain Reaction (PCR) (Michaud et al. 2011). Purified DNA was bi-directionally sequenced using BigDye® Terminator chemistry on an ABI *3730xl* genetic analyzer (Applied Biosystems®, Life Technologies, Grand Island USA) at Retrogen Inc. Custom DNA Sequencing Facility (San Diego, USA).

Ten microsatellite loci were amplified using PCR primers described in Schrey and Heist (2002) (Iox-12, Iox-30) and Kacev et al. (unpublished data) (Iox-B3, Iox-M1, Iox-M36, Iox-M115, Iox-D123, Iox-M59, Iox-M110, Iox-M192). The forward primer of each pair was tailed with an M13 tag that was incorporated with an M13 labelled fluorescent dye during PCR cycling (Schuelke 2000). Reactions were conducted in 5 μL volumes comprising 15–30 ng template DNA, 3 mM $MgCl_2$, 1× MangoTaq™ reaction buffer, 0.1 mM each dNTP, 0.1 pmol M13 tailed forward primer, 0.3 pmol reverse primer, 0.1 pmol M13 fluorescently labeled primer, 0.5 μg bovine serum albumin and 0.25 U MangoTaq™ DNA polymerase (Bioline, Taunton USA). PCR cycling consisted of initial denaturation at 94°C followed by 'touchdown' cycling of 30 s denaturation at 94° C, 45 s annealing, and 1 min extension at 72° C. Annealing temperature began at 65° C and decreased by 2° C at each touchdown, stabilising at 57° C for 30 cycles. Products were separated on an ABI *3730xl* genetic analyzer (Applied Biosystems®, Life Technologies, Grand Island USA). Reference samples for each locus were included in all PCR programs and during capillary separation of fragments so as to ensure consistency in genotype calling. Any reactions that failed to amplify initially, or that returned ambiguous genotypes, were re-amplified in order to minimise both missing data and scoring error.

Mitochondrial DNA sequence data

DNA sequences were edited and aligned using Geneious® Pro v. 6.1.7 (Biomatters Ltd Auckland, New Zealand. Available at http://www.geneious.com). Maximum-likelihood values for different models of sequence evolution were obtained using jModelTest v. 0.1.1 (Posada 2008). According to the Corrected Akaike Information Criterion (Sugiura 1978), the Jukes and Cantor model (Jukes and Cantor 1969), without among site rate variation or invariant sites, was the most likely model of DNA substitution. Assuming this model, Arlequin v. 3.5.1.2 (Excoffier and Lischer 2010) was used to assess sequence variation through calculation of the number of observed haplotypes, as well as haplotypic and nucleotide

diversities (Nei 1987). The extent of population differentiation was explored in Arlequin using both haplotype frequency differences and genetic distance, by calculating the parameters F_{ST} and Φ_{ST}. To avoid biases associated with restricted sampling, samples from Western Australia were pooled with those from southern Australia, and samples from the Indo-Pacific were pooled with those from eastern Australia for all frequency-based analyses. An analysis of molecular variance (AMOVA) did not indicate any significant difference between these sampling locations (Western Australia vs. southern Australia: P = 0.4 and Indo-Pacific vs. eastern Australia: P = 0.7) confirming the validity of this pooling scheme. Fixation indices were tested for significance using 100,000 permutations. The null hypothesis that haplotypes are randomly distributed among sampling locations was also tested using an exact test of population differentiation (Raymond and Rousset (1995). Significance of all Pairwise comparisons was interpreted following non-parametric Bonferroni correction for inflated type 1 error that can arise when performing multiple simultaneous tests (Rice 1989). Hierarchical AMOVA was also conducted in Arlequin using both F_{ST} and Φ_{ST}, with total variance partitioned into within population, among population and among regional covariance components (Cockerham 1973). Significance was tested with 10,100 permutations. Network v. 4.6.1.1 (Fluxus Technology Ltd) was used to reconstruct genealogical relationships among haplotypes using a median-joining network (Bandelt et al. 1999) of all possible maximum parsimony trees. Epsilon was set to 0 and hyper-variable sites were down weighted. The resulting network was illustrated in Network Publisher v. 2.0.0.1 (Fluxus Technology Ltd).

Nuclear microsatellite data

Microsatellite alleles were visually inspected, binned and sized according to the GeneScan™ 500 LIZ™ size standard (Applied Biosystems®, Life Technologies, Grand Island USA) using the Third Order Least Squares algorithm in the microsatellite plugin for Geneious® Pro v6.1.7 (Biomatters Ltd Auckland, New Zealand http://www.geneious.com). Genotypes were checked for signatures of possible scoring errors due to null alleles, short allele dominance, scoring of stutter peaks and typographic error using Microchecker v. 2.2.3 (Van Oosterhout et al. 2004).

Genepop v. 4.2 (Raymond and Rousset 1995) was used to assess whether microsatellite allele frequencies conformed to expectations under models of both Hardy-Weinberg and linkage equilibrium. Again, Bonferroni corrections for multiple comparisons were applied prior to interpretation. Samples from Western Australia were again pooled with those from southern Australia, and samples from the Indo-Pacific were pooled with those from eastern

Australia for frequency-based analyses after confirming it was appropriate to do so using an AMOVA (P = 0.08 and 0.1, respectively). Genetic diversity was characterised by calculating allele frequencies, number of alleles, effective number of alleles and observed, expected and unbiased expected heterozygosities per population averaged over loci in GenAlEx v. 6.5 (Peakall and Smouse 2012). Allelic richness was calculated in FSTAT v. 2.9.3.2 (Goudet 2001) and interpreted as a standardized measure of genetic diversity that is independent of sample size.

Population differentiation based on microsatellite data was investigated in GenAlEx by calculating Nei's G_{ST}, a multiallelic expansion of Wright's F_{ST}. Hedrick's G_{ST}", which is standardized by the observed within population diversity and includes correction for bias due to sampling a small number of populations, was also calculated following Meirmans and Hedrick (2011). AMOVA was also conducted in Arlequin for microsatellite data based on both allelic (F_{ST}) and genotypic (R_{ST}) data, with total variance again being partitioned into within population, among population and among regional covariance components. Significance was assessed with 10,100 permutations.

The program Powsim 4.1 (Ryman and Palm 2006) was used to determine the alpha error and statistical power with which significant genetic differentiation could be determined using our data set. We simulated data with the characteristics of our observed data set by sampling alleles, at the average observed allele frequency across populations, from the same number of observed loci, into subpopulations of the same number and size as our observed. Subpopulations were then allowed to drift apart for a user-specified number of generations in order to attain a pre-defined level of differentiation. Statistical power was determined as the proportion of simulations for which Fisher's exact and Chi-square tests showed a significant deviation from a null hypothesis (H_0) of identical allele frequencies in all subpopulations (i.e. significant genetic differentiation). Simulations were carried out using a series of F_{ST} values ranging from 0.0005 to 0.05, and 500 replicates for each value. Statistical α (type I) error was assessed in a similar way by sampling alleles into subpopulations but omitting the drift steps (i.e. $F_{ST} = 0$) and calculating the probability of rejecting H_0 when it is true.

Population structure was further investigated by implementing model-based clustering of genotypic data using the program Structure v.2.3.4 (Pritchard et al. 2000). The model assumes *K* populations, each characterised by a set of allele frequencies at each locus. Individuals are probabilistically assigned to one or more populations based on their multilocus genotypes, assuming both Hardy-Weinberg and linkage equilibrium. Since vagility

is high in shortfin makos, allele frequencies were assumed to be similar across populations (Falush et al. 2003) and individuals were assigned using the admixture model of ancestry in which each individual may draw a fraction of its genome from each of the *K* populations. Prior information regarding sampling location was allowed to inform ancestry in order to assist clustering (Hubisz et al. 2009). Inference was conducted over 1,000,000 iterations with a burn-in phase of 100,000 iterations. Five independent runs were performed, varying *K* (the number of assumed populations) from one to the number of sampled localities. Priors for the average and standard deviation of *F* (drift within populations) were set to set 0.01 and 0.05 respectively, following Falush et al. (2003). A uniform prior (0, 10) on α (the parameter shaping the distribution of admixture proportion) was assumed. Following Evanno et al. (2005), ΔK (the second order rate of change of the log probability of the data given *K* (Ln P(X|*K*) was calculated using Structure Harvester v.0.6.93 (Earl and vonHoldt 2012) and used to guide inference regarding the number of populations represented in the data. Replicate clustering analyses were aligned using CLUMPP v. 1.1.2 (Jakobsson and Rosenberg 2007 and visualized using distruct v. 1.1 (Rosenberg 2004).

Sex-biased dispersal

We used several approaches to investigate the possibility of differential dispersal patterns among sexes. Firstly, we compared measures of population differentiation as indicated by genetic markers with different modes of inheritance (Prugnolle and de Meeus 2002). Specifically, we compared the magnitude of genetic structure as estimated by F_{ST} (calculated as detailed above) based on maternally inherited mitochondrial DNA with that based on bi-parentally inherited nuclear microsatellite data. Since the magnitude of inferred genetic structure can differ between markers with different modes of inheritance due to differences in mutation rate and/or effective population size (Chesser and Baker 1996), we also calculated F_{ST} for both marker types for two separate data sets that were separated by sex. Additionally, several analyses were conducted that are based on bi-parentally inherited markers alone. The likelihood of local assignment for each individual (i.e. the likelihood that an individual originates from its sampled location) was calculated as described in Paetkau et al. (1995) using GeneClass2 v.2.0 (Piry et al. 2004). Log transformed likelihood values were then corrected for population effects following Favre et al. (1997) resulting in corrected Assignment Indices (AI_c) averaging zero per population and with negative values that indicate lower than average probability of being born locally (migrants). AI_c values were compared for males and females with the expectation that the more dispersive sex would show a more negative frequency distribution (Favre et al. 1997; Mossman and Waser 1999). Various test statistics described by Goudet et al. (2002) were calculated to compare the

parameters F_{ST}, relatedness and the mean and variance of AI_c among males and females. Any bias was tested for significance using a randomisation approach (10,000 permutations) under the null hypothesis that males and females disperse equally, rendering these statistics independent of sex.

The probability that dispersal is unbiased by sex was estimated as the proportion of times the randomized test statistic was larger than, or equal to, the observed statistic (Goudet et al. 2002). Both one- (males assumed to be dispersive sex a priori) and two-tailed tests (no a-priori knowledge regarding dispersive sex) were conducted. All calculations and randomization tests were performed using the program FSTAT v. 2.9.3.2.

Following Banks & Peakall (2012), we compared multivariate spatial autocorrelation analyses (Smouse & Peakall 1999; Peakall et al. 2003) across sexes to look for any sex-bias in fine-scale spatial patterns of genetic structure. Pairwise genetic distances were calculated following Peakall et al. (1995) and Smouse and Peakall (1999). Autocorrelation coefficients (r, Smouse and Peakall 1999) were calculated across a range of distance classes that varied so as to incorporate comparisons within sampling localities, among adjacent localities and more distant comparisons. 95% confidence intervals (CIs) about *r* were calculated by bootstrapping (Peakall et al. 2003) and the null hypothesis of no sex-biased dispersal was accepted if there was overlap in the CI's between the sexes. The alternative hypothesis predicts that *r* values are significantly greater in the more philopatric sex. Heterogeneous autocorrelation across sexes was also assessed using single- (t^2) and multi-distance (ω) class criteria as implemented in the non-parametric heterogeneity tests described by Smouse et al. (2008). These analyses were conducted in GenAlEx and assessed for significance using 10,000 permutations and 10,000 bootstrap replicates. Analyses of sex-biased dispersal were conducted on a slightly reduced data set consisting only of individuals for whom sex data was available (85% of all individuals sampled). This data set consisted of 152 females (F) and 150 males (M) with the following breakdown across sampling locations: North Pacific 41 F: 40M, South Africa 34 F: 57 M, eastern Australia 28 F: 20 M, southern Australia 21 F: 22 M, and New Zealand 28 F: 12 M.

Contemporary effective population size

NeEstimator v. 2.0 (Do et al. 2014) was used to estimate contemporary effective population size (CN_e) based on linkage disequilibrium due to drift (Hill 1981). Linkage disequilibrium was calculated using the composite Burrows method (Weir 1979, 1996) and adjusted for bias that

may arise when sample size is small relative to true effective size (Waples 2006) and due to sampling a finite number of individuals (Waples and Do 2010). Low frequency alleles can upwardly bias CN_e estimates, while removing alleles from the analysis reduces precision. Waples and Do 2010 recommended that this bias-precision trade-off is most balanced when using allele frequency exclusion criterions (P_{crit}) within the range 0.02 to 0.05 if sample sizes are greater than 25. We therefore estimated CN_e excluding alleles with frequencies < 0.02. If a finite point estimate was not obtained, the P_{crit} value was raised by 0.01 and re-estimated. The finite point estimate that was obtained with the lowest P_{crit} value, ideally within the range of least bias-precision trade-off, was accepted as a best estimate. CN_e was estimated separately for each sampling location. Ideally however, CN_e should be estimated for genetically discrete subpopulations since population sub-structure is known to influence linkage disequilibrium and hence estimates of CN_e (Waples and England 2011). Since we detected some substructure in mtDNA for the northern Atlantic, northern Indian and possibly the South Africa sampling locations CN_e was estimated for these independently. Since there was no detectable sub-structure within the Australasian region however, samples from eastern Australia, southern Australia and New Zealand were pooled in order to estimate CN_e for the region as whole.

Results

Conventional tag-recapture

Movements patterns and time at liberty

A total of 7,328 shortfin makos were tagged and released in Australian waters between 1973 and February 2014. Of the tagged individuals, 158 (2.2% of 7,328) were recaptured between October 1977 and March 2013 (Appendix 1 shows summary statistics for recaptured individuals). Of the recaptures, 132 (83.5%) were tagged in New South Wales (NSW), 19 (12%) in Victoria, 3 (1.9%) in Tasmania, 2 (1.3%) in South Australia and 2 (1.3%) in New Zealand (Fig. 1).

A total of 72% (95/132) shortfin makos tagged off NSW were recaptured in waters adjacent to that State and 8.3% (11/132) were recaptured off Victoria (Fig. 1). Of the 19 sharks tagged off Victoria, 78.9% (15/19) were subsequently recaptured in waters adjacent to that State. There were several instances of sharks being recaptured at the tagging site. Eighteen sharks were tagged off Bermagui (NSW) and five of those were recaptured in the same location (following 41–313 days at liberty). Similarly, eight sharks were tagged at the Browns Mountain Seamount off Sydney (NSW) and five (63%) were recaptured at the same location (following 0 to 21 days at liberty).

A total of 56% of recaptures occurred following <6 months at liberty; 12% after 1–2 years, and 9.5% after 2–5 years. Notably, one shark released from Port Macquarie, NSW was recaptured off Port Hacking (NSW) following 11.98 years at liberty. Six sharks were recaptured following long-distance migrations from Australia across the: southwest Pacific Ocean to New Caledonia (n = 2), Tasman Sea to New Zealand (n = 1), Coral Sea (n = 2) to Papua New Guinea and the Solomon Islands. One individual traversed the equator to the Philippines (n = 1) (Fig. 5). Two individuals tagged off New Zealand were recaptured off NSW and two sharks tagged off eastern Tasmania were recaptured off Queensland (Fig. 5). Only one shark tagged off NSW was recaptured off Western Australia (Fig. 5)

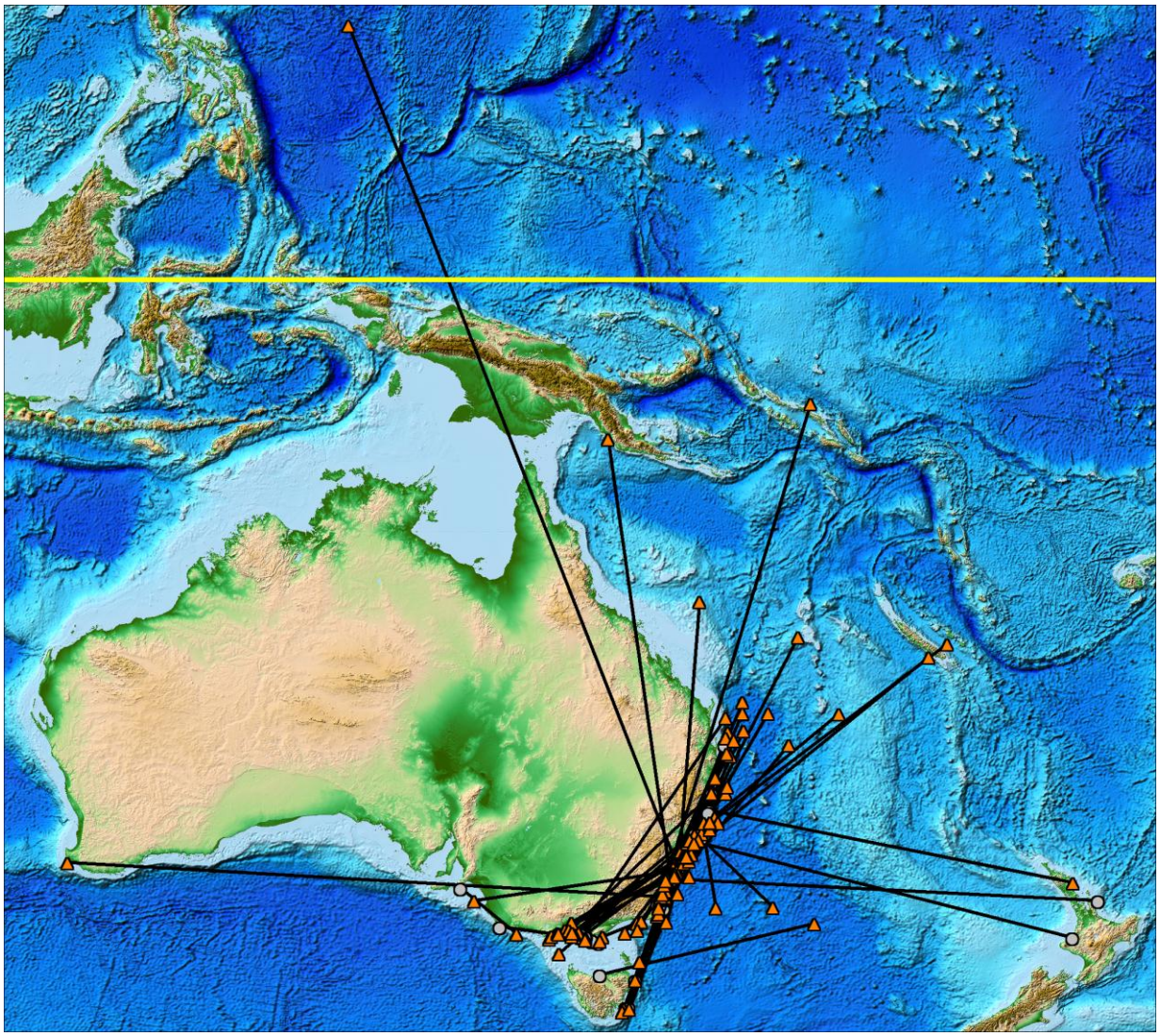

Figure 5. Map showing tagging (grey circles) and recapture locations (orange triangles) for shortfin makos. Black vectors showing minimal distances travelled. The yellow line shows the location of the equator.

Displacement distance and bearing of movements

Displacement distances between capture and release locations ranged between 0 and 5,940 km (mean = 532 ± 62.04 km, median 232.13 km, 5th percentile = 2.33 and 95th percentile = 2,050.60 km). We separated the two main tagging regions. For sharks tagged off NSW (n = 132) the displacement distances ranged between 0 and 5,940 km (mean = 513 ± 67.65 km; 5th percentile = 2.33; 95th percentile = 1,992.91 km). For sharks tagged off Victoria (n=19) the displacement distances ranged between 0.71 and 2,070.95 km (mean = 347.49 ± 139.39 km; 5th percentile = 0.71; 95th percentile = 2,070.95 km). Bearing of travel from the tagging location is shown for all sharks in Fig 6A.The mean bearing of travel by shortfin makos from the tagging locations was 150 ± 8.18°. Two directions of movement were dominant for sharks tagged off NSW (Fig. 6B). These included SSW along the east Australian shelf area of the southwest Pacific Ocean, from eastern Australia into Bass Strait, and NNE to the Coral Sea and offshore areas of the southwest Pacific Ocean. While the number of recaptures was substantially smaller for sharks tagged in Victoria (*c.f.* NSW), these individuals exhibited both westward and eastward movements (Fig. 6C).

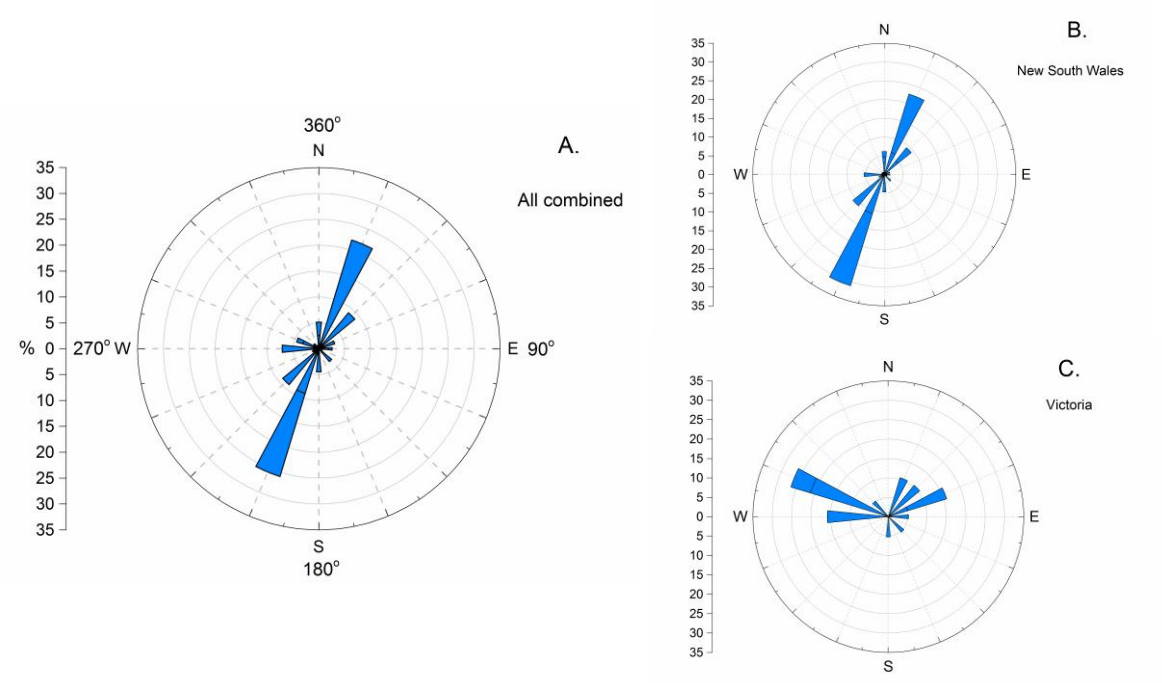

Figure 6. A. Wind-rose percentage frequency plots showing bearing of movement of shortfin mako from their tagging location based on conventional tag-recapture data (n = 158). B. Movement bearings for sharks tagged in NSW (n = 132). C. Movement bearings for sharks tagged off Victoria (n = 19).

Satellite tracking

Movement patterns and time at liberty

Satellite tags were deployed on 13 shortfin makos at locations in the GAB, Bonney Upwelling Region, south-east South Australia (SE SA) and Portland (Victoria), as well as the shelf slope submarine canyon complex in eastern Bass Strait between March 2008 and July 2013 (Fig. 2). Deployment summary statistics are provided in Table 1.

Sharks ranged in size (total length; TL) between 170 and 270 cm and comprised five males (170–220 cm) and eight females (180–270 cm). Satellite tags provided 13,371 position estimates (mean per individual = 1,028 ± 129) of ARGOS classes 3–B, over durations ranging between 249 and 672 days (mean = 418 ± 37 d), for a total of 4,603 days. Six tags provided tracks with durations >1 yr (mean = 1.1 ± 0.1 yr).

Movement summary statistics for individual shortfin makos (M1–M13) are shown in Table 2 and CRAWL model fits to the ARGOS data showing the spatial scale occupied by all individuals (M1–M13) are shown in Figure 14. Shortfin makos tagged in the GAB and Bonney Upwelling Region occupied a spatial range that extended into tropical oceanic waters (13.66° S, 155.99° E) of the southwest Pacific Ocean, to the southeast Indian (Southern Ocean) and the Indian Ocean (Figs. 7–14). Shortfin makos exhibited fidelity to the GAB from longitudes of 125–135 ˚E, near the northern extents of the Bonney Upwelling Region, in Bass Strait, shelf waters off the south coast of WA, the Subtropical Front (North-South orientated SST frontal zone at latitudes of 40–44 ˚S) (M1–M10,Figs. 7–11).

The area off SW WA between Cape Leeuwin, Naturaliste Plateau and Perth Canyon, WA demarked a point where five shortfin makos including M3, M7–9, and M13, left continental shelf waters to commence oceanic movement phases in the Indian Ocean (Figs 8, 10, 11 and 13). Four sharks including M4 (Fig. 8), M8 (Fig. 10), M10 (Fig. 11) and M13 (Fig. 13) travelled southward to the Subtropical Front. Three shortfin makos that were tagged in the GAB (M7–M9) also travelled northward via the Perth and Carnarvon Canyons to the Bartlett and Karma Sea-mounts in the NE Indian Ocean (Figs. 10 and 11). These seamounts are located ~1,260 km NW of Exmouth and ~200 km SSE of Christmas Island, Indian Ocean. These movements included the northern-most migration by a tracked shark (M9) (Fig. 11), which was 12.13 °S, 106.35 °E. One shortfin mako (M11) was tagged in the Bass Strait canyons, travelled to the Coral Sea, via the Queensland Tablemount, and returned to the tagging region via the Everard Canyon (Bass Strait) (Fig. 12). Another individual (M12) (Fig. 12) spent time in eastern Australia shelf and slope waters and then crossed the Tasman Sea to New Zealand shelf waters (37.80 °S, 174.69 °E) via a series of mid-oceanic seamounts

and rises. This was followed by movements into shelf waters and a northward migration of ~2,370 km to tropical waters located 335 km to the east of New Caledonia. This migration extended from shelf waters off Auckland and included the area ~190 km east of Norfolk Island. This individual crossed the New Hebrides Trench to the east of New Caledonia. The northern-most point of travel was 165.59 °E, 19.28 °S, located between New Caledonia and Port Villa. One shark (M13) that was tagged in the Bonney Upwelling Region off Port MacDonnell, South Australia, undertook an extensive west-ward oceanic migration across the central Indian Ocean. It sporadically moved along the Subtropical Front region (-61.08 °E, 43.96 °S) to a position (49.16 °E, 40.11 °S) ~ 200 km from the African continent and 5,800 km west of Cape Leeuwin, WA. This represented the western-most extent of movements by shortfin makos tracked in the GAB.

Estimated minimum distance travelled

A total of 195,685 km of tracking data were collected for the 13 tracked individuals. This represented an average of 15,053 ± 1,326 km per individual over an average period of 402 ± 35 days. Aggregation of the CRAWL model filtered ARGOS data showed minimal horizontal distances travelled ranged from 8,776 km in 262 days to 24,213 km in 551 days (Table 2). Minimum horizontal distances estimated using the CRAWL model did not differ significantly (Two sample t- test, t stat = 0.38, df = 14, P = 0.71) from those estimated previously using state-space models (Rogers et al. 2015).

Displacement distance and bearing of movements

Distal displacement distances from the tagging locations in the GAB, Bonney Upwelling Region, and eastern Bass Strait ranged from 1,500 to 7,520 km (mean = 3,356 ± 509.40 km). A total of 69% (9/13) of the individuals showed distal displacements of >2,000 km and 38% (5/13) of the tracks extended to areas that were >4,000 km from the tagging locations. Shortfin makos tagged in the GAB and Bonney Upwelling Region travelled within an arc from the GAB to W and NW into the Indian Ocean (mean bearing from tagging location = 228 ± 13.8°) (Table 3). Shortfin makos tagged in the eastern Bass Strait (M11 and M12) travelled within an arc to the east across the Tasman Sea and NNE to the Coral Sea (mean bearings from tagging location 173 ± 5.40°and 66 ± 1.26°, respectively) (Table 2). Mean bearing of CRAWL filtered locations from tagging locations for each individual are shown in Table 2.

Table 2. Details of mean bearing of the track per individual from the tagging location to each CRAWL filtered position, mean rate of movement (ROM), minimum distance travelled and distal displacement distance.

Shark #	ARGOS ID Frequency	Mean bearing	Mean rate of movement (ROM, km. d^{-1})	Minimum distance travelled (km)	Distal displacement distance (km)
M1	55947	281 ± 1.22	23	15,672	1,834
M2	55951	252 ± 4.70	23	11,299	1,854
M3	52465	175 ± 2.53	38	17,545	2,560
M4	52471	243 ± 1.00	34	8,776	1,500
M5	115559	290 ± 0.30	39	12,541	2,074
M6	115562	287 ± 1.57	45	11,148	1,297
M7	52466	248 ± 3.02	46	21,586	4,256
M8	52478	210 ± 2.17	50	14,693	4,280
M9	115561	288 ± 1.05	53	16,899	4,942
M10	55952	153 ± 3.47	41	19,964	5,130
M11	115162	173 ± 5.40	34	10,511	2,346
M12	115159	66 ± 1.26	34	10,838	2,730
M13	52481	275 ± 0.28	44	24,213	7,520

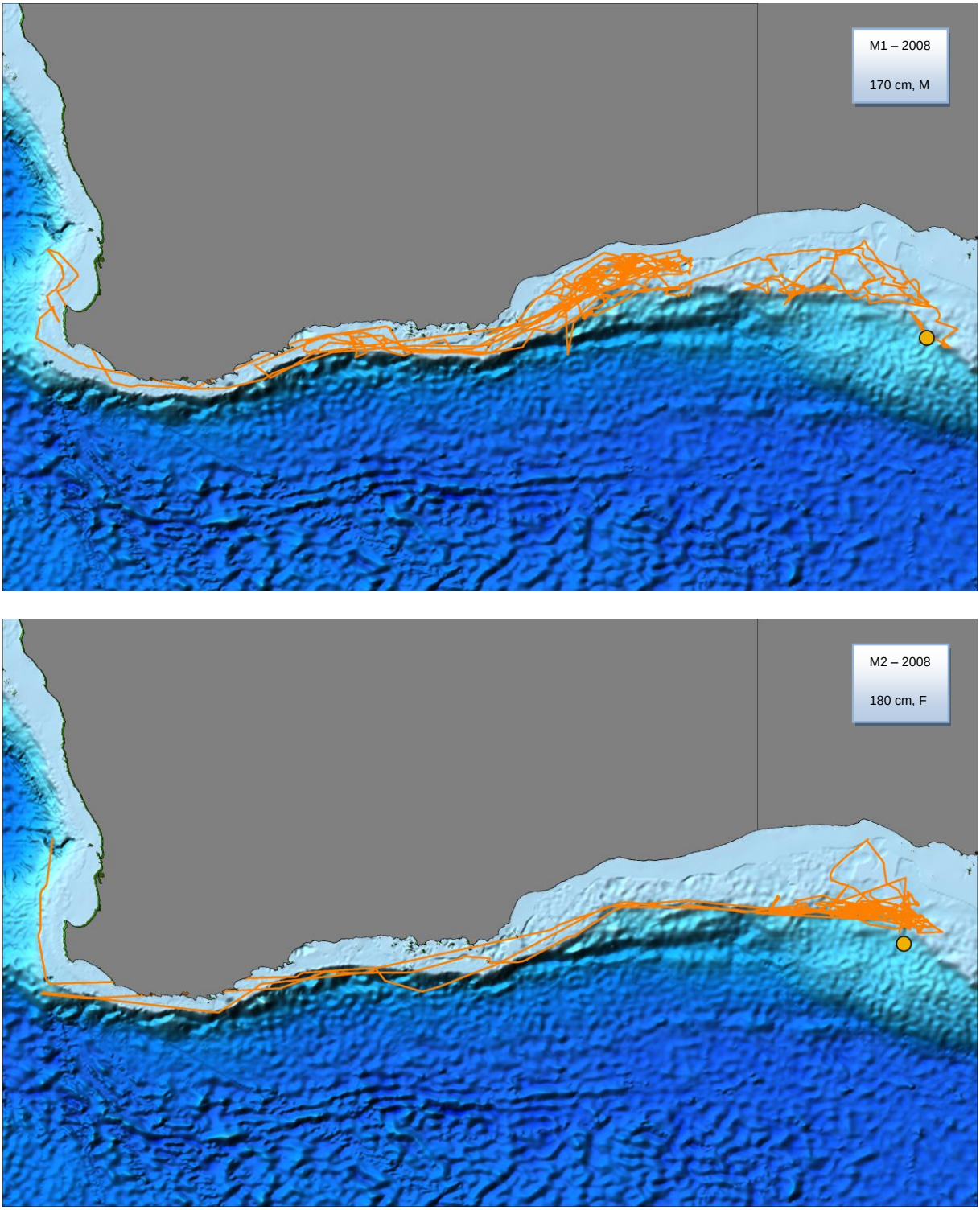

Figure 7. CRAWL model fits to ARGOS data showed the spatial range occupied by shortfin makos, M1 and M2 in the GAB and Indian Ocean. The orange symbol indicates the deployment location.

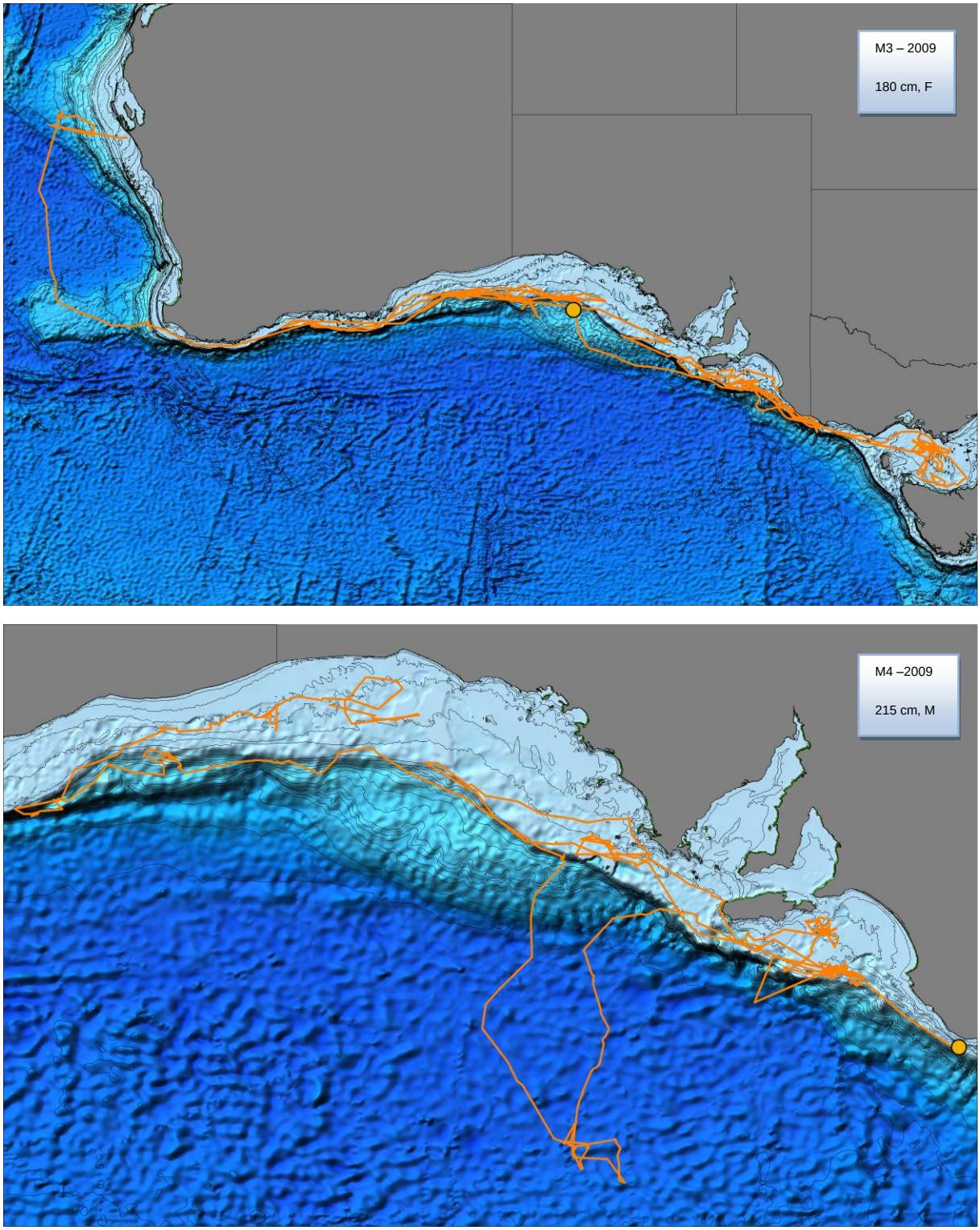

Figure 8. CRAWL model fits to ARGOS data showing the spatial scale occupied by shortfin makos, M3 and M4 in the GAB, Bonney Upwelling Region, Subtropical Front, Indian Ocean and Bass Strait. The orange symbol indicates the deployment location.

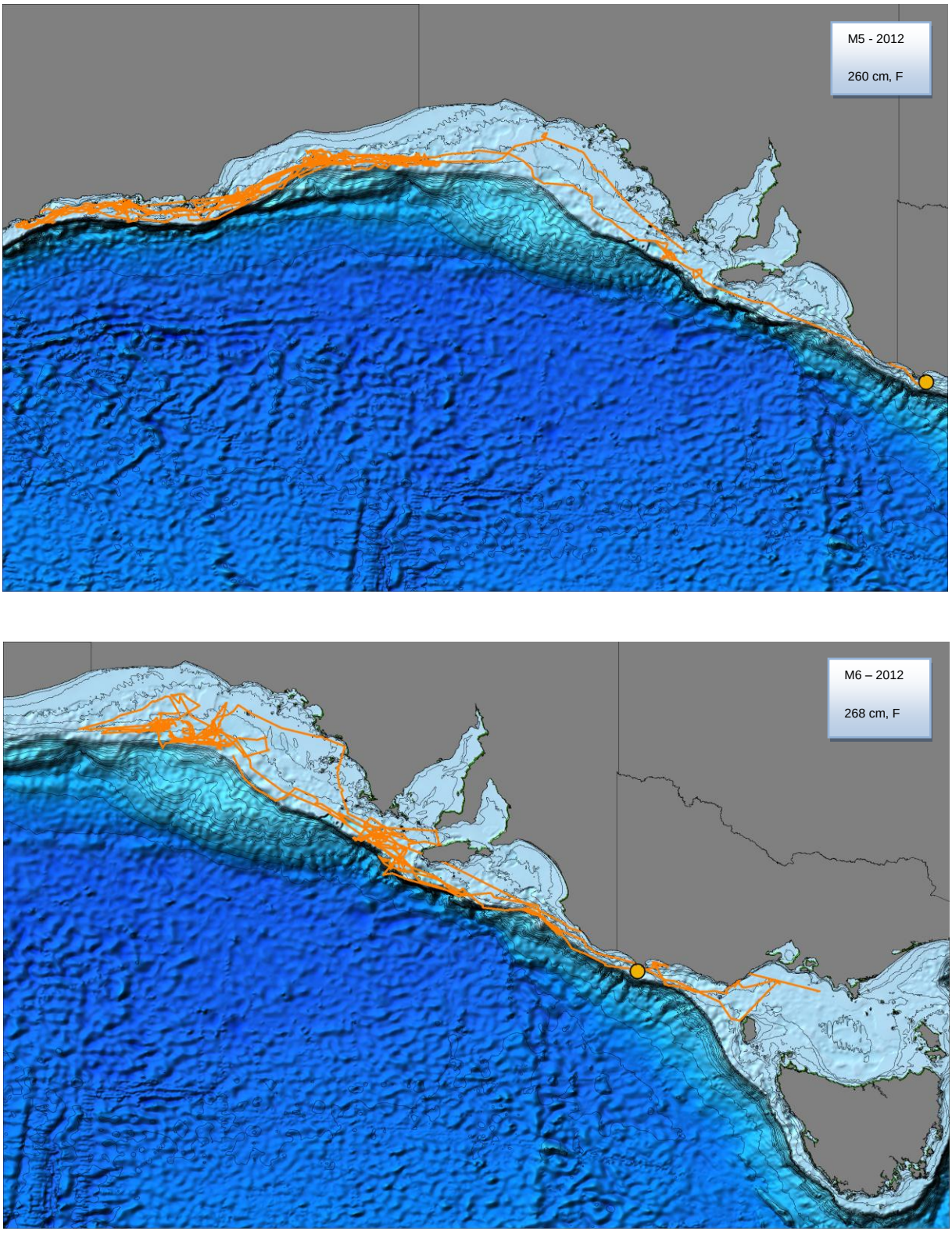

Figure 9. CRAWL model fits to ARGOS data showing the spatial scale occupied by shortfin makos, M5 and M6 in the GAB, Bonney Upwelling Region, and Bass Strait. The orange symbol indicates the deployment location.

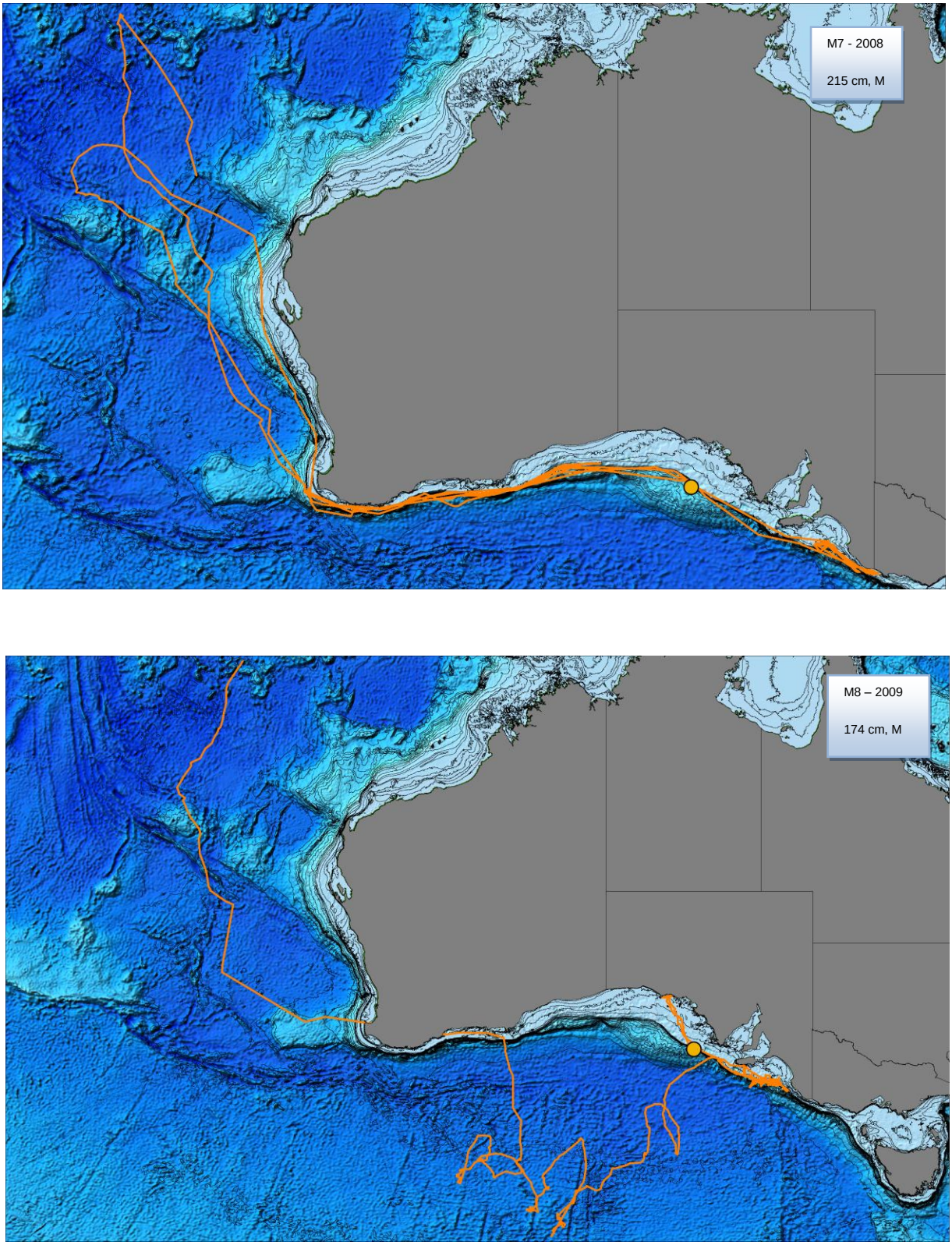

Figure 10. CRAWL model fits to ARGOS data showing the spatial scale occupied by shortfin makos, M7 and M8 in the GAB, Bonney Upwelling Region, Subtropical Front, and Indian Ocean. The orange symbol indicates the deployment location.

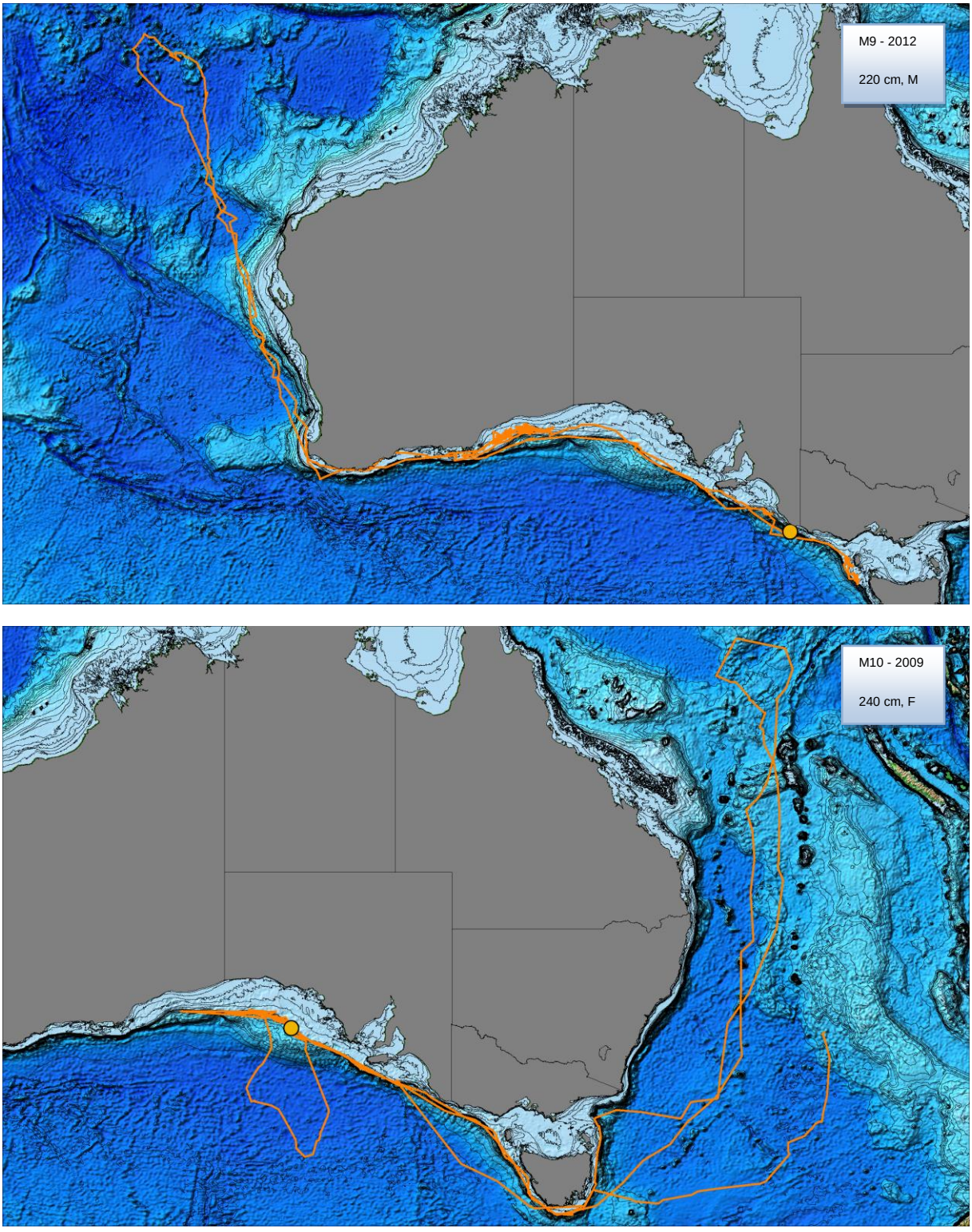

Figure 11. CRAWL model fits to ARGOS data showing the spatial scale occupied by shortfin makos, M9 and M10 in the GAB, Bonney Upwelling Region, Subtropical Front, Tasman Sea, Coral Sea, SW Pacific and Indian Ocean. The orange symbol indicates the deployment location.

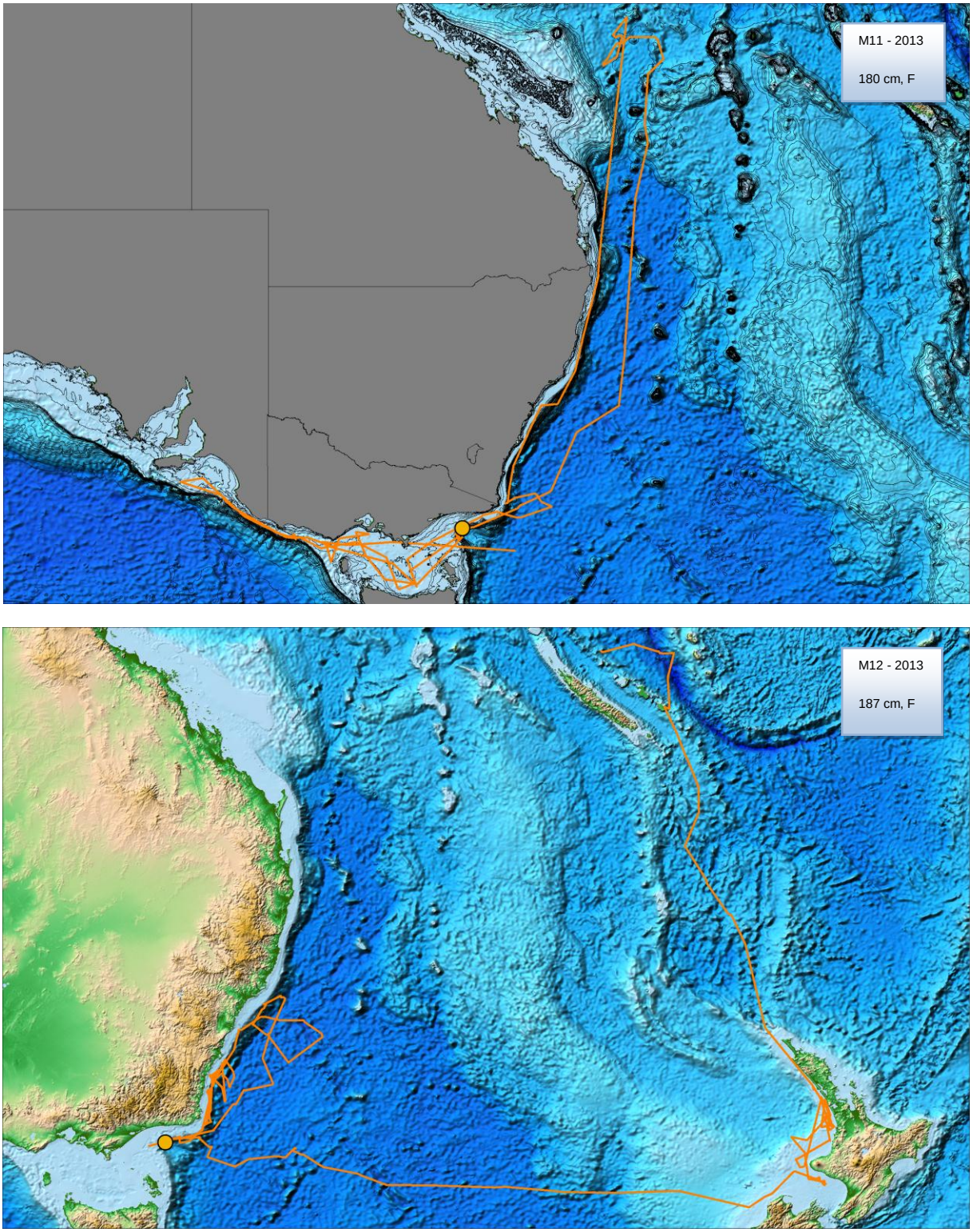

Figure 12. CRAWL model fits to ARGOS data showing the spatial scale occupied by shortfin makos, M11 and M12 in the Bonney Upwelling Region, Tasman Sea, Coral Sea, SW Pacific, New Zealand shelf waters and New Caledonia. The orange symbol indicates the deployment location.

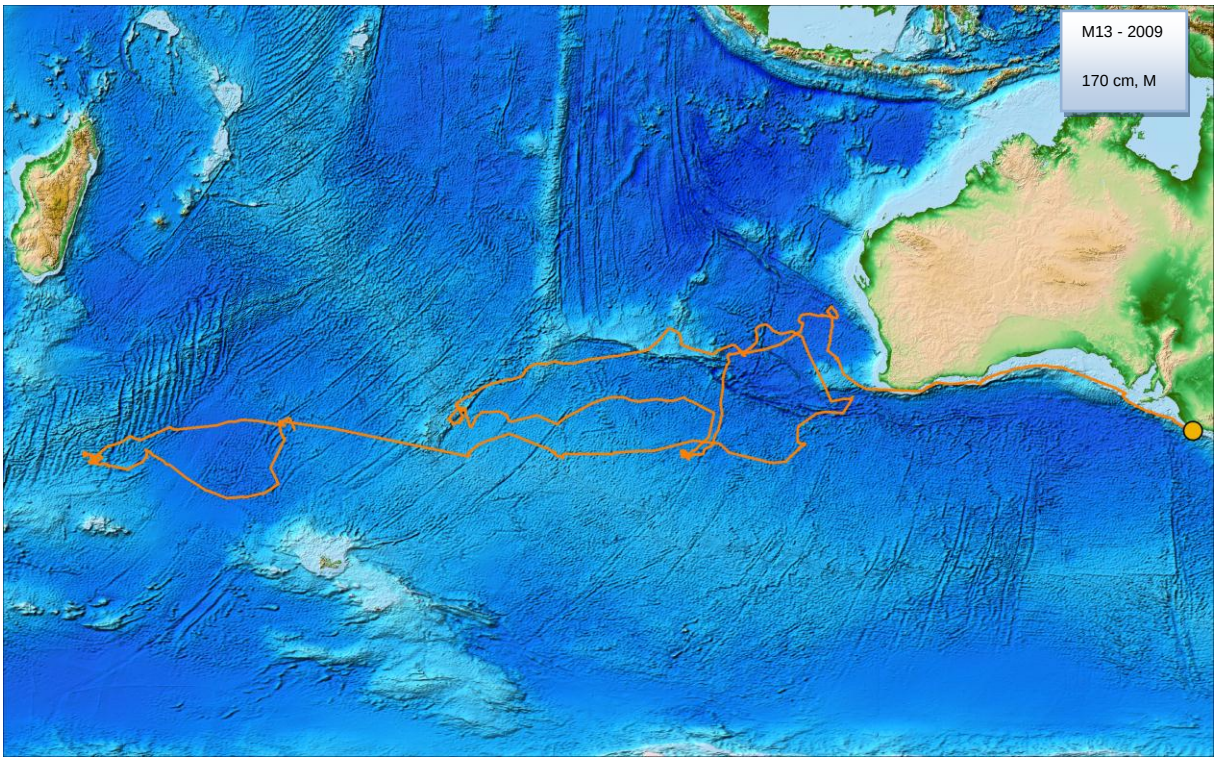

Figure 13. CRAWL model fit to ARGOS data showing the spatial scale occupied by shortfin mako M13 from the Bonney Upwelling Region across the GAB and during a trans-Indian Ocean migration. The orange symbol indicates the deployment location.

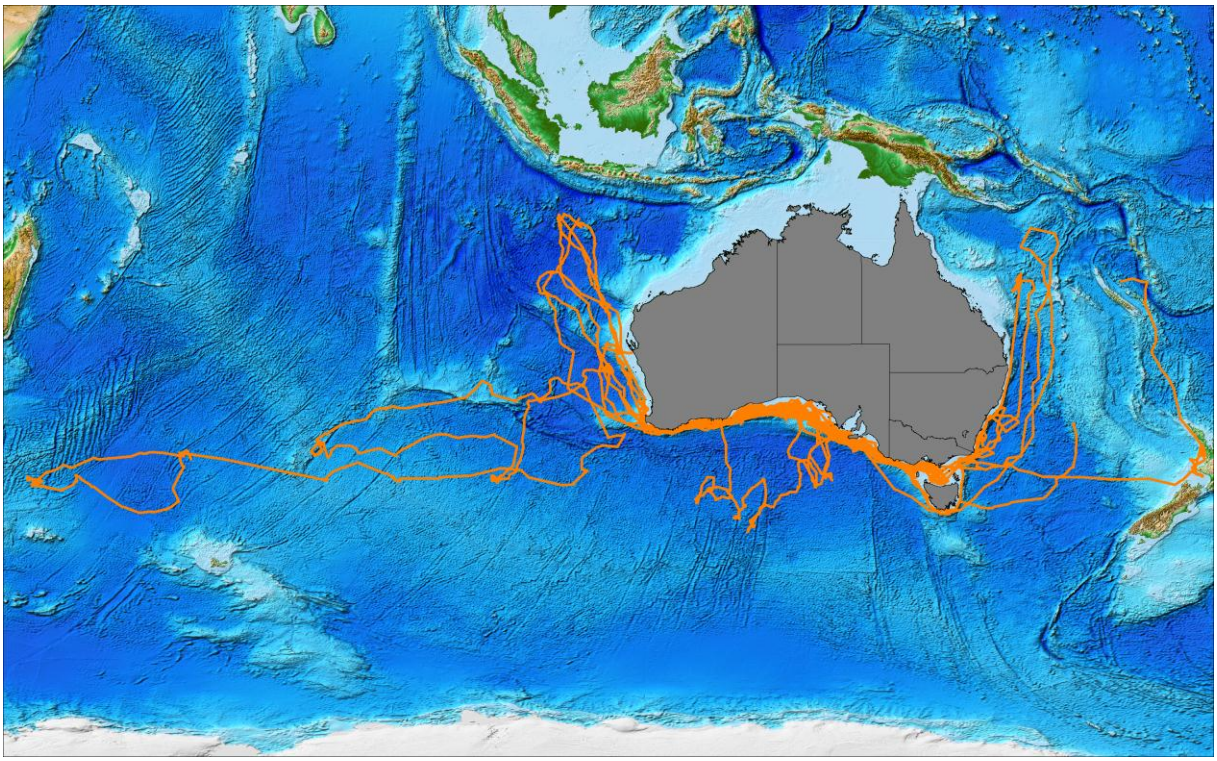

Figure 14. CRAWL model fit to ARGOS data showing the spatial scale occupied by all shortfin makos M1–13 combined between 2008 and 2014.

Population genetics

Mitochondrial DNA sequence data - summary statistics and genetic diversity

The mitochondrial control region was sequenced for 365 shortfin makos resulting in 48 unique haplotypes, defined by 31 polymorphic sites (Table 3), which were sampled across eight broad geographic regions encompassing 62 individual locations (Fig. 4).

Overall, haplotypic diversity was 0.894 ± 0.013 while nucleotide diversity was low at 0.004 ± 0.003. Population level measures of diversity, including sample size, number of haplotypes, haplotypic and nucleotide diversity are shown in Table 3. Haplotypic and nucleotide diversities per population ranged from 0.574 ± 0.067 to 0.940 ± 0.020 and 0.002 ± 0.001 to 0.005 ± 0.003, respectively, with averages of 0.875 ± 0.040 and 0.004 ± 0.002, respectively.

Mitochondrial DNA sequence data - Genealogical relationships

The haplotype network (Fig. 15) is dominated by a single, abundant haplotype that was sampled in ~30% (108/365) of individuals, and from all locations. The network is diverse and characterised by closely related haplotypes with most separated by only a single substitution. Three substitutions was the maximum that was required to link any two haplotypes parsimoniously. Although haplotype frequencies differ across sampling sites, the network does not indicate any strong geographic partitioning of haplotypes. One third of haplotypes (16/48) were unique to a single location, 13 of which were singletons (were only sampled once), however most haplotypes are found at several, often geographically disparate locations.

Table 3. Genetic diversity at mitochondrial DNA and nuclear microsatellite markers. Data were obtained from *n* number of individuals. Mitochondrial diversity is summarised by the number of haplotypes (*N*), haplotypic diversity (*h*) and nucleotide diversity (π). Microsatellite diversity is summarised by the number of alleles per locus (*N*), effective number of alleles (N_e), allelic richness (A_r), observed heterozygosity (H_o), expected heterozygosity (H_e) and unbiased expected heterozygosity (uH_e). All estimates for microsatellite data are averaged over loci.

	Mitochondrial DNA				**Microsatellites**						
Sampling region	***n***	***N***	***h***	***π***	***n***	***N***	N_e	A_r	H_o	H_e	uH_e
Northern Atlantic	30	11	0.846	0.005	28	12.500	7.873	6.683	0.828	0.815	0.830
Northern Indian (Oman)	77	16	0.574	0.002	84	15.600	8.925	6.842	0.856	0.842	0.848
South Africa	92	24	0.911	0.004	91	15.800	8.991	6.789	0.852	0.845	0.850
Indo-Pacific (Indonesia/Taiwan)	22	14	0.918	0.004	13	9.200	6.543	6.657	0.839	0.791	0.826
Eastern Australia	60	28	0.940	0.005	44	14.500	9.336	6.924	0.862	0.844	0.853
Southern Australia	36	16	0.927	0.005	46	14.100	9.165	6.846	0.813	0.830	0.839
Western Australia	9	8	0.972	0.003	7	7.100	5.272	6.699	0.748	0.742	0.802
New Zealand	39	18	0.912	0.005	42	15.500	9.420	7.166	0.838	0.855	0.865
Total	365	48	0.894	0.004	355	13.038	8.191	6.902	0.839	0.838	0.847

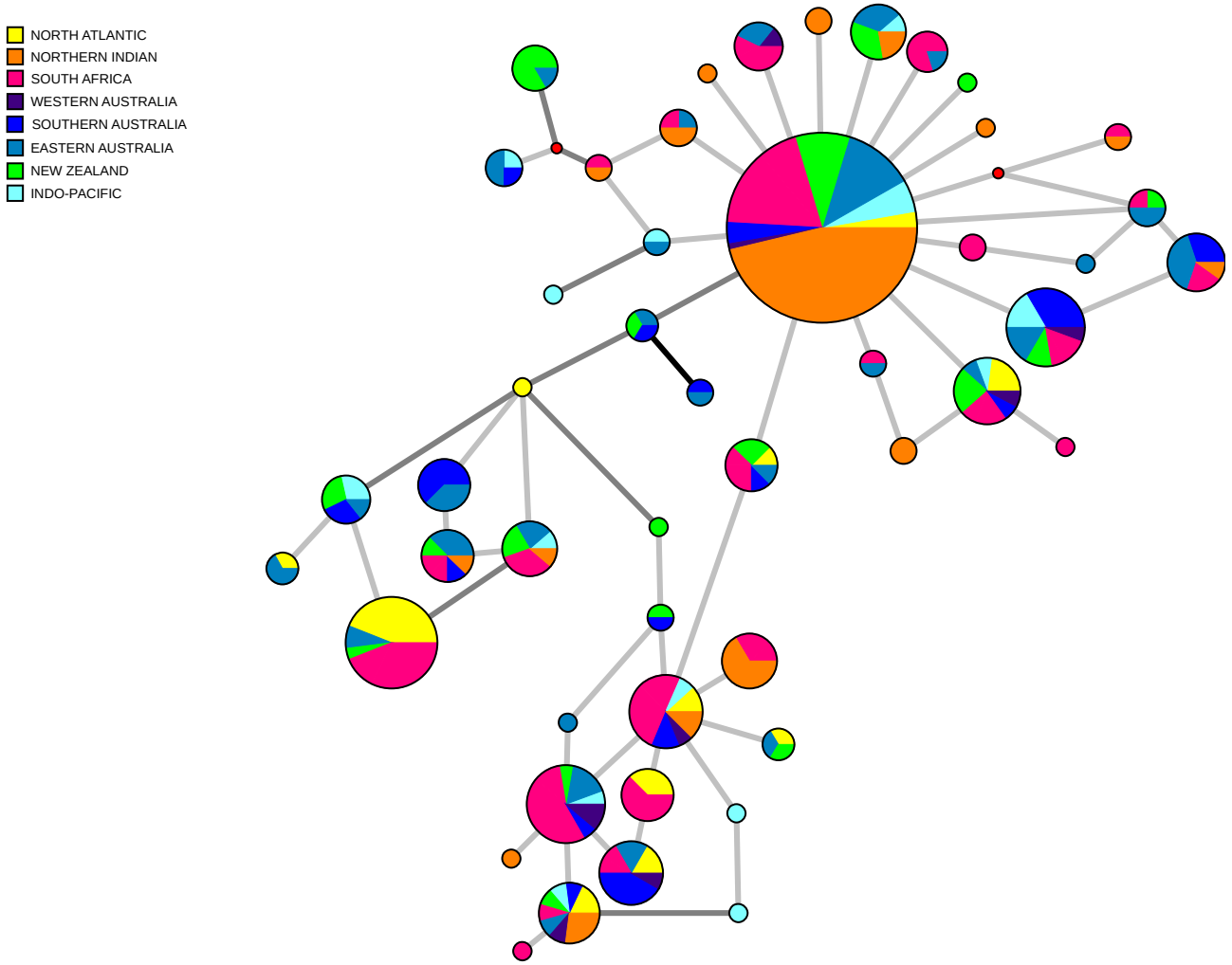

Figure 15. Median joining network of 10 equally parsimonious trees. Each haplotype is shown as a circle, the area of which is proportional to the haplotypes frequency in the data set. Small solid red circles are intermediate states that were not observed in the data set. Light grey, dark grey and black lines represent 1, 2 and 3 mutational steps between haplotypes, respectively.

Mitochondrial DNA sequence data – population differentiation

Pairwise fixation indices provide an indication of population differentiation, with an upper ceiling of one that indicates complete differentiation (fixation for different alleles). Measures of population differentiation may be based solely on differences in haplotype frequencies among locations (F_{ST}). Alternatively, they may also incorporate additional information about nucleotide diversity as an indication of haplotype similarity (Φ_{ST}). Both measures may be susceptible to different biases depending on the proportion and patterns of shared diversity among populations. It has thus become common practice to report both metrics (Bird et al. 2011, Holsinger et al. 2009). Values of F_{ST} and Φ_{ST} were low to moderate. Both Northern Hemisphere locations (Northern Atlantic and Northern Indian Ocean) were significantly differentiated from all Southern Hemisphere localities based on F_{ST}, Φ_{ST} and exact tests of population differentiation (Table 4). Weak but significant differentiation was detected between South Africa and southern Australia based on F_{ST}, but not between South Africa and any other Australasian location (eastern Australia or New Zealand.). This result was not corroborated by Φ_{ST} estimates in which South Africa was not significantly differentiated from any of the Australasian locations (southern Australia, eastern Australia or New Zealand.). Conversely, South Africa was significantly differentiated from all other locations based on exact tests of population differentiation (Table 4). Within Australasia, significant differentiation was detected between southern Australia and New Zealand based on F_{ST}, Φ_{ST} and exact tests of population differentiation (Table 4).

Population differentiation was also assessed using Analysis of Molecular Variance (AMOVA). Interpretations presented herein are based on Φ_{ST}, but results from AMOVA based on F_{ST} were qualitatively similar. The global Φ_{ST} estimate was low (Φ_{ST} = 0.080), but significant (P = 0.000). Total variation in the data set could be separated into five major regions: the northern Atlantic, the northern Indian, South Africa, western Australasia (western and southern Australia) and eastern Australasia (Indo-Pacific, eastern Australia and New Zealand). While most of the variation in the data set was found within populations (91.5%, F_{ST} = 0.085, P = 0.000), among region variance accounted for a significant 8.2% (F_{CT} = 0.082, P = 0.009) of the total variation. Partitioning among regions was weaker (2.0%) when considering only South Africa and the Australasian locations (South Africa vs. western Australasia (western and southern Australia) vs. eastern Australasia (Indo-Pacific, eastern Australia and New Zealand)), although still significant (F_{CT} = 0.020, P = 0.032). However, the among-region variance component was not significant (F_{CT} = -0.006, P = 0.666) in an AMOVA on data in which all Australasian locations were grouped together (South Africa vs. western, southern and eastern Australia, Indo-Pacific and New Zealand). The global Φ_{ST} was non-significant

(1.63% of total variation, Φ_{ST} = 0.016, P=0.06) when considering all sampling locations in Australasia (Indo-Pacific, eastern Australia, western Australia, southern Australia and New Zealand). Similarly, there was no significant difference (3.5% of total variation, Φ_{CT} = 0.035, P = 0.100) between regions when partitioning the data set into eastern (Indo-Pacific, eastern Australia, New Zealand) and western (western Australia, southern Australia) Australasia.

Nuclear microsatellite DNA data - summary statistics and genetic diversity

Ten microsatellite loci were genotyped for 355 shortfin makos sampled across the eight broad geographic locations (Fig. 4, Table 3). There was no evidence of scoring errors due to short allele dominance or typographic error. Two loci, Iox-12 and Iox-D123, showed evidence of null alleles. These were in low frequency (<10% based on all estimators; Van Oosterhout et al. 2004), detected in samples from a single location and due to significant excess of homozygotes observed in two and one genotype classes respectively. Following Bonferroni correction, all loci and populations conformed to expectations under a model of Hardy-Weinberg equilibrium. These loci therefore, were not excluded from further analyses. Linkage disequilibrium was detected for three locus pairs (Iox-M110 and Iox-B3, Iox-12 and Iox-30, Iox-M192 and Iox-D123), however these results too could be accounted for by significant comparisons in single sampling locations and so were not excluded from final analyses.

Genetic diversity at microsatellite loci was moderate to high. The number of alleles per locus (*N*) ranged between 9 and 30, with means per population ranging from 7.10 to 15.80 (Table 3). The effective number of alleles per locus ranged between 5.27 and 9.42 across populations. Allelic richness was relatively consistent across populations, ranging between 6.66 and 7.17. Unbiased expected heterozygosity was also relatively consistent across populations, ranging between 0.80 and 0.87. Observed heterozygosity ranged from 0.75 to 0.86 (Table3). Lower sample sizes from western Australia and the Indo-Pacific resulted in slightly reduced diversity (Table 3) and greater divergence between expected and observed heterozygosities.

Table 4. Pairwise measures of population differentiation based on mitochondrial DNA. F_{ST} values are below the diagonal and Φ_{ST} values are above the diagonal. Significance was assessed using a non-parametric permutation approach. * indicates a comparison that represents significant differentiation at the 95% confidence level following Bonferroni correction. Exact tests of population differentiation were also conducted. λ in the lower diagonal of the matrix indicates resultant significant comparisons.

	northern Atlantic	**northern Indian**	**South Africa**	**eastern Australia**	**southern Australia**	**New Zealand**
northern Atlantic		0.396*	0.114*	0.139*	0.147*	0.152*
northern Indian	0.257λ*		0.100*	0.073*	0.186*	0.077*
South Africa	0.041λ*	0.119λ*		0.004	0.027	0.020
eastern Australia	0.072λ*	0.109λ*	0.007λ		0.021	0.002
southern Australia	0.080λ*	0.197λ*	0.029λ*	0.011		0.063*
New Zealand	0.077λ*	0.115λ*	0.016λ	-0.002	0.032 λ*	

Nuclear microsatellite DNA data – population differentiation

As was the case when estimating population differentiation based on mitochondrial DNA, measures of population differentiation based on microsatellite data may be based on allelic frequency differences among locations (F_{ST}) or also incorporate information about the evolutionary distance between alleles (R_{ST}). The majority of the variation in the microsatellite data occurred within populations (99.9%) and the global multilocus F_{ST} (considering samples from all locations across both hemispheres) estimate was low (F_{ST} = 0.002), but marginally significant (P = 0.020). Individual locus F_{ST} estimates were low, ranging between -0.003 and 0.009. The significant multilocus F_{ST} result was driven by significant F_{ST} values at just two of the 10 loci (Iox-M192, F_{ST} = 0.005, P = 0.004; Iox-M36 F_{ST} = 0.009, P = 0.001). The multilocus R_{ST} estimate was also low (R_{ST} = 0.002) but non-significant (P = 0.250).

The same population pairwise comparisons as were performed for the mitochondrial data were also made for the microsatellite data. Somewhat contrasting the results from mtDNA where significant differentiation was detected when comparing northern and southern hemisphere, for the microsatellite data all population pairwise estimates of G_{ST} and G_{ST}'' were low and only a single pairwise comparison, that between South Africa and southern Australia, indicated significant differentiation (Table 5). Significant divergence between South Africa and southern Australia however, was not supported by AMOVA of microsatellite data. When partitioning the data by region, ie. northern Atlantic vs. northern Indian vs. South Africa vs. Australasia (eastern Australia, southern Australia and New Zealand grouped together), the among-region variance component was non-significant, accounting for < 1% of total variation in the dataset (F_{CT} = 0.002, P = 0.196). Likewise, the among-population component was also non-significant (F_{SC} = 0.001, P = 0.623). The majority (99.8%) of variation was found within populations. This result was consistent across AMOVA analyses based on allelic (F_{ST}) and genotypic (R_{ST}) data, thus only the results from the allelic-based analysis are presented.

Fig. 16 shows the statistical power of our microsatellite data, given the sample sizes, number of loci, and average allele frequencies characterizing our empirical data set, to detect various levels of true population differentiation (F_{ST}). Our data set has good statistical power with a 100% probability of detecting a true F_{ST} as low as 0.0025 and a high probability (65 – 70%) of detecting an F_{ST} as low as 0.001. The alpha error (corresponding to the probability of obtaining false significances when the true F_{ST} = 0) was ≤ 5%.

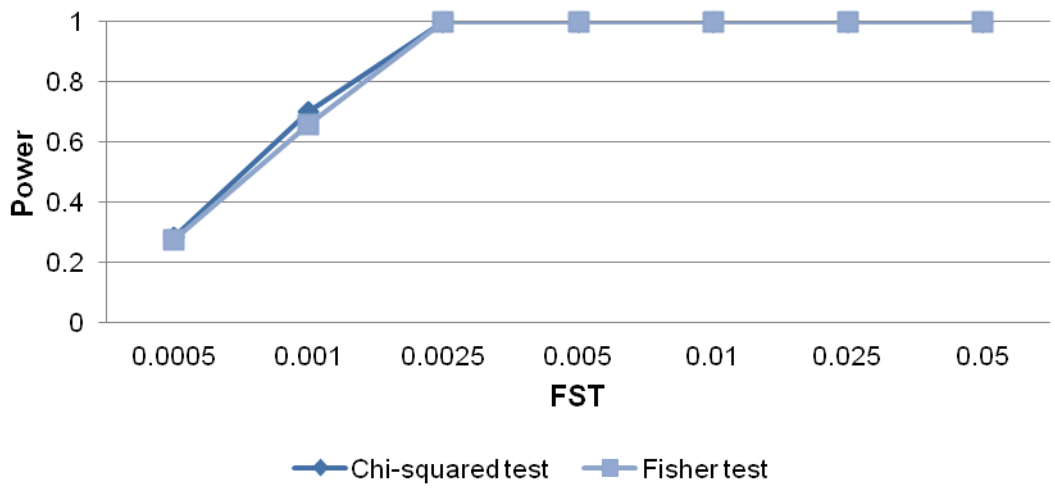

Figure 16. Statistical power of microsatellite data to detect various levels of true population differentiation (F_{ST}).

Model-based clustering analyses performed in Structure also indicated high connectivity among all sampling locations (Fig. 17). The mean estimated log probability of the data was highest for K = 1, while the modal value of the distribution of ΔK (Evanno et al. 2005) suggested that 2 clusters could be identified in the data. The ΔK metric cannot be estimated for K=1 and so panmixia could not be assessed as a possible scenario using this approach. Further, this metric does not take into account the scale of ΔK. We observed values that were two orders of magnitude smaller than is typically observed for cases of real structure. In addition, the bar plots of the estimated cluster membership coefficients for each individual did not show support for K = 2. Although subtle differences in allele frequencies were detected across sampling sites, individuals were assigned in similar proportions to each of the two clusters (Fig. 17). There was considerable variance in parameter estimates across runs for each individual K, which indicates non-convergence of the analysis despite running for a sufficient length of time. Together these observations are consistent with there being little to no signal of population structure in the data.

Table 5. Pairwise measures of population differentiation based on nuclear microsatellite data. G_{ST} values are below the diagonal and G_{ST}'' values are above the diagonal. Significance was assessed using a non-parametric permutation approach. Populations that were significantly differentiated at the 95% confidence level, following Bonferroni correction for multiple comparisons, are indicated by an *.

	northern Atlantic	**northern Indian**	**South Africa**	**eastern Australia**	**southern Australia**	**New Zealand**
northern Atlantic		0.017	0.025	0.008	0.031	0.017
northern Indian	0.001		0.016	0.007	0.015	0.015
South Africa	0.002	0.001		0.016	0.043*	0.011
eastern Australia	0.001	0.001	0.001		0.000	-0.005
southern Australia	0.003	0.001	0.003*	0.000		0.025
New Zealand	0.001	0.001	0.001	0.000	0.002	

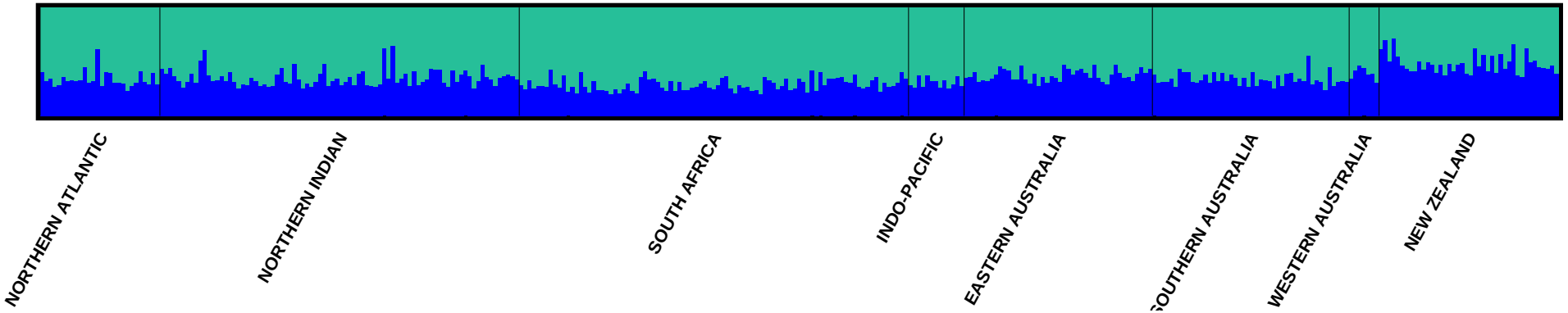

Figure 17. Plot of the estimated membership coefficients for each individual in each of two genetic clusters (K=2), as inferred using the program *Structure*. Each individual is represented by a vertical column. Individuals are grouped by sampling site.

Nuclear microsatellite DNA data – sex-biased dispersal

Pairwise fixation indices were higher between sampling locations for mitochondrial DNA markers than for microsatellite markers, however this is expected given the four-fold lower effective population size of mitochondrial DNA relative to nuclear DNA. There were no obvious differences in patterns of differentiation when comparing males and females of either marker type (Table 6). Fixation indices for both marker types were generally low in both sexes, however Pairwise estimates of Φ_{ST} were usually (although not always) higher in females than in males for mitochondrial DNA (Table 6a). This pattern was not observed in the microsatellite data (Table 6b). F_{ST} and relatedness based on microsatellite markers were both low overall, but higher in females (F_{ST} = 0.003, r = 0.006, respectively) than in males (F_{ST} = 0.000, r = -0.001). This difference bordered on significance (P = ~ 0.050), however the observed values of the test statistics for these parameters were within the range of the null distribution that dispersal is independent of sex (Figure 18). F_{IS} was higher in males (F_{IS} = 0.009) than females (F_{IS} = 0.001) but this difference was not significant (P = 0.203, Table 7, Figure 18). Corrected assignment (AI_c) values ranged between −8.01 and 7.94 for males and −6.23 and 10.78 for females (Figure 18). Mean AI_c was higher for females (0.190) than for males (-0.191), however this difference was not statistically significant (P = 0.158, Table 7). Variance of AI_c was also higher for females (11.865) than for males (9.112) but this difference was also not significant (P = 0.838, Table 7). The observed value of the test statistics for both the mean and variance of AI_c fell within the range of the null distribution representing the probability that dispersal is unbiased by sex (Fig. 18). The frequency distributions of AI_c values for males and females were largely overlapping (Fig. 18) and both sexes showed a similar proportion of values in the negative portion of the distribution (54% for females and 52% for males).

Spatial patterns of genetic structure were similar across sexes (Fig. 19). The null hypothesis of correlogram homogeneity across sexes was accepted in all three heterogeneity tests. The male and female 95% bootstrap confidence intervals about r overlapped in all distance classes (Fig. 19). The single distance class t^2 tests were all non-significant (Table 8), as was the multi-class ω test of overall correlogram heterogeneity (ω = 6.226, P = 0.411). Significant departure from the null of hypothesis of randomly distributed genotypes in space was detected for both males and females with low but significant positive autocorrelation among genotypes detected at small (100 km) distance classes (r_{MALES} = 0.009, P = 0.000; $r_{FEMALES}$ = 0.008, P = 0.003 for the first distance class; ω_{MALES} = 59.401, P = 0.000; $\omega_{FEMALES}$ = 33.078, P = 0.007; Table 8; Fig. 19).

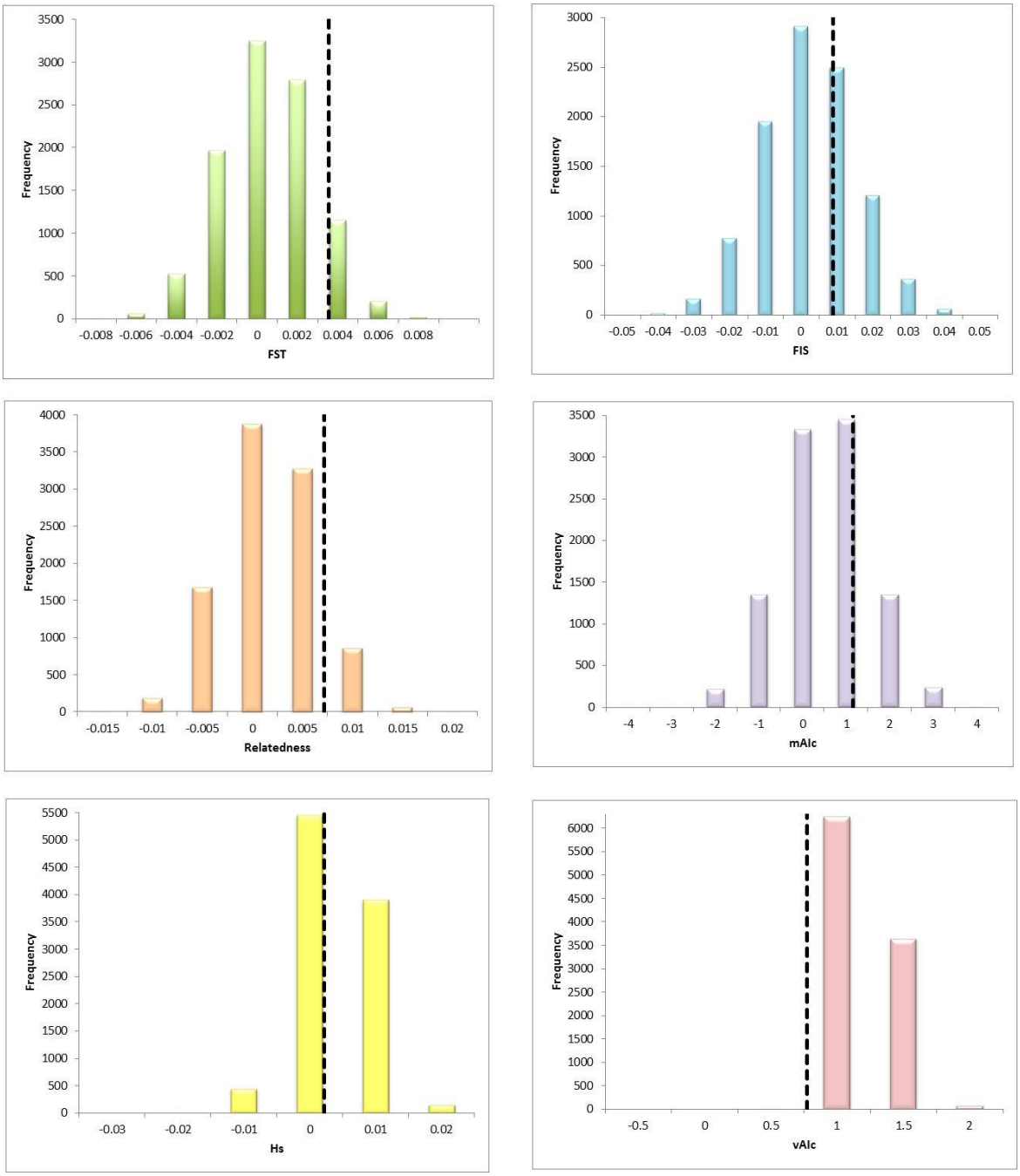

Figure 18. Distribution of the randomized test statistics (F_{st}, F_{IS}, relatedness, r, $m\text{AI}_c$, $v\text{AI}_c$, $A\text{I}_c$) for detecting sex biased dispersal and frequency distribution of assignment indices for males and females. The vertical dashed line corresponds to the observed value of the test statistics. Assignment Indices were calculated and used to assess sex differences in assignment.

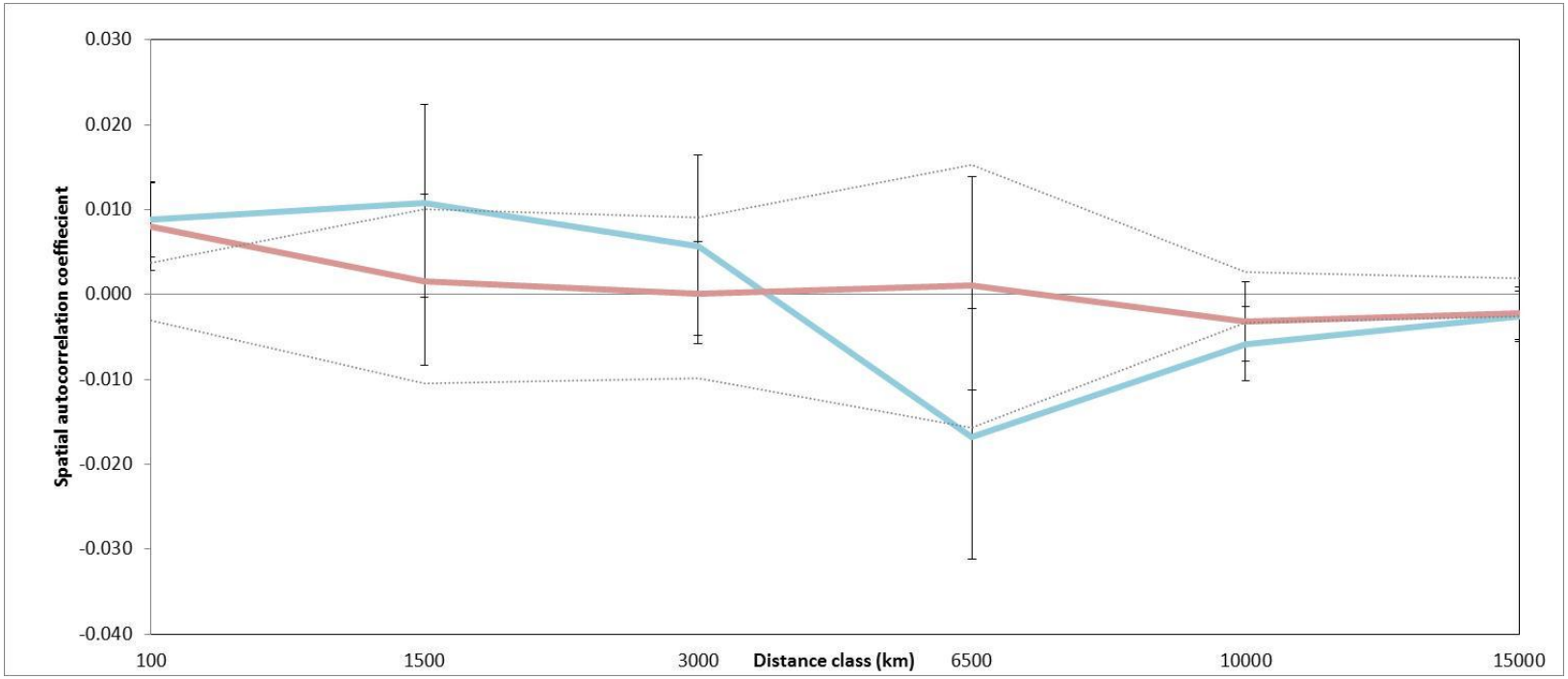

Figure 19. Correlogram plots of the spatial autocorrelation coefficient, *r* as a function of geographical distance for males (in blue) and females (in red). Upper and lower bounds for the 95% confidence interval for the null hypothesis of no spatial structure (*r* = 0) based on 10, 000 random permutations of the data among distance classes are depicted as black dotted lines. 95% confidence intervals about *r* were determined using 10, 000 bootstrap replicates. Geographic distances (km) presented are the maximum distance of each class.

Table 6. Comparisons of pairwise measures of population differentiation for females (below diagonal) and males (above diagonal) based on Φ_{ST} values for mitochondrial DNA (a) and G_{ST}'' values for nuclear microsatellite data (b). Significance was assessed using a non-parametric permutation approach. Populations that were significantly differentiated at the 95% confidence level, following Bonferroni correction for multiple comparisons are represented using a superscripted star (*)

(a)	**northern Indian**	**South Africa**	**eastern Australia**	**southern Australia**	**New Zealand**
northern Indian		0.082*	0.079*	0.168*	0.098
South Africa	0.168*		0.002	0.015	0.008
eastern Australia	0.135*	-0.001		-0.005	-0.0161
southern Australia	0.205*	0.051*	0.012		0.016
New Zealand	0.130*	0.020	-0.006	0.028	

(b)	**Northern Indian**	**South Africa**	**Eastern Australia**	**Southern Australia**	**New Zealand**
northern Indian		0.005	0.010	0.008	0.017
South Africa	0.009		0.009	0.009	0.015
eastern Australia	0.009	0.010		0.010	0.017
southern Australia	0.009	0.014	0.012		0.020
New Zealand	0.010	0.009	0.008	0.014	

Table 7. *F*-statistics, relatedness (*r*), mean assignment (mAI_C) and variance assignment (vAI_C) for each sex. Significance was assessed using the randomisation method.

	F_{ST}	*r*	F_{IS}	mAI_C	vAI_C
Males	-0.0004	-0.0007	0.0092	-0.1914	11.8649
Females	0.0029	0.0059	0.0010	0.1901	9.1119
P-value	0.0510	0.0501	0.2033	0.1578	0.8376

Table 8. Tests of spatial autocorrelation and among sex correlogram heterogeneity. Numbers of comparisons (*n*), autocorrelation coefficients, *r* and *P*-values are shown for each distance class as well as a multiclass test criterion (ω) of the departure from the null hypothesis of $r = 0$. Single-class (t^2) and multiclass (ω) test criteria and associated *P*-values for the test of correlogram homogeneity across sexes are also shown.

		Distance class (km)							
Spatial autocorrelation		**100**	**1500**	**3000**	**6500**	**10000**	**15000**	**ω test**	***P*-value**
Males	**n**	2851	366	407	170	2773	4608	59.401	0.000
	r	0.009	0.011	0.006	-0.017	-0.006	-0.003		
	***P*-value**	0.000	0.019	0.112	0.979	0.999	0.977		
Females	**n**	2851	366	407	170	2773	4608	33.078	0.007
	r	0.008	0.002	0.000	0.001	-0.003	-0.002		
	***P*-value**	0.003	0.396	0.592	0.219	0.997	0.725		
Among sex heterogeneity								**ω test**	***P*-value**
	t^2	0.062	1.401	0.836	2.977	0.703	0.031	6.226	0.411
	***P*-value**	0.800	0.237	0.362	0.084	0.398	0.862		

Effective population size estimates

Applying $CN_{e\ crit}$ values within the range of acceptable bias-precision trade-off ($0.020 < P_{crit} < 0.050$) resulted in finite point estimates of CN_e for most sampling locations, ranging in order of magnitude from hundreds to several thousand (Table 9). A finite estimate could not be obtained for eastern Australia. Negative estimates of CN_e were obtained for this location across a range of P_{crit} values (0.020 – 0.20). The lower bounds of the 95% confidence intervals were in the hundreds for all locations (except eastern Australia which was unbounded), while upper bounds were mostly infinite (Table 9). Estimated effective population size for the Australasian region (Indo-Pacific, eastern, southern, and western Australia and New Zealand) was 2,550.6 (95% CI = 831, ∞). An infinite measure of CN_e is an artefact of the linkage disequilibrium method used here and essentially an indication of insufficient power due to various biases and difficulties, that are well documented in the literature (Luikart et al. 2010, Waples and Do 2010, Hare et al. 2011), associated with estimating CN_e in large populations of highly diverse animals with overlapping generations. Since populations cannot be infinite in size, these estimates are more appropriately reported as inestimable in Table 9. Finite lower and upper bounds on the 95% confidence interval surrounding the estimate were only obtained for the northern Indian location. Population size was comparatively small at this location with a point estimate of 252.3. The lower and upper bounds were 169.6 and 465.4, respectively (Table 9).

Table 9. Estimates of effective population size (CN_e) and associated upper and lower bounds of the 95% confidence interval (CI). Bias-precision trade-off is most balanced when using allele frequency exclusion criterions (P_{crit}) within the range 0.02 to 0.05.

Regions	**Sample size**	***CN*$_e$**	**95% CI lower**	**95% CI upper**	**P_{crit}**
northern Atlantic	28	1208.8	109.1	inestimable	0.04
northern Indian	84	252.3	169.6	465.4	0.02
South Africa	91	1409.9	413.7	inestimable	0.03
eastern Australia	57	Infinitely large	inestimable	inestimable	0.02 – 0.2
southern Australia	53	5692.5	368.7	inestimable	0.02
New Zealand	42	566.6	203.8	inestimable	0.02
Australasian (eastern Australia, southern Australia, New Zealand)	152	2550.6	831	inestimable	0.02

Discussion

During this study, we investigated the population structure and movement patterns of shortfin mako populations in the Australasian and central Indo-Pacific using conventional tagging, long-term satellite telemetry, mitochondrial DNA and nuclear DNA datasets. We provide high-resolution information regarding the spatial connectivity of shortfin mako populations in the Australasian and Central Indo-Pacific Region that can inform discussions regarding regional-scale management options for this species.

Although genetic population structure has been investigated previously for the shortfin mako, all prior studies have largely addressed differentiation at the inter-oceanic scale, with a focus on the Pacific Ocean basin. Sampling from the Australasian region has been limited and prohibited assessments at scales suitable for informing fishery management decisions within the Australian Exclusive Economic Zone. Additionally, sampling of shortfin makos in the Southern and Indian Ocean basins was particularly sparse prior to this study, limiting our ability to make inferences about connectivity between Australasian and neighbouring populations. Previous studies of the movement of this species using tracking data have mostly focused on the southwest Pacific Ocean off eastern Australia and sample sizes were relatively small (e.g. Stevens et al. 2010). This study represents the first multidisciplinary study of the movement and population connectivity of the shortfin mako throughout the Australasian region, using information from both genetic and tracking datasets and including representatives from the Indian Ocean, allowing these factors to be more rigorously assessed.

Matrilineal population differentiation

There have been three prior studies of population genetic structure based on mitochondrial DNA in shortfin mako (Heist et al. 1996; Taguchi et al 2011; Michaud et al. 2011). Divergence between the Atlantic and Pacific Ocean basins was a common result in all of these studies, as well as evidence of reduced cross-equatorial connectivity. While Heist et al. (1996) and Taguchi et al. (2011) were unable to distinguish north and south Pacific sampling sites, improved sampling (840 individuals from five regions in the Pacific, and one in the Atlantic Ocean) by Michaud et al. (2011) revealed significant differences between the north and south Pacific, and the southeast and southwest Pacific. Taguchi et al. (2011) was the only one of these studies to consider samples from the Indian Ocean. The eastern Indian Ocean was found to be divergent from all sampling sites, except the north Atlantic. This included significant differentiation between the eastern Indian Ocean and east coast of Australia, indicating possible east-west matrilineal population structure in the shortfin mako in Australian waters. However, sparse sampling of highly genetically diverse, mobile animals

can easily lead to frequency differences that give a falsely inflated sense of population structure, and therefore these patterns must be interpreted with caution given the relatively small sample sizes analysed by Taguchi et al. (2011).

Similar to previous studies (Heist et al. 1996; Taguchi et al. 2011), we found considerable mitochondrial DNA genetic diversity in shortfin makos. Haplotypic diversity was higher than 0.9 at most sampling sites (Fig. 15, Table 3), which is toward the higher end of the range typically found for elasmobranchs (Hoelzel et al. 2006; Keeney and Heist 2006; Castro et al. 2007; Dudgeon et al. 2008; Schultz et al. 2008; Chabot and Allen 2009; Benavides et al. 2011; Blower et al. 2012) and typical of other highly mobile pelagic species (Graves 1998). Also consistent with previous work, our mitochondrial DNA data set showed little evidence of trans-equatorial migration. Both Northern Hemisphere sampling locations (north Atlantic and northern Indian) were significantly differentiated from all other sampling sites (Table 4). We were unable to distinguish the Indo Pacific sampling site from those in the Australian region, however this sample included just five individuals sampled from the Northern Hemisphere. The majority of samples included in the Indo Pacific site were sampled from fish markets in Indonesia, and were likely caught in the Southern Hemisphere. Our data, therefore, does not allow a comprehensive assessment of trans-equatorial gene flow between Australian populations and those in the northern Pacific however, Michaud et al. (2011) describe significant differentiation between the northwest and southwest Pacific, indicating that trans-equatorial migration is similarly limited in this region.

Michaud et al. (2011) hypothesised that haplotype sharing between the Atlantic and Australia/New Zealand indicates that gene flow between the Pacific and Atlantic populations, occurs primarily through the Indian Ocean. Limited sampling from both the Indian Ocean and Australasian region prevented further investigation in their study. Our analyses provide some support for this hypothesis, as we did not distinguish South Africa from the Australasian populations and all pairwise fixation indices involving comparisons between these two regions were low relative to comparisons between Northern and Southern Hemisphere sampling sites. All pairwise Φ_{ST} estimates between South Africa and the Australasian region were non-significant, indicating that gene flow occurs across the Indian Ocean (Table 4). This result is consistent with Taguchi et al. (2011) who could not distinguish western Indian Ocean sampling sites from those in the eastern Indian Ocean, or the Pacific Ocean. Our exact tests of population differentiation, however, indicated significant differentiation between Australasian and South African sampling sites, and a single pairwise comparison between South Africa and southern Australia was also significant based on F_{ST} (Table 4). These significant comparisons should be interpreted with caution, however, given the small magnitude of observed pairwise fixation indices. The frequency data inherent in the analysis of population structure is particularly susceptible to noise due to random sampling error both at the intralocus (number of individuals) and interlocus (number of loci sampled) levels. This is exacerbated in high gene flow species, such as shortfin mako, such that it

is expected to find some statistically significant differences among geographic regions as a result (Waples 1998). Taguchi et al. (2011) reported a highly differentiated eastern Indian Ocean population, although this was based on limited sampling from this region. Despite extensive efforts, few samples were obtained from the eastern Indian Ocean off Western Australia, which precludes us from commenting regarding the validity of the finding of Taguchi et al. (2011). Obtaining additional samples from this region should be a priority for future sampling efforts. Doing so will also allow a more rigorous assessment of connectivity across the Indian Ocean between South Africa and Australasia, as well as assessing connectivity between the east and west coasts of Australia.

Taguchi et al. (2011) indicated possible population structure between the eastern and western coasts of Australia. The Bassian Isthmus in southern Australia is a well characterised biogeographic barrier that is thought to have influenced population subdivision between coasts in a diversity of marine species (Waters 2008). Blower et al. (2012) reported maternal genetic population subdivision between eastern and southwestern coastal regions of Australia in the white shark *Carcharodon carcharias*, a close relative of the shortfin mako (Naylor et al. 2012). In contrast, we did not find any evidence of matrilineal population structure in shortfin makos sampled from around the Australian continent. The AMOVA comparing samples collected off the eastern and western coasts of Australia was non-significant, and none of the pairwise comparisons of fixation indices indicated significant divergence between locations within Australian waters. Interestingly, however, the single pairwise comparison between southern Australia and New Zealand indicated significant divergence. The Φ_{ST} estimate between southern Australia and New Zealand is lower than those observed between Northern and Southern Hemisphere sampling sites, indicating that gene flow between these locations is less constrained than across the equator, but nevertheless restricted enough to represent significant divergence (Table 4). There are two possible explanations for this observation. The first is that this signal is an artefact of restricted sampling from a highly diverse set of haplotypes, whereby minor differences in haplotype frequencies can result in low, but statistically significant estimates of Φ_{ST} (Waples 1998). Alternatively, gene flow throughout this region may occur in a 'stepping stone' fashion whereby southern Australia and New Zealand are connected via the east coast of Australia, but gene flow between those two locations specifically is constrained. AMOVA in which eastern, western Australia and New Zealand were separated into distinct regions was non-significant so we cannot refute that Australia and New Zealand represent a single matrilineal stock.

Nuclear population differentiation

There has been only one prior microsatellite analysis of population structure in shortfin mako. Schrey and Heist (2003) reported very weak evidence of population structure based on samples

from both the Northern and Southern Hemispheres in the Atlantic and Pacific Ocean basins, as well as the Atlantic and Indian coasts of South Africa. Multi-locus measures of population subdivision were low and non-significant based on F_{ST}, however, R_{ST} was statistically significant, driven by a single pairwise comparison between the North Atlantic and North Pacific samples. The authors recommended interpreting the significance of this result with caution, in light of the small amount of migration necessary to drive the magnitude of this parameter so low that the signal of genetic differences among samples is obscured by the noise inherent in finite sampling (Waples 1998). Moreover, this analysis was based on just four microsatellite loci. Since each gene locus is an independent sample of evolutionary history, the stochastic processes of migration and genetic drift, it is expected that these parameters can vary greatly between loci. It is therefore desirable to base assessments on a larger number of independent loci than was available for analysis in Schrey and Heist (2003). Sampling from both Australia and the Indian Ocean were limited (Australia n = 43 and South Africa n = 26) allowing little inference regarding fine-scale spatial structure in the region.

Similar to Schrey and Heist (2003), we found lower genetic differentiation in the microsatellite data than for mitochondrial DNA data. Only a single pairwise comparison, South Africa versus southern Australia, suggested significant differentiation (Table 5), however, this was not supported by AMOVA. The model-based clustering analysis suggested only subtle differences in allele frequencies across regions and sampling locations (Fig. 16), and was consistent with there being little to no signal of population structure. Like Schrey and Heist (2003), we also interpret the significance of the comparison between South Africa and Australia with caution given that the estimate of F_{ST} is low. It is possible that this result is also an artefact of noise related to finite sampling of this highly diverse species (Waples 1998). From a management perspective, it is more important to determine whether these differences are biologically meaningful such that these units warrant management as separate stocks. Conversely, we also caution against interpreting the overall lack of significant differences in microsatellite data to mean that shortfin mako represent a single, globally panmictic stock. A small number (<10, Spieth 1974; Mills and Allendorf 1996) of migrants will homogenise allele frequencies across regions, rendering potentially biologically meaningful stock differences undetectable by this data set. This does not mean however, that the rate of migration, which is the more important parameter from a management perspective because it governs how rapidly a stock may be replenished following harvest, is high enough to warrant management as a single population. In organisms, such as elasmobranchs, with relatively low fecundity, the number of migrants required per generation to allow stock rebuilding is orders of magnitude higher (hundreds to thousands) than to homogenise allele frequencies and estimating migration rate with this level of precision from genetic data is extremely difficult for high gene flow species (Waples 1998). It is therefore important that both the mitochondrial and microsatellite data be interpreted in conjunction with direct estimates of

dispersal via tracking studies to delineate population structure in high gene flow species such as the shortfin mako. Essentially, genetic data offer an across generation estimation of the extent of movement via gene flow. Tracking data provides a within-lifetime estimate of movement and combining the two can better elucidate whether a signal of panmixia is likely driven by few, relatively rare dispersal events or whether a species is highly vagile, promoting high connectivity between locations. Combining the two data types can also reveal patterns that may have been overlooked if relying solely on one data type. For example, a signature of reproductive philopatry may be overlooked in wide ranging animals if individuals are sampled for genetic analysis during the dispersed phase, which would promote an artificial signature of panmixia.

Sex-biased dispersal

Sex-biased dispersal is a pattern where individuals of one sex remain philopatric to a particular site for breeding, while those of the opposite sex disperse. Generally, dispersal tends to be male-biased with polygynous breeding systems such as mammals, while female-biased dispersal is predicted for monogamous systems, e.g. birds (Greenwood 1980). It is important to identify and manage species that exhibit sex-biased dispersal accordingly to avoid selective overharvest of the more philopatric sex, if fishing practices are concentrated in their comparatively smaller range. Furthermore, identifying areas to which females exhibit philopatry can aid in locating pupping and nursery grounds (Hueter 1998). Male-biased dispersal has been demonstrated in a number of elasmobranch species (Keeney et al. 2003; Keeney et al. 2005; Duncan et al. 2006; Schultz et al. 2008; Daly-Engel et al. 2012) including the white shark (Pardini et al. 2001; Blower et al. 2012), which also shows trans-oceanic migrations by both sexes (Bonfil et al. 2005; Bruce et al. 2006). Schrey and Heist (2003) suggested sex-biased dispersal as a possible mechanism to explain the magnitude of the difference in degree of genetic structure inferred from mitochondrial DNA and microsatellite markers between ocean basins in shortfin mako (mitochondrial DNA is maternally inherited and therefore strong mitochondrial structure in the absence of microsatellite structure can indicate female philopatry). Sexual segregation, based on sex-ratios of catches in high seas long-line fishery bycatch data has also been identified for shortfin makos in the South-east Pacific Ocean, with females found in higher frequencies with increasing proximity to the South American continent (Mucienties et al. 2009). However, an observer program in the ETBF in the SW Pacific found that for 1,126 shortfin makos for which sex was determined, 42% were male, and 58% were female (Bruce 2014), and both regional and seasonal differences were apparent in proportions of sexes in observer based monitoring of pelagic long-line catches off New Zealand (Francis 2013). Together these studies indicate that shortfin makos exhibit some degree of female philopatry, however, how best to integrate this information with current management strategies and Recovery Plans remains unclear. As with all HMS, it is difficult to distinguish movements for breeding that have genetic consequences and implications for long-term population dynamics and survival, from

other types of movement. Our data suggests a trend toward male-biased dispersal, although for the most part this observation was not statistically supported. Fixation indices were higher for mitochondrial DNA than for microsatellite markers and the magnitude of this difference exceeds the expectation if it were driven only by differences in the relative effective population sizes of these two markers (Table 4 and Table 5). Pairwise estimates of Φ_{ST} were usually higher in females than in males for mitochondrial DNA (Table 6a), although this pattern was not observed in the microsatellite data (Table 6b). Sample sizes are reduced further in analyses that are split by sex and therefore the significance of these results must be interpreted with caution for reasons that were outlined previously.

Allele frequencies across sampling sites should be more similar for individuals of the dispersing sex than those of the more philopatric sex. The expectation therefore, is for F_{ST} and relatedness (*r)* to be highest in the more philopatric sex. Additionally, because the dispersing sex should largely consist of immigrant and less related individuals, we expect them to have a lower probability of local assignment and greater variance in assignment index than the philopatric sex (Goudet et al. 2002). The observed values for these parameters (Table 7) in this study were consistent with these expectations, indicating male-biased dispersal in shortfin mako. However, the test statistics based on the difference in these parameters between sexes fell within the randomised distribution representing the null hypothesis of no sex-biased dispersal (Fig.18).

There are several caveats to the interpretation of these results. These tests lack power to detect sex-biased dispersal unless the bias is very strong (> 80:20) and dispersal occurs at intermediate rates (Goudet et al. 2002). It is highly possible that our analyses are lacking in power due to both of these factors. Both tracking data and the low observed fixation indices based on genetic data suggest that both male and female shortfin mako are highly mobile. If females exhibit philopatry it seems more likely that this will be towards generalised oceanic areas, rather than discrete pupping grounds, both of which indicate that any bias that may exist is likely to be weak and operating at the ocean basin scale (i.e. females are philopatric to particular ocean basins, but not to discrete sites within them). Moreover, this high mobility and genetic diversity observed in the shortfin mako implies that populations are likely to be large and diffuse. In turn, this implies that very large sample sizes will be required to estimate allele frequencies with sufficient precision to detect immigrant genotypes. Finally, these tests are only applicable if dispersal occurs prior to reproduction and sampling occurs after dispersal (Goudet et al. 2002). This prerequisite is extremely difficult to ensure in HMS. Mature shortfin mako are generally rare, such that our sample consists of a mixture of mostly juvenile and sub-adult individuals sampled over several years from multiple cohorts. It is possible that this unavoidable sampling scheme is masking any signal of statistically supported sex-biased dispersal in these particular analyses, although the trend indicates a male-bias.

We did not detect any differences in spatial genetic structure across sexes based on the spatial autocorrelation analysis. Ability to detect a sex bias using this method is also highly dependent upon sample size and requires the development of strong spatial genetic structure in the more philopatric sex before a difference will be rendered statistically significant (Smouse et al. 2008; Banks and Peakall 2012), which is unlikely to occur in HMS. Although we detected low, but significant positive autocorrelation among genotypes at small distance classes, the magnitude of autocorrelation was similar in males and females and bootstrap confidence intervals were overlapping. Banks and Peakall (2012) stressed the importance of sampling at or below the scale at which dispersal is restricted in the more philopatric sex in order to concentrate pairwise data points at that spatial scale. This analysis and our inferences regarding sex-biased dispersal in general, would thus benefit greatly from more information regarding the movements of adult individuals of both sexes. Satellite tracking of mature individuals together with genetic analysis of a large sample of mature sharks collected during the breeding season is required.

The magnitude of the difference in population structure detected across marker types (mitochondrial vs. microsatellite markers) indicates that sex-biased dispersal may be occurring at the ocean-basin scale. However, it is important to note that our samples consist largely of juvenile and subadult individuals that may not yet have dispersed from their natal region, which would elevate the degree of structure observed in this class. We nevertheless recommend that this species be managed accordingly pending more fine-scale information that may become available via tracking and genetic analysis of adult individuals. As discussed by Schrey and Heist (2003), it makes sense that female-mediated gene flow is reduced between hemispheres because Northern and Southern Hemisphere females must be on opposite seasonal reproductive cycles since parturition occurs in the spring (Mollet et al. 2000). Females may benefit from familiarity and predictability of prey resources by remaining philopatric to a particular hemisphere for breeding and pupping, while males on the other hand are more flexible in terms of adjusting to the local time of breeding following long distance dispersal events between hemispheres. Additionally, given that mating and parturition are separated by at least 12 to 18 months, if females don't adhere to strict pupping grounds it makes sense for males to roam more widely to gain access to fertile females.

Effective population size

Various benchmarks, ranging from 500–5,000 individuals have been suggested for the minimum effective population size, CN_e, required for avoiding inbreeding and maintaining evolutionary potential. However, these guidelines are based on population genetics theory and the simplistic assumption of an idealised population. Violations of any of the assumptions of this theory, such as overlapping generations, fluctuating population size, unequal sex ratio, non-random mating or

selection, will affect the accuracy and precision of these estimates. Moreover, it is difficult to genotype a sufficient number of molecular markers to have the statistical power necessary to make precise estimates of CN_e when populations are large and diverse, because the drift signal is so small that there is often little information about the upper bound of the estimate under these circumstances (Luikart et al. 2010, Waples and Do 2010, Hare et al. 2011). In this way, estimating CN_e is subject to many of the same limitations that have been discussed previously when trying to quantify migration in high gene flow species (Waples 1998). Useful information may still be obtained from analyses of CN_e under these circumstances, such as the lowest possible level of CN_e (Waples and Do 2010; Hare et al. 2011), which might be a useful predictor of population bottlenecks. We suggest that for highly mobile species with potentially large population sizes, whose scarcity, cryptic nature and resultant limited accessibility, means sampling tends to occur opportunistically across cohorts, that this parameter is best applied cautiously as an indicator of the magnitude of population size, rather than interpreted as providing precise point estimates.

During this study, we were unable to obtain a point estimate for the eastern Australia sampling location (Table 9). Negative estimates of CN_e were obtained for this location from analyses applying a range of P_{crit} values (0.02–0.2). Negative estimates of CN_e occur when the contribution of sampling error to linkage disquilibrium is larger than expected, thus producing a negative adjusted estimate of linkage disequilibrium and hence a negative estimate of CN_e. The correct interpretation of such a result being that there is no evidence for linkage disequilibrium due to drift, rather it can all be explained by sampling error, thus implying an infinitely large effective population. Essentially this result is an artefact of the method as a result of limited sampling from a large population and is rather best interpreted as inestimable. Since we did not find any evidence of population structure within the Australasian region, individual estimates for each location within the region essentially approximate the broader population. The estimate for the Australasian region based on all of these samples combined (Indo-Pacific, eastern, southern, western Australia and New Zealand) is considered the most informative. The point estimate for this region was 2,551, with a lower confidence interval bound of 831 and an infinite upper bound. Cautiously interpreting this estimate by taking the lower confidence bound as the lowest possible estimate of CN_e indicates that the Australasian shortfin mako population is above the accepted thresholds for avoiding inbreeding depression and meets the threshold (CN_e 500–1000) for maintaining evolutionary potential (genetic diversity) described by Frankham et al. (2010). Pending more precise estimates of CN_e for shortfin mako, the precautionary principle should be applied by managing the Australasian population based on this lower bound with the aim of avoiding reductions in population size. It must be acknowledged that this interpretation assumes an unbiased point estimate of CN_e. The most likely source of bias in our analysis is sampling from multiple cohorts with overlapping generations. The effect of this on estimating CN_e remains little known (Waples and Do 2010), but is potentially substantial (Luikart et al. 2010). Waples and Do (2010) estimate that sampling from a number of cohorts equal to the generation length will

approximate CN_e, but this is not likely given our present sampling scheme. We are thus unable to quantify how much bias has been introduced as a result of violating this assumption of the analysis.

Obtaining more precise estimates of CN_e in the future will require a more intensive and costly sampling effort. Present estimates suggest that the effective population size of shortfin mako in the Australasian region is likely to be in the order of thousands of individuals. It has been suggested that precise estimates of N_e require sampling ~10% of the effective size of the population (Waples and Do 2010; Hare et al. 2011), which in this case means increasing sampling effort to include hundreds to thousands of samples. Sampling from clearly defined cohorts may also contribute substantially to minimising potential bias associated with these estimates, while also allowing independent estimates of CN_e using alternative methods (Jorde and Ryman 1995) for comparison to those obtained using linkage disquilibrium single time-point estimators, as a way of cross-validation (Hare 2001; Portnoy 2009; Dudgeon et al. 2012). Estimating the population census size, perhaps via mark-recapture methods based on game fishing data, would also be particularly useful. Once accurate estimates of CN_e are obtained, this would facilitate estimating the N_e/N_c ratio which is a useful parameter that can inform about both the population dynamics and conservation status of a species (Portnoy 2009; Luikart et al. 2010). Finally, emerging high throughput sequencing technologies offer the potential to screen comparatively large numbers of loci and alleles. This means that it may be possible in the future to obtain better confidence bounds on precise point estimates of CN_e even for species with large population sizes (Hare et al. 2011). Importantly, the point estimate obtained for the northern Indian Ocean population based on our analysis was 252, which was lower than that obtained for any other location and also had finite lower and upper bounds of 169.6 and 465.4, respectively. Although microsatellite diversity in samples from this location appeared to be similar to levels found at other locations, mitochondrial diversity was noticeably reduced (Table 3). This observation, taken together with the smaller estimate of CN_e, possibly indicates a population bottleneck has occurred in the northern Indian Ocean. This requires further investigation using tests designed to explicitly detect population declines, but it is worth noting that based on the afore mentioned conservation threshold, this population may be at risk of detrimental effects associated with small or declining population size and may warrant further attention from resource managers.

This study benefited from access to a substantial existing tag-recapture data-set for shortfin makos that was collected by recreational, game and commercial fishers and managed by the NSW Game Fish Tagging Program. Long-term tag-recapture data provided a valuable means to assess distribution and connectivity in the Australasian and Central Indo-Pacific Region, and allowed qualitative comparisons with dispersal patterns elucidated from satellite telemetry and genetic data. Long distance movements (>1000 km) based on conventional tag-recaptures

comprised 16% of the recaptures and provided further evidence that shortfin mako populations in the Australasian and Central Indo-Pacific Region utilise oceanic habitats with spatial scales in the magnitude of 1,000s of km. There was only a single cross-equatorial recapture of a shortfin mako over the history of the conventional tagging program and when combined with the telemetry data this suggests that northward movements into equatorial regions (<12° S) may be relatively uncommon. This is consistent with the results from the genetic data, which also demonstrated reduced cross-equatorial connectivity.

When considering the geographical isolation of much of Australia's shelf waters, conventional tag-recapture data must be viewed cautiously in-terms of potential power to elucidate patterns of connectivity outside popular mako game fishing regions, given that there are few opportunities for sharks to be recaptured by recreational fishers in isolated regions of south and southwest Australia. Outside the eastern recreational/game fishery, the reporting of recaptures relies on cooperation of commercial line and gillnet fisheries, and long-range charter fleets that are either not aware of the tagging program, e.g. in High Seas areas beyond the exclusive economic zone (200 nm), or where shortfin makos may be taken on foreign owned commercial fishing vessels operating in isolated areas that are potentially less likely to provide tag return data. Movements from eastern Australia into the Coral Sea, tropical southwest Pacific Ocean (e.g. New Caledonia), and to and from New Zealand were recorded in the conventional tagging data, which conferred with the spatial scales of movements determined from the satellite telemetry data and is consistent with the high degree of genetic connectivity that was observed between locations throughout this region. Of note, was the low frequency of conventional tag recaptures to the west of Victoria, however, rather than being reflective of an east west divide we interpret this to be explained by the isolation of the GAB and southwestern Australia and a lack of access and fishing effort by game and recreational fishers in areas inhabited by shortfin makos. Neither the satellite telemetry data, nor the genetic data provided strong evidence of reduced connectivity between the east and west coasts of Australia.

The spatial distribution of shortfin makos that were satellite tagged in the GAB and Bonney Upwelling Region extended into northern tropical oceanic waters, south to the Subtropical Front and in the SW Pacific Ocean and Coral Sea. Fidelity of juvenile shortfin makos was a key feature between 125 ˚ and 135 ˚E in the Great Australian Bight (Rogers et al. unpublished data), and the Naturaliste Plateau in the SE Indian Ocean represented a 'gateway' where shortfin makos tended to leave the continental shelf and begin oceanic movements towards seamounts located ~1,260 km NW of Exmouth and ~200 km SSE of Christmas Island. The tropical migrations included the northern-most movement by a tracked individual (106.35°E, 12.13°S). One shark tagged in the Bonney Upwelling Region migrated across the central Indian Ocean to an area ~200 km from the African continent (49.16°E, 40.11°S), representing the western-most movement, while the eastern-

most movement was across the Tasman Sea to New Zealand shelf waters (174.69°E, 37.80°S). This was followed by a northern migration by the same individual of ~2,370 km to tropical waters to the east of New Caledonia. During the final stages of the preparation of this report, this tag was still active and this shark inhabited shelf and oceanic waters to the north of New Zealand.

In summary, the telemetry component of this study showed that shortfin makos exhibited several distinct movement stages. These were either combinations of/or single components of shelf-oceanic, shelf-residential and highly migratory-oceanic movements. Below we summarise the spatial scales that defined the movements of individual shortfin makos over different timeframes in the Australasian and Central Indo-Pacific Region based on minimal distances travelled.

1) Great Australian Bight, Subtropical Front and Indian Ocean (8,776–24,213 km: 262–672 d).

2) Great Australian Bight and western Bass Strait (11,148 km: 249 d).

3) Great Australian Bight, Subtropical Front and NE Indian Ocean (14,693–21,586 km: 320–469 d).

4) Great Australian Bight, Subtropical Front and Coral Sea (10,511–19,964 km: 311–482 d).

5) Eastern Bass Strait, New Zealand and New Caledonia (10,838 km: 318 d, tag still active).

Movements over similar geographical scales have been described for shortfin makos during long-term telemetry studies in the NE Pacific Ocean, where tropical temperature fronts (at ~ -12–15°S) align with turning points during return oceanic migrations to shelf waters of the California Current ecosystem (Block et al. 2011), supporting our findings that this species is among the most mobile of the large pelagic sharks. This high mobility coupled with their 'slow' life history characteristics and broad vertical habitat preferences (Stevens et al. 2010; Abascal et al. 2011) means that individuals are likely to interact with a range of fishing gears during the course of their lifespan. Patterns of high dispersal observed in the long-term conventional tagging and telemetry datasets, mitochondrial and microsatellite DNA were all in support of the definition of this species as 'Highly Migratory' in the Australasian and Central Indo-Pacific Region and further indicated there was high spatial connectivity of populations of shortfin mako.

Conclusions

In summary, based on the 36 year conventional game fish tagging data-set, a 7-year satellite tracking dataset, and microsatellite and mitochondrial DNA analyses from 365 samples collected in six key regions, the most appropriate scale at which to manage the population fished in Australian State and Commonwealth waters are the boundaries of the Australian and Central Indo Pacific Region (New Zealand – south west Pacific – Australasian/Indo Pacific Region). This will need to be refined as further satellite tracking data are collected, and as further genetic data are collected from the north and south east Pacific Ocean, and southern Indian Ocean.

To summarise the findings of this study for management purposes, we created a 'conceptual connectivity plot' that demonstrates a broad spatial overview and comparison of the scales of connectivity highlighted by each of the four data sets (Fig. 20). Importantly, while differences between hemispheres were not detectable in the microsatellite data, mitochondrial DNA, telemetry and conventional tagging data all indicated there was minimal connectivity at that geographic scale. Connectivity between the Australian region and neighbouring South African waters via the Indian Ocean is more complicated to interpret. Despite some evidence of cross Indian Ocean linkages, the exact tests of population differentiation based on mitochondrial DNA suggested that connectivity may be reduced (Table 4).

No individuals were tracked from coast to coast across the entire Indian Ocean using satellite telemetry, however a single individual tagged in the Bonney Upwelling Region off southern Australia was recorded as far west as the Crozet Plateau in the Indian Ocean (2000 km east of South Africa), and mitochondrial Φ_{ST} estimates (Table 4) and microsatellite DNA analyses (Table 5) indicated connectivity across this region. There was also a high degree of haplotype sharing between South Africa and Australasian locations.

It is possible that the combination of the eastward flowing South Indian Current, STF, and east-west running bathymetric features, including the Naturaliste Plateau, Diamantina Fracture Zone and Broken Ridge form oceanic migratory pathways that facilitate trans-Indian Ocean linkages between these populations.

Further investigations into the extent of connectivity between Australian and South African waters would benefit from tracking information from adult individuals, as well as genetic data from improved sampling of individuals off Western Australia. Other priorities include identification of regions in the Australasian and Central Indo-Pacific Region used for nursery, pupping and parturition, and to improve information on the size of breeding populations.

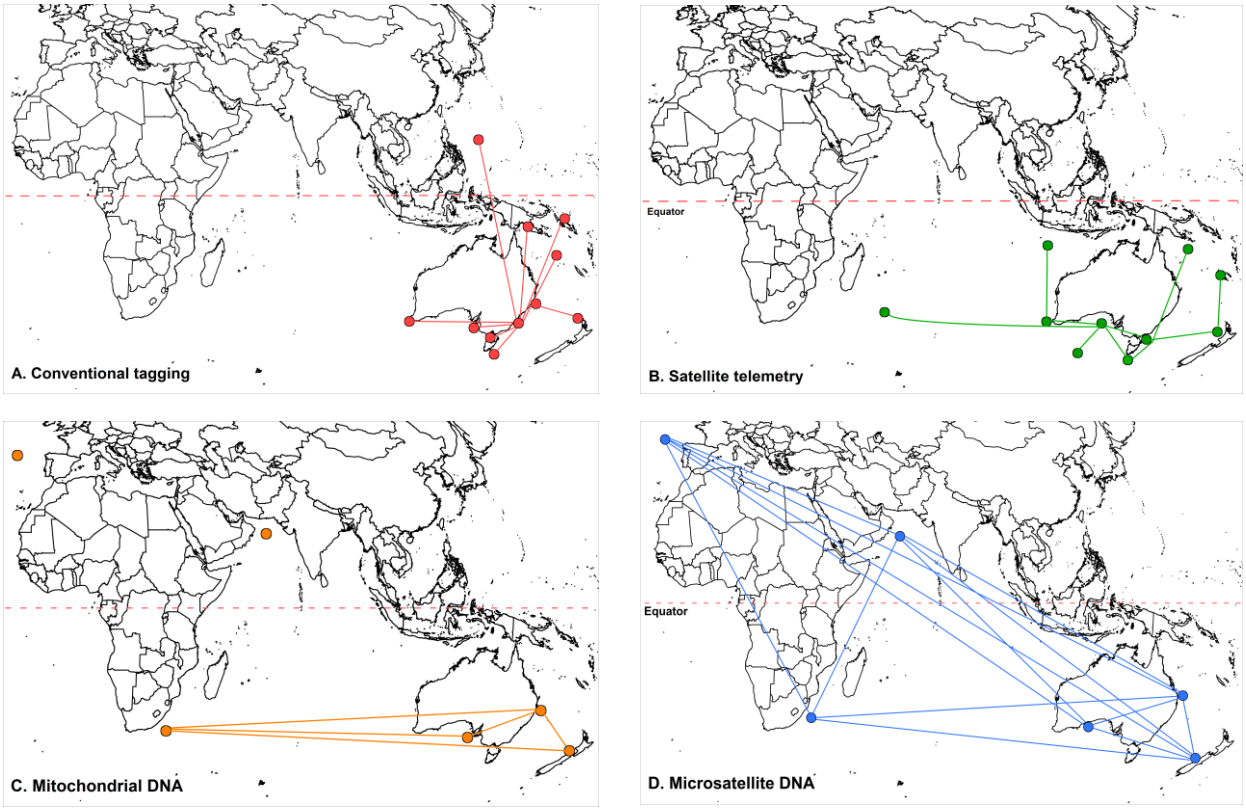

Figure. 20. Conceptual connectivity plots showing linkages determined from the four different data-sets in the Australasian and central Indo Pacific and South Africa, and the two 'out-groups', Northern Indian Ocean (Oman), and the North Atlantic (Portugal). **A.** Red symbols and lines: conventional tagging. **B**. Green symbols and lines: satellite tracking. **C.** Orange symbols and lines: mitochondrial DNA. **D**. Blue symbols and lines: microsatellite DNA.

Implications

- Findings of this study resolve the spatial range, individual movements, stock structure and effective population size of shortfin mako populations in the Australasian and Central Indo-Pacific Region, enhancing our ability to inform future risk assessment processes.
- This study provides key information that could be incorporated during the IUCN, EBPC, CITES and CMS assessment processes.

Recommendations

- Based on this study, shortfin mako should be managed as an independent, panmictic stock in Australasia (with New Zealand), but separate from the South African population and the Northern Hemisphere.
- This study highlights that to adequately manage potential impacts on shortfin mako populations, there is a need for the appropriate RFMOs to consider threatening processes within the broad spatial distribution of the Australasian and central Indo-Pacific Region. Findings could be integrated into discussions of appropriate spatial scales for fishery bycatch regulations of shortfin makos for fisheries managed by Western and Central Pacific Fishing Commission, Indian Ocean Tuna Commission, and International Commission for the Conservation of Atlantic Tunas, and Australian State and Commonwealth fisheries management authorities.
- The estimate of effective population size for shortfin makos in the Australasian region is in the order of thousands of individuals. The lower CI bound (831) of the point estimate of effective population size of 2,551 is a suitable basal point for discussions pertaining to the status of the Australasian population with the aim of avoiding declines from this level. Further efforts should be made to improve the precision of these estimates via more intensive sampling effort.
- Ecological risk assessments undertaken by Western and Central Pacific Fishing Commission, Indian Ocean Tuna Commission, and International Commission for the Conservation of Atlantic Tunas have identified the shortfin mako to be among the most vulnerable shark species to pelagic long-line fisheries in the Indian, western and central Pacific Oceans (Commission for the Conservation of Southern Bluefin Tuna's, CCSBT Working Group, 2013). The CCSBT Ecologically Related Species Working Group (ERSWG) could integrate the new information on movement and stock structure as part of ecological risk assessment processes to improve and mitigate ecological impacts of fishing on the shortfin mako population in the Australasian and central Indo-Pacific Region.

Further Development

This project, along with the findings of the workshop to synthesise available data on mako and porbeagle sharks in Australasian waters (Bruce 2014) together form important basal information required to further develop regional-scale management policies for these pelagic sharks in the future. To feed into this process, further spatially explicit risk assessment analyses could be conducted using the data-streams generated during this project. This could include the assessment of cumulative impacts of multiple processes on the critical habitats of these pelagic shark species.

In summary, further development of this research should also seek to:

- Better understand the patterns of growth dynamics of shortfin makos in relation to recently resolved migratory behaviours in the Australasian and Central Indo-Pacific Region.
- Resolve sex-biased dispersal hypotheses.
- Improve satellite tracking data-sets off eastern Australia with a focus on mature-sized sharks.
- Identify regions in the Australasian and Central Indo-Pacific Region used by shortfin makos for nursery, pupping and parturition processes.
- Improve the precision of preliminary estimates of the order of magnitude of breeding population sizes provided in this report.

During this project we established a collaboration with researchers at the NOAA Southwest Fisheries Science Centre, California USA, that are currently generating a DNA data set (both mitochondrial and microsatellite) for shortfin mako sampled from the northern and southeastern Pacific regions. We have taken measures to ensure that their emerging data sets are entirely comparable with our own, via the exchange of reference individuals and by targeting an identical suite of genetic markers. The aim is to combine these data sets to obtain a global perspective of genetic structure in this highly mobile species. This will also allow us to assess the degree of connectivity between Australasian and neighbouring Southern Hemisphere populations, which we were unable to sample as a part of this study.

Extension and Adoption

- Findings of this study represent important facets of the scientific information required to develop Australian Commonwealth Government Environment Department Threatened Species Recovery Plans.

- Findings of this study will be delivered in verbal presentations and in publication formats at the next available forum of the relevant RFMOs, and sent to the Executive Officers and relevant representatives of each pelagic fishery.

- Information will be made available to the Australian Fisheries Management Authority, Western and Central Pacific Fishing Commission, Indian Ocean Tuna Commission, International Commission for the Conservation of Atlantic Tunas, and Australian State management authorities for incorporation during fisheries ecological/bycatch risk and stock assessments processes at regional levels.

- Findings will be presented at international conferences and made available in the Australasian and central Indo-Pacific region on Government websites, including those of the FRDC and SARDI Aquatic Sciences.

References

Abascal, F. J., Quintans, M., Ramos-Cartelle, A., and Mejuto, J. (2011). Movements and environmental preferences of the shortfin mako, *Isurus oxyrinchus*, in the southeastern Pacific Ocean. *Marine Biology* 158, 1175–1184.

Ahonen, H., Harcourt, R.G., and Stow, A. J. (2009). Nuclear and mitochondrial DNA reveals isolation of imperilled grey nurse shark populations (*Carcharias taurus*). *Molecular Ecology* 18, 4409–4421.

Amante, C., and Eakins, B. W. (2009). ETOPO1 1 Arc-Minute Global Relief Model: Procedures, Data Sources and Analysis. NOAA Technical Memorandum NESDIS NGDC-24, 19 pp.

Avise, J. C. (2004). Molecular Markers, Natural History and Evolution 2nd Edition. Sunderland, Massachusetts, Sinauer Associates, Inc.

Bandelt, H. J, Forster, P., and Rohl, A. (1999). Median-joining networks for inferring intraspecific phylogenies. *Molecular Biology and Evolution* 16, 37–48.

Banks, S. C., and Peakall, R. (2012). Genetic spatial autocorrelation can readily detect sex-biased dispersal. *Molecular Ecology* 21, 2092–2105.

Baum, J. and Worm, B. (2009). Cascading top-down effects of changing oceanic predator abundances. *Journal of Animal Ecology* 78, 699–714.

Benavides, M. T., Feldheim, K. A., Duffy, C. A., Wintner S., Braccini, J. M., Boomer J., Huveneers C., *et al.* (2011). Phylogeography of the copper shark (*Carcharhinus brachyurus*) in the southern hemisphere: implications for the conservation of a coastal apex predator. *Marine and Freshwater Research* 62(7), 861–869.

Bird, C., Karl, S., Smouse, P., and Toonen, R. 2011. Detecting and measuring genetic differentiation. *In* Crustacean Issues 19 Phylogeography and Population Genetics in Crustacea. *Edited by* C. Held, S. Koenemann and C. Schubart. CRC Press. pp. 31-55.

Block, B. A., Jonsen, I. D., Jorgensen, S. J., Winship, A. J., Shaffer, S. A., Bograd, S. J., Hazen, E. L., Foley, D. G., Breed, G. A., Harrison, A.-L., Ganong, J. E., Swithenbank, A. , Castleton, M., Dewar, H., Mate, B. R., Shillinger, G. L., Schaefer, K. M., Benson, S. R., Weise, M. J., Henry, R. W., and Costa, D. P. (2011). Tracking apex marine predator movements in a dynamic ocean. *Nature* 475 (7354), 86–90.

Blower, D. C., Pandolfi, J. M., Bruce, B. D., Gomez-Cabrera, M., and Ovenden, J. R. (2012). Population genetics of Australian white sharks reveals fine-scale spatial structure,

transoceanic dispersal events and low effective population sizes. *Marine Ecology Progress Series* 455, 229–244.

Bonfil, R., Meÿer, M., Scholl, M. C., and Johnson, R., *et al.* (2005). Transoceanic migration, spatial dynamics and population linkages of white sharks. *Science* 310, 100–103.

Bruce, B. D., Stevens, J. D., and Malcolm, H. (2006). Movements and swimming behaviour of white sharks (*Carcharodon carcharias*) in Australian waters*. Marine Biology* 150, 161–172.

Bruce B. D. (2014) Shark Futures: A synthesis of available data on mako and porbeagle sharks in Australasian waters - Current status and future directions. Final Report to the Fisheries Research and Development Corporation - FRDC 2011/045. CSIRO Marine & Atmospheric Research Hobart Tasmania. 159 pp.

Castro, A. L. F., Stewart, B. S., Wilson, S.G., Hueter, R. E., Meekan, M. G., Motta, P. J., Bowen, B. W., *et al.* (2007). Population genetic structure of the Earth's largest fish, the whale shark (*Rhincodon typus*). *Molecular Ecology* 16, 5183–5192.

Chabot C. L., and Allen L. G. (2009). Global population structure of the tope (*Galeorhinus galeus*) inferred by mitochondrial control region sequence data. *Molecular Ecology* 18, 545–552.

Chapman, D. D., Simpfendorfer, C. A., Wiley, T. R., Poulakis, G. R., Curtis, C., Tringali, M., Carlson, J. K., *et al.* (2011). Genetic diversity despite population collapse in a critically endangered marine fish: the smalltooth sawfish (*Pristis pectinata*). *Journal of Heredity* 102, 643–652.

Chesser, R. K., and Baker, R. J. (1996). Effective sizes and dynamics of uniparentally and diparentally inherited genes. *Genetics* 144, 1225–1235.

Cockerham, C. (1973). Analysis of gene frequencies. *Genetics* 74, 679–700.

Compagno, L., M. Dando, *et al.* (2005). Sharks of the World, Princeton University Press.

Daly-Engel Toby, S., Seraphin Kanesa, D., Holland, K. N., Coffey, J. P., Nance, H. A., Toonen, R. J., and Bowen, B. W. (2012). Global phylogeography with mixed-marker analysis reveals male-mediated dispersal in the endangered scalloped hammerhead shark (*Sphyrna lewini*). *PLoS ONE* 7(1), e29986.

Dingle, H. and Drake, V. A. (2007). What Is Migration? *Bioscience* 57(2), 113–121.

Do, C, Waples, R. S., Peel, D., Macbeth, G. M., Tillett, B. J., and Ovenden, J. R. (2014). NeEstimator V2: re- implementation of software for the estimation of contemporary

effective population size (N_e) from genetic data. *Molecular Ecology Resources* 14, 209–214.

Dudgeon, C. L., Blower, D. C., Broderick, D., Giles, J. L., Holmes, B. J., Kashiwagi T, Krück NC , *et al*. (2012). A review of the application of molecular genetics for fisheries management and conservation of sharks and rays. *Journal of Fish Biology* 80, 1789–1843.

Dudgeon, C. L., Broderick, D., and Ovenden, J. R. (2008). IUCN classification zones concord with, but underestimate, the population genetic structure of the zebra shark *Stegostoma fasciatum* in the Indo-West Pacific*. Molecular Ecology* 18, 248–261.

Dulvy, N. K., Baum, J. K., Clarke, S. C., Compagno, L. J. V., Corte´s, E., Domingo, A., Fordham, S., Fowler, S. L., Francis, M. P., Gibson, C., Martı´nez, J., Musick, J. A., Soldo, A., Stevens, J. D., and Valenti, S. (2008). You can swim but you can't hide: the global status and conservation of oceanic pelagic sharks and rays. *Aquatic Conservation: Marine & Freshwater Ecosystems* 18, 459–482. doi:10.1002/AQC.975.

Duncan, K. M., Martin, A. P., Bowen, B. W., and De Couet, H. G. (2006). Global phylogeography of the scalloped hammerhead shark (*Sphyrna lewini*). *Molecular Ecology* 15, 2239–2251.

Earl, D. A., and vonHoldt, B. M. (2012). STRUCTURE HARVESTER: a website and program for visualizing STRUCTURE output and implementing the Evanno method. *Conservation Genetics Resources* 4, 359–361.

Evanno, G, Regnaut, S., and Goudet, J. (2005). Detecting the number of clusters of individuals using the software STRUCTURE: a simulation study*. Molecular Ecol*ogy14, 2611–2620.

Excoffier, L., and Lischer, H. E. L., (2010). Arlequin suite Ver 3.5: a new series of programs to perform population genetics analyses under Linux and Windows. *Molecular Ecology Resources* 10, 564−567.

Falush, D., Stephens, M., and Pritchard, J. K. (2003). Inference of population structure using multilocus genotype data: linked loci and correlated allele frequencies. *Genetics* 164, 1567–1587.

Favre, L., Balloux, F., Goudet, J., and Perrin, N. (1997). Female-biased dispersal in the monogamous mammal *Crocidura russula*: evidence from field data and microsatellite patterns. *Proceedings of the Royal Society of London Series B* 264, 127–132.

Ferretti, F., Worm, B., Britten, G. L., Heithaus, M. R., and Lotze, H. K. (2010). Patterns and ecosystem consequences of shark declines in the ocean. *Ecology Letters* 13, 1055–1071.

Francis, M., Griggs, L. H., and Baird, S. J. (2001). Pelagic shark bycatch in the New Zealand tuna longline fishery. *Marine and Freshwater Research* 52, 165–178.

Francis, M. P., and Duffy, C. (2005). Length at maturity in three pelagic sharks (*Lamna nasus, Isurus oxyrinchus*, and *Prionace glauca*) from New Zealand. *Fisheries Bulletin* 103, 489–500.

Francis, M. P. (2013). Commercial catch composition of highly migratory elasmobranchs. New Zealand Fisheries Assessment Report 2013/68. ISBN 1179-5352. 79 pp.

Frankham, R., Ballou, J. D., and Briscoe D. A. (2010). Introduction to Conservation Genetics. Cambridge, Cambridge University Press.

GeoScience Australia 2009. http://www.ga.gov.au/

Goudet, J., Perrin, N., and Waser, P. (2002). Tests for sex biased dispersal using genetic markers. *Molecular Ecology* 11, 1103–1114.

Goudet, J. (2001). FSTAT, a program to estimate and test gene diversities and fixation indices (version 2.9.3). http://www.unil/ch/izea/softwares/fstat.html.

Graves, J. E. (1998). Molecular insights into the population structures of cosmopolitan marine fishes. *The Journal of Heredity* 89, 427–437.

Greenwood, P. J. (1980). Mating systems, philopatry and dispersal in birds and mammals. *Animal Behaviour* 28, 1140–1162.

Hare, M. P. (2001). Prospects for nuclear gene phylogeography. *Trends in Ecology and Evolution* 16, 700–706.

Hare, M. P., Nunney, L., Schwartz, M. K., Ruzzante, D. E., Burford, M., Waples, R. S., Ruegg, K., *et al.* (2011). Understanding and estimating effective population size for practical application in marine species management. *Conservation Biol*ogy 25, 438 –449.

Heist, E. J., and Musick, J. A., *et al.* (1996). Genetic population structure of the shortfin mako (*Isurus oxyrinchus*) inferred from restriction fragment length polymorphism analysis of mitochondrial DNA. *Canadian Journal of Fisheries and Aquatic Sciences* 53, 583–588.

Heithaus, M., and Frid, A., *et al.* (2008). Predicting ecological consequences of marine top predator declines. *Trends in Ecology & Evolution* 23, 202–210.

Hill, W. G. (1981). Estimation of effective population size from data on linkage disequilibrium. *Genetical Research* 38, 209– 216.

Hoelzel, A. R., Shivji, M., Magnussen, J., and Francis, M.P. (2006). Low worldwide genetic diversity in the basking shark (*Cetorhinus maximus*). *Biology Letters* 2, 639–642.

Holdsworth, J. and Saul, P. (2010). New Zealand billfish and gamefish tagging, 2008–09, Bluewater Marine Research, 34 pp.

Holts, D. (1988). Review of U.S. west coast commercial shark fisheries. *Marine Fisheries Review* 50, 1–8.

Holts, D. and Bedford, D. (1993). Horizontal and vertical movements of the shortfin mako shark *Isurus oxyrinchus*, in the southern California Bight. *Australian Journal of Marine and Freshwater Research* 44, 901–909.

Hubisz, M., Falush, D., Stephens, M., and Pritchard, J. K. (2009). Inferring weak population structure with the assistance of sample group information. *Molecular Ecology Resources* 9, 1322–1332.

Hueter RE (1998). Philopatry, natal homing and localized stock depletion in sharks. Shark News 12, 1–2.

Jakobsson, M., and Rosenberg, N. A. (2007). CLUMPP: a cluster matching and permutation program for dealing with label switching and multimodality in analysis of population structure. *Bioinformatics* 23, 1801–1806.

Johnson, D., London, J., Lea, M. -A., and Durban, J. (2008). Continuous-time correlated random walk model for animal telemetry data. *Ecology* 89(5), 1208–1215.

Jorde, P. E., and Ryman, N. (1995). Temporal allele frequency change and estimation of effective size in populations with overlapping generations. *Genetics* 139, 1077–1090.

Jorgensen, S. J., Reeb, C. A., *et al*. (2010). Philopatry and migration of Pacific white sharks. *Proceedings of the Royal Society B: Biological Sciences* 277(1682), 679–688.

Jukes, T. H, and Cantor CR (1969). Evolution of protein molecules. Mammalian protein metabolism H. Munro. New York Academic Press. 21–132.

Kacev, D. (in prep). The development of novel microsatellite loci for shortfin mako sharks, *Isurus oxyrinchus* (order Lamniformes).

Keeney D., Heupel, R., Hueter, R., and Heist, E. (2003). Genetic heterogeneity among blacktip shark, *Carcharhinus limbatus*, continental nurseries along the U.S. Atlantic and Gulf of Mexico. *Marine Biology* 143, 1039–1046.

Keeney, D., Heupel, R., Hueter, R., and Heist E. (2005). Microsatellite and mitochondrial DNA analyses of the genetic structure of blacktip shark (*Carcharhinus limbatus*) nurseries in the northwestern Atlantic, Gulf of Mexico, and Caribbean Sea. *Molecular Ecol*ogy 14, 1911–1923.

Keeney, D. B., and Heist, E.J. (2006). Worldwide phylogeography of the blacktip shark (*Carcharhinus limbatus*) inferred from mitochondrial DNA reveals isolation of western Atlantic populations coupled with recent Pacific dispersal. *Molecular Ecology* 15, 3669–3679.

Klimley, A. P., Beavers, S. C., *et al.* (2002). Movements and swimming behavior of three species of sharks in La Jolla Canyon, California*. Environmental Biology of Fishes* 63, 117–135.

Kohler, N., Turner, P., *et al.* (2002). Tag and recapture data for three pelagic shark species: blue shark (*Prionace glauca*), shortfin mako (*Isurus oxyrinchus*), and porbeagle (*Lamna nasus*) in the North Atlantic Ocean. *Collective Volume of Scientific Papers* ICCAT 54, 1231–1260.

Loefer, J., Sedberry, G. *et al.* (2005). Vertical movements of a shortfin mako in the western North Atlantic as determined by pop-up satellite tagging. *Southeastern Naturalist* 4, 237–246.

Luikart, G., Ryman, N., Tallmon, D. A., Schwartz, M. K., and Allendorf, F. W. (2010). Estimation of census and effective population sizes: the increasing usefulness of DNA-based approaches. *Conservation Genetics* 11, 355–373.

Luikart, G., Sherwin, W. B., Steele, B. M. and Allendorf, F. W. (1998). (1998). Usefulness of molecular markers for detecting population bottlenecks via monitoring genetic change. *Molecular Ecology* 7, 963–974.

Meirmans, P. G., and Hedrick, P. W. (2011). Assessing population structure: FST and related measures. *Molecular Ecology Resources* 11, 5–18.

Michaud A, Hyde J. R., Kohin, S., and Vetter, R. (2011). Mitochondrial DNA sequence data reveals barriers to dispersal in the highly migratory shortfin mako shark *(Isurus oxyrinchus*). In: Report of the Shark Working Group Workshop. Annex 4. International Scientific Committee for Tuna and Tuna-like Species in the North Pacific Ocean. 38 pp.

Mills, L. S, and Allendorf, F. W. (1996). The one-migrant-per-generation rule in conservation and management. *Conservation Biology* 10, 1509−1518.

Mollet, H. F., Cliff, G., Harold, L. Pratt Jr., and Stevens, J. D. (2000). Reproductive biology of the female shortfin mako, *Isurus oxyrinchus* Rafinesque, 1810, with comments on the embryonic development of lamnoids. *Fisheries Bulletin* 98, 299–318.

Mossman, C. A, and Waser, P. M. (1999). Genetic detection of sex-biased dispersal. *Molecular Ecology Notes* 8, 1063–1067.

Mucientes, G. R., Queiroz, N., Sousa, L. L., Tarroso, P., and Sims, D. W. (2009). Sexual segregation of pelagic sharks and the potential threat from fisheries. *Biology Letters* 5, 156–159.

Musyl, M. K., Domeier, M. L., Nasby-Lucas, N., Brill, R. W., McNaughton, L. M., Swimmer, J. Y., Lutcavage, M. S., Wilson, S. G., Galuardi, B., and Liddle, J. B. (2011). Performance of pop-up satellite archival tags. *Marine Ecology Progress Series*. 433, 1–28.

Nams, V. O. (2006). Detecting oriented movement of animals. *Animal Behaviour* 72, 1197–1203.

Nance, H. A., Klimley, P., Galvan-Magana, F., Martınez-Ortiz, J., and Marko, P. B. (2011). Demographic Processes Underlying Subtle Patterns of Population Structure in the Scalloped Hammerhead Shark, *Sphyrna lewini*. *PLoS ONE* 6, e21459.

Naylor, G. J. P., Caira, J. N., Jensen, K., Rosana, K. M., White, W. T., and Last, P. R. (2012). A DNA sequence-based approach to the identification of shark and ray species and its implications for global elasmobranch diversity and parasitology. *Bulletin American Museum Natural History* 367, 1–262.

Nei, M. (1987). Molecular Evolutionary Genetics. New York, Columbia University Press. Pp 512.

Paetkau, D., Calvert, W., Stirling, I., and Strobeck, C. (1995). Microsatellite analysis of population structure in Canadian polar bears. *Molecular Ecology* 4, 347–354.

Pardini, A. T., Jones, C. S., Noble, L. R., Kreiser, B., Malcolm, H., Bruce B. D., Stevens, J. D., *et al.* (2001). Sex-biased dispersal of great white sharks. *Nature* 412, 139–140.

Peakall, R., Ruibal, M., and Lindenmayer, D. B. (2003). Spatial autocorrelation analysis offers new insights into gene flow in the Australian bush rat, *Rattus fuscipes*. *Evolution* 57, 1182–1195.

Peakall, R., Smouse, P. E., and Huff, D. R. (1995). Evolutionary implications of allozyme and RAPD variation in diploid populations of Buffalograss *Buchloe dactyloides*. *Molecular Ecology* 4, 135–147.

Peakall, R., and Smouse, P. E. (2012). GenAlEx 6.5: genetic analysis in Excel. Population genetic software for teaching and research – an update. *Bioinformatics* 28, 2537–2539.

Piry, S., Alapetite, A., Cornuet, J. M., Paetkau, D., Baudouin, L., and Estoup, A. (2004). GeneClass2: A software for genetic assignment and first-generation migrant detection. *Journal of Heredity* 95, 536–539.

Portnoy, D. S., McDowell, J. R., McCandless, C. T., Musick, J. A., and Graves, J. E. (2009). (2009). Effective size closely approximates the census size in the heavily exploited western Atlantic population of the sandbar shark, *Carcharhinus plumbeus*. *Conservation Genetics* 10, 1697–1705.

Posada, D. (2008). jModelTest: Phylogenetic Model Averaging. *Molecular Biology and Evolution* 25, 1253–1256.

Pritchard, J. K., Stephens, M., and Donnelly, P. (2000). Inference of population structure using multilocus genotype data. *Genetics* 155, 945–959.

Prugnolle, F., and de Meeus, T. (2002). Inferring sex-biased dispersal from population genetic tools: a review. *Heredity* 88, 161–165.

Palumbi, S. R. (2003). Population genetics, demographic connectivity, and the design of marine reserves. *Ecological Applications* 13 Supplement, S146–S158.

Raymond, M., and Rousset, F. (1995). Population genetics software for exact tests and ecumenicism. *Journal of Heredity* 86, 248–249.

Rice, W. R. (1989). Analyzing tables of statistical tests. *Evolution* 43, 223–225.

Rogers P. J., Huveneers, C., Page, B., Goldsworthy, S. D., Coyne, M., Lowther, A. D., Mitchell, J. G., and Seuront, L. (2015). Living on the continental shelf edge: habitat use of juvenile shortfin makos *Isurus oxyrinchus* in the Great Australian Bight, southern Australia. *Fisheries Oceanography*. 24: 3, 205–218.

Rosenberg, N. A. (2004). Distruct: a program for the graphical display of population structure. *Molecular Ecology Notes* 4,137–138.

Ryman, N., and Palm, S. 2006. POWSIM: a computer program for assessing statistical power when testing for genetic differentiation. *Molecular Ecology* 6, 600–602.

Schrey, A. and Heist, E. (2002). Microsatellite markers for the shortfin mako and cross-species amplification in lamniformes. *Conservation Genetics* 3, 459–461.

Schrey, A. and Heist, E. J. (2003). Microsatellite analysis of population structure in the shortfin mako (*Isurus oxyrinchus*). *Canadian Journal of Fisheries and Aquatic Sciences* 60, 670–675.

Schuelke, M. (2000). An economic method for the fluorescent labelling of PCR fragments. *Nature Biotechnology* 18, 233–234.

Schultz, J. K., Feldheim, K. A., Gruber, S. H., Ashley, M. V., McGovern, T. M., and Bowen, B. W. (2008). Global phylogeography and seascape genetics of the lemon sharks (genus Negaprion). *Molecular Ecology* 17, 5336–5348.

Sepulveda, C. A., Kohin, S. *et al.* (2004). Movement patterns, depth preferences, and stomach temperatures of free-swimming juvenile mako sharks, *Isurus oxyrinchus*, in the Southern California Bight. *Marine Biology* 145, 191–199.

Smouse, P. E., Peakall, R., and Gonzales, E. (2008). A heterogeneity test for fine-scale genetic structure. *Molecular Ecology* 17, 3389–3400.

Smouse, P. E., and Peakall, R. (1999). Spatial autocorrelation analysis of individual multiallele and multilocus genetic structure. *Heredity* 82, 561–573.

Spieth, P. T. (1974). Gene flow and genetic differentiation. *Genetics* 78, 961–965.

Stevens, J. D. (1992). Blue and mako shark by-catch in the Japanese longline fishery off South-eastern Australia. *Australian Journal of Marine and Freshwater Research* 43, 227–236.

Stevens, J., R. Bradford, *et al*. (2010). Satellite tagging of blue sharks (*Prionace glauca*) and other pelagic sharks off eastern Australia: depth behaviour, temperature experience and movements. *Marine Biology* 157, 575–591.

Sugiura N (1978). Further analysis of the data by Akaike's information criterion and the finite corrections. Communication in Statistics - Theory and Methods. A7, 13–26.

Sunnucks, P., and Hales, D. (1996). Numerous transposed sequences of mitochondrial cytochrome oxidase in aphids of the genus Sitobion (Hemiptera: Aphididae). *Molecular Biology and Evolution* 13, 510–523.

Taguchi, M., Kitamura, T., and Yokawa, K. (2011). Genetic population structure of shortfin mako (*Isurus oxyrinchus*) inferred from mitochondrial DNA on inter-oceanic scale. National Research Institute of Far Seas Fisheries, Japan. 11 pp.

Van Oosterhout, C., Hutchinson, W. F., Wills, D. P. M., and Shipley, P. (2004). Micro-checker: software for identifying and correcting genotyping errors in microsatellite data. *Molecular Ecology Notes* 4, 535–538.

Waples RS (1998). Separating the wheat from the chaff — patterns of genetic differentiation in high gene flow species. *Journal of Heredity* 89, 438–450.

Waples RS (2006). A bias correction for estimates of effective population size based on linkage disequilibrium at unlinked gene loci. *Conserv. Genet.* 7, 167–184.

Waples, R. S., and England, P. R. (2011). Estimating contemporary effective population size on the basis of linkage disequilibrium in the face of migration. *Genetics* 189, 633−644.

Waples, R. S., and Do, C. (2010). Linkage disequilibrium estimates of contemporary Ne using highly variable genetic markers: a largely untapped resource for applied conservation and evolution. *Evolutionary Applications* 3, 244−262.

Waters, J. M. (2008) Marine biogeographical disjunction in temperate Australia: Historical landbridge, contemporary currents, or both? *Diversity and Distributions* 14, 692–700.

Weir BS (1979). Inferences about linkage disequilibrium. *Biometrics* 35, 235–254.

Weir BS (1996). Genetic Data Analysis. Sunderland, MA., Sinauer.

Wraith, J. and S. Kohin (2010). Cooperative Anglers and NMFS SWFSC Billfish Newsletter.

Appendices

Appendix 1. List of researchers and project staff.

Formulation of project: Paul Rogers and Shannon Corrigan.

Management of project (Primary Investigator): Paul Rogers.

Data management: Paul Rogers (Conventional tagging and satellite telemetry), and Shannon Corrigan (Genetics).

Laboratory analyses: Shannon Corrigan (Genetics).

Fieldwork: Paul Rogers (Satellite telemetry and tissue sampling).

Data analyses: Paul Rogers (Conventional tagging and satellite telemetry), Andrew Lowther (Spatial modelling of satellite telemetry data), and Shannon Corrigan (Genetics).

Report preparation: Paul Rogers (Conventional tagging and satellite telemetry), and Shannon Corrigan (Genetics).

Appendix 2. Details of conventional game fish tag-recapture events.

Tag #	Release date	Release location	Recapture date	Recapture location	Days at liberty	Distance (km)
1	02-Oct-77	Sydney	30-Oct-77	Redhead	28	52
2	16-Oct-77	Sydney Heads	30-May-78	Sussex Inlet	226	167
3	19-Oct-77	The Peak	06-Nov-77	Broken Bay	18	47
4	27-Mar-79	Unknown	29-Jul-79	Morna Point	124	49
5	28-Dec-80	Swansea	25-Apr-82	Swansea	483	2
6	03-Oct-81	Swansea	10-Jan-82	Terrigal	99	379
7	24-Apr-82	Manly	12-Feb-83	Botany Bay	294	26
8	18-Sep-83	Broken Bay	18-Sep-88	Botany Bay	1827	51
9	17-May-85	Shell Harbour	03-Nov-85	Gibber Reef	170	327
10	11-Aug-85	Point Plomer	25-Apr-86	Tutukaka NZ	257	2051
11	01-Sep-85	Point Plomer	13-May-86	Montague Island	254	605
12	19-Oct-85	Port Stephens	21-Feb-88	Wybung Head	855	69
13	31-Mar-86	Port Stephens	27-May-87	Cape Howe	422	630
14	17-Oct-86	Port Stephens	04-Oct-87	Sydney wide	352	56
15	18-Oct-86	Port Stephens	23-May-87	Box Head	217	113
16	06-Sep-87	Port Macquarie	29-Aug-99	Port Hacking	4375	334
17	18-Oct-87	Garie Beach	26-Sep-88	Coogee	344	35
18	02-Oct-88	Port Macquarie	27-Mar-89	Merimbula	176	623
19	02-Oct-88	Port Macquarie	17-Nov-89	The Banks	411	431
20	01-Oct-89	Sydney	24-Oct-89	Kiama	23	158
21	25-Apr-90	Bermagui	12-Jun-91	Solomon Islands	413	3369
22	29-Apr-90	Montague Island	05-Apr-91	Nadgee River	341	133
23	02-Dec-90	Corrimal	08-May-91	Narooma	157	206
24	14-Apr-91	Tura Head	03-Oct-93	Wollongong	903	302
25	08-Sep-91	Port Stephens Heads	15-Jun-94	King Island	1011	1072
26	26-Apr-92	Bermagui	27-Aug-92	Brisbane	7	1228
27	26-Apr-92	Norah Head	03-May-92	Port Hacking	123	90
28	18-Oct-92	Wave Recording Buoy	24-Feb-93	Gabo Island	129	568
29	02-Nov-92	Port Kembla Wide	16-Jan-93	Cape Conran	75	423
30	28-Nov-92	Redhead	01-Sep-93	Coffs Harbour	277	370
31	24-Jan-93	Bermagui	22-May-93	Bermagui	118	2
32	10-Jul-93	Jervis Bay Canyons	25-Aug-94	Ulladulla	411	23
33	10-Jul-93	Jervis Bay Canyons	10-Oct-94	Norah Head	457	223
34	10-Oct-93	Port Macquarie	16-Oct-93	Forster	6	51
35	26-Dec-93	Eve's Ravene	29-Jan-94	Maringo Beach	34	114
36	24-Apr-94	Narooma	01-Oct-95	Norah Head Canyons	525	363
37	17-Sep-94	Bellambi Point	01-Sep-95	New Caledonia	349	1993
38	27-Feb-95	Bermagui	18-Apr-95	Bermagui	50	25
39	09-Mar-95	Bermagui	14-Apr-95	Eden	36	77
40	06-Jun-95	Bermagui	01-Oct-95	Redhead	117	410
41	27-Jul-95	Kurnell	31-Jul-97	Marion Reef	735	1676
42	13-Aug-95	Swansea	26-May-96	Port Hacking	287	120
43	03-Sep-95	Botany Bay	23-May-96	Tuross Canyons	263	261
44	09-Sep-95	Botany Bay	30-Sep-95	Redhead	21	111
45	28-Oct-95	Shoalhaven Bight	13-May-96	Kangaroo Island	198	1102
46	19-Nov-95	Hare Bay	24-Jan-96	Sydney	66	168
47	27-Jan-96	Bermagui	08-Mar-96	Bermagui	41	21

48	10-Mar-96	Bermagui	28-Apr-98	Fortescue Bay	779	756
49	28-Mar-96	Shoalhaven Bight	15-Jun-00	Bermagui	1540	206
50	06-Apr-96	Bermagui	24-Apr-96	Montague Island	18	23
51	27-Apr-96	Port Hacking	10-Feb-97	Gabo Island	289	414
52	12-May-96	Jervis Bay Canyons	02-Jun-96	Bendalong	21	70
53	16-May-96	Bermagui	03-Oct-98	Bird Island	870	376
54	07-Jun-96	Bermagui	04-Aug-96	Terrigal	58	353
55	25-Jul-96	Wybung Head	07-Feb-97	Port Arthur	197	1156
56	24-Aug-96	Botany Bay	03-Jan-97	Bermagui	132	302
57	08-Sep-96	Port Hacking	03-Oct-96	Port Stephens	25	188
58	05-Oct-96	Botany Bay	06-Dec-97	Kingfish A Oil Rig	427	582
59	05-Oct-96	Stanwell Park	27-May-98	Bermagui	599	262
60	07-Oct-96	Shellharbour	03-Dec-96	Ulladulla	57	56
61	01-Dec-96	Long Reef	15-Dec-96	The Peak	14	29
62	27-Mar-97	Bermagui	21-Apr-98	Fraser Island	390	1351
63	18-May-97	Bermagui	06-Dec-98	Cape Leeuwin	567	3200
64	18-Jul-97	Bermagui	27-May-98	Bermagui	313	24
65	05-Oct-97	Port Hacking	22-Feb-99	Jervis Bay	314	127
66	05-Oct-97	Swansea	15-Aug-98	Loyalty Islands, Noumea	505	1995
67	03-Jan-98	Wollongong	28-May-98	Mudjimba Island	145	939
68	24-Jan-98	Pirates Bay	15-Mar-98	Cape Moreton	50	1861
69	21-Mar-98	Phillip Island	26-Feb-99	Fraser Is	342	1639
70	18-Apr-98	Mowarry Point	17-May-98	Bulli	29	360
71	24-Apr-98	Bermagui	15-Sep-98	Bermagui	144	15
72	12-May-98	Tuross Canyons	27-May-98	Bermagui	15	35
73	05-Jul-98	Jervis Bay Canyons	23-Mar-99	Moreton Island	261	988
74	03-Sep-98	Port Hacking	04-Apr-99	Bermagui	213	293
75	03-Oct-98	Bulli	14-Jun-99	Tuross	107	242
76	03-Oct-98	Port Hacking	18-Jul-99	Moreton Island	189	823
77	03-Oct-98	Swansea	10-Apr-99	Terrigal	254	39
78	03-Oct-98	The Banks	18-Jan-99	Lakes Entrance	288	428
79	04-Oct-98	Kiama	15-Nov-98	Swansea	20	196
80	04-Oct-98	Kiama	05-May-01	Fraser Seamount	42	1153
81	04-Oct-98	Stanwell Park	24-Oct-98	Jervis Bay Canyons	217	112
82	04-Oct-98	Stanwell Park	09-May-99	The Banks Wide	944	80
83	14-Nov-98	Beecroft Head	16-May-99	Port Hacking	183	118
84	06-Mar-99	Port Stephens	23-Jun-99	Eden	109	477
85	24-Mar-99	Waitara	14-Apr-01	Swansea	752	2135
86	10-Jul-99	Jervis Bay Canyons	01-Aug-00	Myall Lakes	388	359
87	26-Jul-99	Eden	26-Sep-99	Seal Rocks	62	633
88	22-Aug-99	Botany Bay	02-Oct-99	Port Hacking	41	26
89	18-Sep-99	Wollongong	26-Sep-99	Seal Rocks	8	334
90	25-Sep-99	Jervis Bay Canyons	03-Feb-00	Long Reef	131	163
91	07-May-00	Sydney	22-May-02	Sydney	745	0
92	20-May-00	Swansea	21-Jun-00	North Solitary Island	32	410
93	05-Aug-00	Botany Bay	22-Nov-03	Jervis Bay	1204	136
94	22-Sep-00	Black Head	07-Oct-00	Wollongong	15	79
95	24-Sep-00	Drum And Drumsticks	25-Oct-00	Botany Bay	1	129
96	24-Sep-00	Quarry	25-Sep-00	Coffs Harbour	31	4
97	05-Nov-00	Botany Bay	04-Feb-01	Port Phillip Bay	91	736
98	03-Jun-01	Merimbula	24-Jul-01	Moreton Island	51	1157

99	29-Sep-01	Botany Bay	17-Apr-05	Eden	1296	363
100	13-Oct-01	Shoalhaven Bight	16-Feb-02	Phillip Island	126	664
101	02-Dec-01	Unknown	25-Apr-02	Fraser Island	144	1010
102	25-Jan-02	Bermagui	22-Jun-02	Clarence Headland	148	838
103	23-Feb-02	Port Stephens	15-Sep-02	Port Stephens	204	25
104	20-Apr-02	Unknown	21-Apr-02	Unknown	1	11
105	03-Nov-02	Bermagui	03-Nov-03	Forster	365	559
106	08-Feb-03	Gerroa	15-Sep-04	Phillipine Sea	585	5940
107	13-Dec-03	Currarong	07-Apr-04	Apollo Bay	116	762
108	20-Dec-03	Bass Point	08-Mar-04	Kilcunda	79	681
109	08-Feb-04	The Entrance	22-Jan-05	Hippolyte Rocks	349	1162
110	28-Feb-04	Port Stephens	19-May-04	Montague Island	81	446
111	20-Mar-04	Broken Bay	16-Apr-04	North Stradbroke Island	27	668
112	20-Mar-04	Cape Schanck	18-Jun-04	Stanwell Park	90	733
113	08-Aug-04	Browns Mountain	08-Aug-04	Browns Mountain	0	0
114	26-Feb-05	Pirates Bay	27-Jul-05	Gold Coast Seaway	151	1740
115	05-Mar-05	Mercury Island	09-Jun-05	Ulladulla	96	2295
116	19-Mar-05	Inverloch	11-Feb-06	Barwon Heads	329	100
117	06-Apr-05	Tabourie Lake	17-Oct-06	Port Moresby	559	2924
118	06-Aug-05	Browns Mountain	07-Jan-06	Cape Otway	154	909
119	06-Aug-05	Browns Mountain	07-Jan-06	Apollo Bay	154	889
120	18-Jan-06	Inverloch	22-Jan-06	San Remo	4	37
121	29-Apr-06	Point Lookout	14-Jun-06	Batemans Bay	46	982
122	07-Nov-06	Coffs Harbour	17-Feb-07	Portsea	102	1190
123	11-Feb-07	Port Stephens	06-May-07	Browns Mountain	84	152
124	17-Feb-07	Kilcunda	19-Jan-08	Cape Schanck	336	22
125	18-Feb-07	Cape Schanck	30-Jul-07	Pacific Ocean	162	2071
126	12-Jan-08	Cape Schanck	27-Apr-08	Cape Schanck	106	1
127	11-Oct-08	Shellharbour Shelf	19-Oct-08	Port Hacking	8	97
128	18-Jan-09	Wilsons Promontory	26-Dec-09	Port Albert	342	44
129	24-Jan-09	St Helens	18-Sep-10	Stanwell Park	602	813
130	22-Feb-09	Cape Schanck	04-Feb-10	Barwon Heads	347	40
131	21-Mar-09	Cody Bank	10-Jan-10	Cape Woolamai	295	33
132	08-Apr-09	Tuross Canyons	10-Apr-09	Kiama Canyons	2	158
133	01-Aug-09	Browns Mountain	02-Aug-09	Browns Mountain	1	111
134	22-Aug-09	Kiama Canyons	22-Aug-09	Greenwell Point	0	15
135	20-Sep-09	Stanwell Park Canyons	08-Jan-10	Flinders Island	110	702
136	20-Sep-09	Stanwell Park Canyons	14-Nov-10	Botany Bay	420	51
137	23-Dec-09	Inverloch	28-Dec-09	Portsea	5	98
138	09-Jan-10	Bass Strait	03-May-10	Tasman Sea	114	1140
139	22-Jan-10	Cape Liptrap	25-Jan-10	Cape Conran	3	262
140	18-Sep-10	Port Hacking	14-Aug-11	Browns Mountain	330	15
141	19-Sep-10	Wollongong	27-Nov-10	Jervis Bay	69	108
142	01-Oct-10	Bermagui	25-Aug-13	Drum Canyons	1059	163
143	05-Dec-10	Shellharbour	08-Feb-11	Lake Tabourie	65	107
144	02-Jan-11	Cape Schanck	15-Jan-11	Lorne	13	75
145	07-Jan-11	Port Macdonnell	19-Mar-11	Cape Liptrap	71	450
146	25-Jan-11	Inverloch	30-Jan-11	Flinders	5	67
147	26-Feb-11	D'Estrees Bay	16-Dec-13	Portland	1024	421
148	27-Feb-11	Inverloch	29-Jan-12	Cape Schanck	336	138
149	17-Sep-11	Wollongong	12-Oct-11	Norah Head	25	161

150	25-Nov-11	Jervis Bay	21-Jun-12	Pacific Ocean	209	1717
151	21-Jan-12	Port Welshpool	28-Jan-12	Port Welshpool	7	42
152	04-Aug-12	Browns Mountain	16-Aug-12	Browns Mountain	12	0
153	04-Aug-12	Browns Mountain	25-Aug-12	Browns Mountain	21	2
154	05-Aug-12	Browns Mountain	28-Dec-13	St Helens	510	858
155	09-Sep-12	Browns Mountain	09-Sep-12	Browns Mountain	0	0
156	23-Nov-12	Jervis Bay	11-Jan-13	Cape Schanck	49	666
157	07-Jan-13	Cape Woolamai	20-Jan-13	Cape Woolamai	13	31
158	10-Mar-13	Cape Woolamai	11-Mar-13	Cape Liptrap	1	30

Appendix 3. Intellectual Property.

NSW Department of Primary Industries
Locked Bag 3020 Nowra NSW 2541

NSW Department of Primary Industries
Data Licence

THIS LICENCE AGREEMENT is made on the 22nd day of January 2014

BETWEEN PHIL BOLTON

Representing NSW Department of Primary Industries (the Licensor), ABN 72 189 919 072

AND PAUL ROGERS

Representing SARDI Aquatic Sciences (the Licensee), ABN 53 763 159 658

IT IS HEREBY AGREED THAT:

1. **Definition of terms:**
   - 1.1 'Licensor' means NSW Department of Primary Industries (NSW DPI) ABN 72 189 919 072
     'Licensee' means SARDI Aquatic Sciences ABN 53 763 159 658
   - 1.2 'Data' means the Data described in Annexure A, and any data derived there from.
   - 1.3 "Point of Access" means equipment listed in Item 4 Annexure B being a personal computer or another type of stand alone computer or a single computer terminal on a computer network or any other item of electronic and or mechanical equipment capable of viewing, interpreting, processing, manipulating or otherwise accessing the Data or any derivate data incorporating the Data.
   - 1.4 "Approved Purposes" means any purpose specified in Item1 Annexure B.
2. **Licence:**
   - 2.1 The Licensor grants to the Licensee a non-exclusive and non-transferable Licence to:
     - 2.1.1 use the Data, for and limited to, the Approved Purpose subject always to the conditions in this Agreement.
     - 2.1.2 reproduce the Data at the Point of Access
     - 2.1.3 permit consultants, contractors or subcontractors with whom it has contracted for the provision of services to the Licensee to use the Data at the Point of Access for the Approval Purpose only.
     - 2.1.4 combine the Data with other data of the Licensee and provided that nothing is this clause will derogate from the ownership of the Licensor in the Data or any Data derived from the Data and further provided that nothing in this cause shall, unless the parties otherwise agree at that time, entitle the Licensee to keep a copy of an portion of the Data or any Data derived from the Data upon the termination of this Agreement for any reason and the Licensee will indemnify the Licensor if such combination of data combined with the Data infringes the copyright of any third person
   - 2.2 The rights granted herein are restricted solely to the Licensee and may not be assigned, transferred or sublicence without the prior written permission of the Licensor, which permission may be granted subject to any conditions which the Licensor may require.
   - 2.3 By virtue of this Agreement, the Licensee acquires only the right to use the Data and does not acquire any rights of ownership of the Data and is entitled to use, distribute or sublicence the Data only in accordance with clauses 6 and 7.
3. **Duration:**
   - 3.1 The Licence granted in this agreement shall expire on the date specified in Item 2, Annexure B.
   - 3.2 Upon expiration of the Licence the Licensee shall return the Data and erase all other copies of the Data held in its computer files stored in any media.
4. **Licence Fee**
   - 4.1 In consideration of the grant of the licence the Licensee shall pay to the Licensor a licence fee as specified in Item 3, Annexure B, on delivery of the Data.
   - 4.2 The licence fee is inclusive of the Goods and Services Tax (GST) payable in respect of this Licence for the data. A valid Tax Invoice will be issued on receipt of payment.
   - 4.3 The Licensee may apply for an increase in the number of Points of Access.
   - 4.4 The Licensor may grant to the Licensee rights to an increased number of Points of Access to the Data subject to the payment of an additional fee.

5. **Ownership**

5.1 The Data and any copies that may be made of it, whether in its original form, shall remain the property of the Licensor.

5.2 All copyrights and intellectual property rights in the Data shall remain the property of the Licensor.

6. Copying of the Data:

6.1 The Licensee may make only sufficient copies of the Data as are reasonably required for operational and backup purposes, provided that all copies of the Data are kept in safe keeping and are otherwise subject to the provisions of this Agreement and that any Notice placed on the Data indicating or implying the Licensor's ownership shall where reasonable possible be reproduced in or on such copies.

6.2 The Data may be manipulated, copied as agreed in 6.1, or transfer via any media for the Approved Purposes, but the Licensee must not sublicence, 'lend', 'rent', resell or otherwise provide the Data to a third party in any form, in whole or in part, either temporarily or permanently.

7. Outputs for internal use:

7.1 The Licensee may use the Data to produce outputs only to meet its own internal needs with respect to the Approved Purposes. For the purposes of this clause the acceptance of any payment other than reimbursement for the direct cost of production (including the cost of printing) for any document which includes the Data or any part of it is not a use to meet internal needs.

8. Publication of Data

8.1 Where the licensee combines the data with other data held by the licensee to produce a product, or otherwise derives from the data (whether for internal, private or public use), any product that may include maps, publications and digital data, the Licensee is not entitled to deal with, make available, sell or otherwise dispose of those products unless it has first obtained the written consent of the Licensor. The Licensor may grant or refuse its consent in its absolute discretion and may grant consent subject to any condition or conditions whatsoever.

8.2 The Licensee, if requested, must provide a copy of any reports or publications, including public statement or publicity material resulting from use of the Data to NSW DPI for review within a reasonable time before making the statement or publishing the material. With respect to any required report the Licensee must complete the report to NSW DPI's satisfaction or NSW DPI may return it to the Licensee for satisfactory completion within a reasonable time.

8.3 NSW DPI reserves the rights to use reports or publications developed from the data for non-commercial purposes within NSW DPI including publication on its intranet and internet sites, teaching purposes, for further research and spoken presentations.

9. Endorsement and Acknowledgment:

9.1 The Licensee is to endorse on all maps and other publications including digital products which it may produce using the Data or any copy thereof a statement acknowledging that the Licensor supplied the Data, and that the Licensor remains the owner of the Data.

9.2 The existing "NSW DPI Game Fish Tagging Program" is funded by the NSW Recreational Fishing Saltwater Trust. All publications incorporating these data or derivatives, must acknowledge the NSW Recreational Fishing Saltwater Trust together with NSW DPI.

10. Liability, Release and Indemnity:

10.1 The Licensor does not warrant the Data is error free, or that it meets the Licensee's particular requirements.

10.2 The Licensor warrants that it holds copyright in the Data.

10.3 The Licensee acknowledges the Data may contain errors or omissions

10.4 The Licensee acknowledges that in no event shall the Licensor be liable for indirect, special, incidental or consequential damages (including loss of anticipated revenue) in connection with or arising out of performance of the Data, or otherwise in connection with this Agreement. Any liability shall be limited to the amount of any Licence Fee collected by the Licensor pursuant to this Agreement.

11. Security

11.1 The Licensee shall, subject to section 11.2, treat the Data as private and confidential to the Licensee and shall maintain the Data in safe custody and to the extent that "personal information" is included in any data, shall ensure compliance with the *Privacy and Personal Information Protection Act 1998.*

11.2 The Licensee shall take all reasonable steps to ensure that all persons, including sub-contractors employed by the Licensee, keep the Data confidential and does not disclose the Data to any person or use the Data for any purpose, other than in accordance with the conditions of this Agreement.

11.3 The Licensee agrees to notify the Licensor in writing of any security breaches. Or thefts of the Data, with 7 days of such breaches or thefts being discovered.

11.4 The Licensee accepts responsibility for the acts and defaults of all persons using the Data so supplied.

12. Termination:

12.1 This Licence may be terminated if either party breaches any of the terms of the Agreement and fails to remedy the breach within one month of a written notice from the other party specifying the breach and requesting the remedying thereof.

12.2 The termination of this Licence under 12.1 shall be without prejudice to the rights of either party for moneys due under the Agreement prior to termination.

12.3 The Licensee shall cease using the Data for any purpose from the date of termination of this Licence and shall within 30 days of the date of termination return the Data to the Licensor and erase all copies of the Data in its possession including any derived data.

13. Updates of the Data:

13.1 From time to time the Licensor may have available an updated version of the Data (the "Updated Data"). Updated Data may at the Licensor's sole option or discretion be provided during the term of this Agreement at a price payable by the Licensee to be agreed and evidence by the execution of a document so as to adopt the terms and conditions of this Agreement except as amended therein. Immediately upon its provision the Updated Data shall form part of the Data provided that nothing herein contained shall be deemed to impose any obligation on the Licensor to create and make available to the Licensee such Updated Data.

14. General Terms

14.1 Governing Law - This Agreement shall be governed by and construed in accordance with the law for the time being in force in the State of New South Wales.

14.2 Entire Agreement - This Agreement when executed shall supersede all prior agreements and undertaking between the parties and constitute the entire agreement between the parties relating to the Data

14.3 Notices - Any notice in writing required or permitted to be given in this Agreement shall be delivered to the Licensee personally or forwarded to the Licensee by post, to the Licensee's address shown on this Agreement. Notices to the Licensor shall be delivered or posted to its office for the time being. A notice sent by post shall be deemed to have been given two days after it was posted

IN WITNESS THEREOF the parties have executed this Agreement the day and year hereinbefore written:

Signed on behalf of NSW Department of Primary Industries (the Licensor), by

PHIL BOLTON, FISHERIES MANAGER ..... (Print name and position)

..... (Signature)

In the presence of:

IAN OSTERLOH FISHERIES MANAGEMENT OFFICER ..... (Print name and position)

..... (Signature)

Signed on behalf of SARDI Aquatic Sciences (the Licensee), by

Paul Rogers Research Scientist ..... (Print name and position)

..... (Signature)

In the presence of:

S. MAYFIELD, SARDI ..... (Print name and position)

..... (Signature)

Annexure A

'Data':

An extract from the NSW DPI Game Fish Tagging Program database including selected data for Mako Sharks from 1974 to Present.

Data includes:

A. For all release - recaptures
   1. Tag Number
   2. Date
   3. Location
   4. Length/Weight
   5. Time at Liberty
   6. Distance Travelled
   7. Comments

Annexure B

Item 1 – 'Approved Purposes':

NSW Department of Primary Industries will provide tag data held within the NSW DPI Game Fish Tagging Program database. This data will be used by SARDI in a FRDC TRF project on Mako Shark population structure and connectivity along with any other available conventional/satellite tagging data and genetic analyses.

Item 2 – 'Licence expiration date per Section 3':

12 months from the signature date of this licence agreement.

Item 3 – "Licence Fee per Section 4':

Not applicable in this case.

Item 4 – 'Point of Access':

The data is to be stored by the licensee, Paul Rogers (SARDI), on a secure server. Access to data will not be public. For approved purposes only.